A HYDROLOGICAL MODEL OF HARRINGTON SOUND, BERMUDA AND ITS SURROUNDING CAVE SYSTEMS

A Thesis

by

JONATHAN LEWIS STOFFER

Submitted to the Office of Graduate Studies of
Texas A&M University
in partial fulfillment of the requirements for the degree of

MASTER OF SCIENCE

Approved by:

Chair of Committee, Thomas M. Iliffe
Committee Members, Ayal Anis
George Jackson
Douglas Klein
Head of Department, Michael Masser

May 2013

Major Subject: Wildlife and Fisheries Sciences

ABSTRACT

Harrington Sound, located in east central Bermuda, is almost entirely enclosed by land except for a 26.4 m wide channel called Flatts Inlet. This limited connection to the open ocean restricts Harrington Sound's tides, resulting in a near 3 hour delay and dampening the tidal range to 35% of those on the coast. By comparing the tidal amplitude and surface area of Harrington Sound, tidal exchange can be determined. Past research has shown Flatts Inlet only supplies the Sound with about half of its tidal water. The remaining tidal exchange enters and leaves the Sound either via groundwater influx through pores in the rock or through the traversable passageways of limestone cave systems in the land that encloses the Sound.

The aim of this study was to model hydrodynamic tidal flux and current through marine caves into Harrington Sound. One of the goals of Bermuda's cave habitat protection plan is to track tidal circulation of water through these cave systems. Information on such cave water transport would facilitate future pollution and nutrient exchange studies. This research was initiated during a six week trip to Bermuda by Jonathan Stoffer as he obtained tidal and water quality data from caves along the perimeter of Harrington Sound. Additional flow data was collected with instruments placed by local cave divers. A YSI 600XLM water quality sonde, Norteck Vector Current Meter, and an in-situ level Aqua TROLL were used to monitor tidal amplitude, periodicity, current velocity, and water quality in cave pools and submerged passages. Profiles of the top 1-2 meters of water at each pool were taken at 56 sites. Tidal gauges

were placed in 27 major cave pools surrounding Harrington Sound, as well as Harrington Sound itself, for 48 hours, to monitor tidal propagation through the island. The vector current meter was placed for six weeks to measure water flow in and out of Harrington Sound in six cave passageways known to have high flow rates.

The resulting data have been compared to atmospheric data obtained from the Bermuda Weather Service and analyzed using Microsoft Excel, MATLAB and ArcGIS. The final goal of this project was to create a hydrological model able to predict flow rate and water depth in Bermudian caves with water depth data from the ocean and Harrington Sound.

In constructing a water budget for Harrington Sound, I was able to account for 72.3% of all tidal inflow and 43.3% of all tidal outflow from the Sound as passing through either Flatt's Inlet or one of the six tested caves. In creating my tidal models, I was able to achieve an averaged sum of squared deviation (SSD) normalized against count ranging from 5.1×10^{-4} to 8.4×10^{-4} m^2. The flow model achieved a SSD of 3.8×10^{-3} m^2. My data also suggest that exchange between Harrington Sound and other inland waters, through cave systems, does exist.

DEDICATION

Jim and Jan Stoffer

ACKNOWLEDGMENTS

I would like to thank all those who helped make this research possible. First, I would like to thank Dr. Tom Iliffe for helping me discover a part of the natural world I knew very little about. I would also like to thank the Bermuda Zoological Society for providing the grant that made my work in Bermuda possible. Working in Bermuda was an amazing experience that I will always remember. It is a place I will want to visit over and over again throughout my life.

I would also like to thank those individuals in Bermuda who helped make my work possible. First, I would like to thank Gil Nolan for his relentless support of me, both in the field and in gaining permission to work with local land owners. Second, I would like to thank those buddies who were willing to go out with me when called to duty. Among those I would like to thank the members of the Bermudian branch of the church of Jesus Christ of Latter day Saints, especially the missionaries, for going out with me so often. I would also like to thank those working for the aquarium and the Bermuda Zoological Society for helping me in the field and Pak Leung for helping me with data analysis.

Finally, I would like to thank those members of my committee who helped me analyze the mountain of data this research created and complete my thesis; Ayal Anis, Douglas Klein, and George Jackson.

TABLE OF CONTENTS

LIST OF TABLES

Page

LIST OF FIGURES

Page

CHAPTER I

INTRODUCTION: THE BERMUDA ISLANDS

1.1 Introduction

Bermuda consists of a series of small islands (51 km^2) located in a remote part of the North Atlantic, 1100 km east of South Carolina at 32º N, 64º W (Fig. 1.1). The islands are part of a limestone cap that rests atop a volcanic seamount. The majority of the platform is submerged at 15 to 25 m below sea level and consists of a variety of bays, sounds and lagoons. Harrington Sound, a 4.79 km^2 inshore water body in east central Bermuda, lies almost entirely enclosed within Bermuda's largest island (Fig. 1.1) (Morris et al., 1977). The Sound has a connection to the ocean through a single surface channel, Flatts Inlet. In addition, it is thought that the Sound also exchanges with the ocean through the many cave passageways in the surrounding landmass (Morris et al., 1977).

A review examining hydrology across the Bermudian islands can be found in Morris et al. (1977). Additional short term studies involved direct measurements of hydrological properties in Bermudian caves and anchialine pools include cave water column profiles and tidal data (Iliffe, 1980), an examination of the impacts of a massive dumping event on cave chemistry (Iliffe et al., 1984) and a survey of physical and hydrological profiles in anchialine ponds (Thomas et al., 1991). The results of a 13 month long study of cave temperature and salinity in Walsingham and Crystal Cave,

Bermuda are presented in Iliffe (2000). Data on lag time and tidal range for 27 caves around the island showed that a linear relationship existed between percent tidal range and lag time in caves (R^2=0.85) and that the values for tidal range and lag time were influenced by the caves position relative to Harrington Sound and the ocean. Cave water column profiles and short term current data was collected by Cate (2009) to supplement research on pollution.

The research presented here consists of an examination of hydrology and water exchange through caves connecting Harrington Sound with the ocean. Sample time for previous studies of current and tidal exchange in Bermudian caves ranged from 1 to 12 days (Thomas et al., 1991; Iliffe, 2000; Cate, 2009). Since longer sampling periods are required for resolving tidal patterns through a lunar cycle, my data collection periods lasted over 6 weeks are required so that lunar effects can be resolved.

I present water profiles and monitoring of tidal cycles and current flow through caves around Harrington Sound in this report. I also present a water budget for Harrington Sound based on my own calculations, as well as calculations made by Morris et al. (1977). Finally, I present a model of water level and flow through caves based on variations in water level in Harrington Sound and other inshore waters. This research will contribute to the recovery plan for Bermuda's critically endangered cave fauna which calls for the collection of biological, ecological and general habitat data in a central Geographical Information System (GIS) data base to "gain a better understanding of… hydrography of the cave systems" (Glasspool, 2003: 8).

This opening chapter provides an examination of the current body of knowledge relating to geology, hydrology and biology of Harrington Sound and its surrounding cave systems. Research objectives and hypotheses for this study are also listed and explained. Chapter 2 details profiles of water quality parameters taken in caves around Harrington Sound. Chapter 3 examines tidal range and lag time measurements taken in caves around Harrington Sound. Finally, Chapter 4 discusses the results of current measurements taken in caves around Harrington Sound, as well as provides a water budget for Harrington Sound based on atmospheric conditions and water exchange through cave systems and Flatts Inlet. Chapter 4 also includes a model which predicts water level changes in caves based on water levels in Harrington Sound and the ocean.

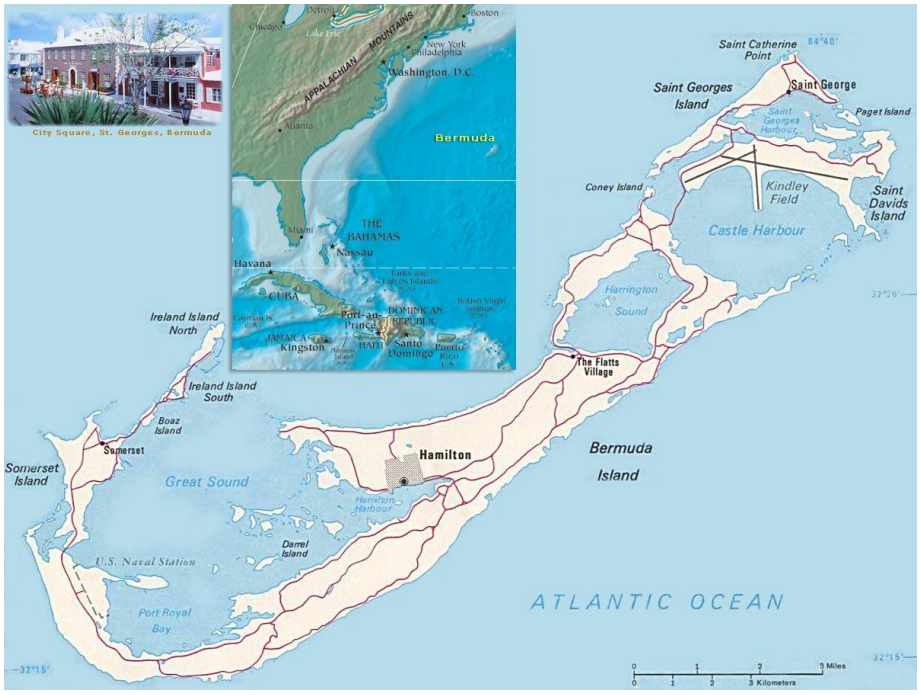

Fig 1.1. Bermuda and its location in relation to the U.S. coastline. Image from http://www.geographicguide.com/america-maps/bermuda.htm

1.2 Bermudian Geology

The Bermuda islands are currently thought to have formed during the closing of the Tethys Ocean and the associated gravitational collapse into the Earth's mantle (Vogt and Jung, 2007). In order to maintain mass balance, magma was forced through weak spots in the crust, creating the volcanic eruptions that formed the islands. These eruptions occurred ca. 47-40 Ma, during the early to middle part of the Middle Eocene and led to the formation of the Bermuda Pedestal (Vogt and Jung, 2007). The pedestal has three topographic highs: the Bermuda islands, and the submerged Plantagenet (Argus) and Challenger Banks, with the latter two rising to about 50 m below the surface (Vacher and Quinn, 2004). After the initial formation of the islands, episodic periods of submersion and exposure during glacial and interglacial periods led to a progressive buildup of eolian limestone. This is evidenced by the presence of paleosols formed during interglacial periods and laced through the limestone (Vacher and Quinn, 2004). Eolianite formations developed in a sequence of early shoaling, sand dune development, vertical growth and lateral accretion on solid formations atop the volcanic basement rocks (Hearty and Vacher, 1994). This long term growth of Bermuda's land mass is depicted in Fig. 1.2. The oldest limestone, the Walsingham formation, dates from the early Pleistocene and is found primarily in the isthmus separating Harrington Sound from Castle Harbour (Fig. 1.2). This is where most of Bermuda's caves are located. Today, Bermuda's exposed rock column is composed of alternating limestone and paleosols of Pleistocene age (Hearty and Vacher, 1994). Bermuda's surface topography

rises up to 76 meters above sea level and consists primarily of rolling hills (Iliffe, 2009). The cave entrances used in this study are at most 20 to 30 meters above sea level.

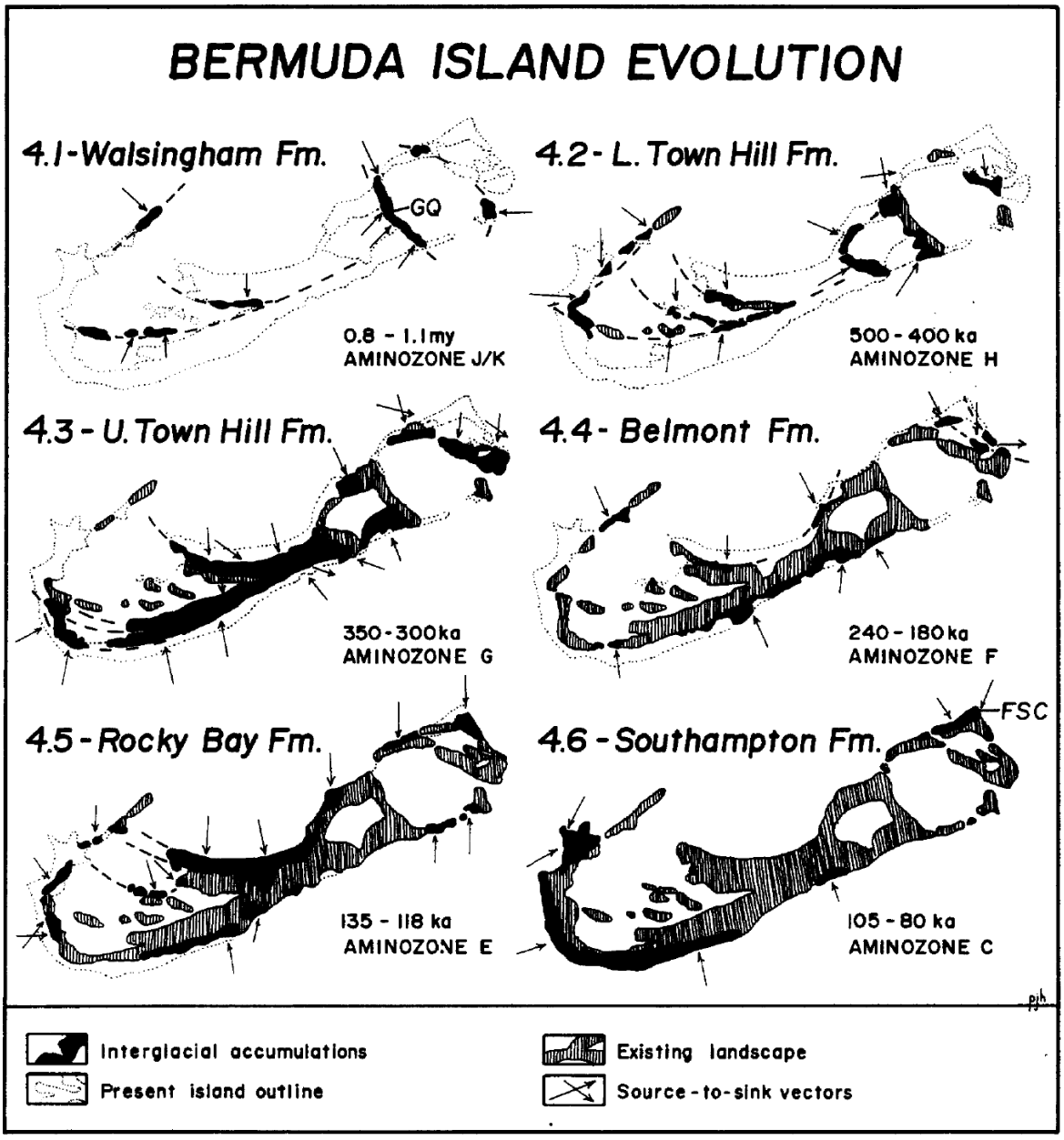

Fig 1.2. Long term development of Bermuda's surface. Given as sequential snapshots of deposition (Hearty and Vacher, 1994).

1.3 Inland Waters and Harrington Sound

The waters surrounding Bermuda are host to a diverse marine landscape, supporting great expanses of coral reefs, and are thus a hot spot of biodiversity requiring environmental protection. In 2008, about 7%, or 294.74 km^2, of the waters surrounding Bermuda were designated as protected coral reefs (Bermuda Department of Statistics, 2009). The majority of Bermuda's reefs are in the North Lagoon, a large area north of the island encompassing submerged portions of the Bermuda pedestal. This lagoon comprises scattered reef pinnacles and shallow flats reaching to 15 to 25 m deep. Major inshore water bodies include the Great Sound system located within the neck of land that wraps around the southwestern side of the island, the St. Georges system just below St. George on the north east side of the island, the Castle Harbour system located between Bermuda's northern islands and its main island, and Harrington Sound, a inshore water body in east central Bermuda (Morris et al., 1977).

Formation of Bermuda's inshore bodies of water, such as its Sounds, are thought to have begun after Bermuda's original formation, when an eolian limestone cap developed on the island (Vacher and Quinn, 2004). During low sea stands, depressions in this cap were dissolved by fresh water accumulation. When sea level rose, these depressions became sites of further dissolution due to fresh-saltwater mixing. With full marine inundation today, bioerosion has driven the continued expansion and formation of Bermuda's inland bodies of water (Neumann, 1965).

The 4.79 km^2 Harrington Sound is almost entirely enclosed within Bermuda's largest island, with between 200 to 1000 meters of land separating it from the ocean on

all sides (Morris et al., 1977). Along the coast of the Sound, deep clefts are cut into the cliff faces, some reaching as much as 4 meters (Thomas, 1996). These clefts were thought to be the result of wind and wave action on the cliff walls (Verrill, 1907; Thomas, 1996). However, this notion was challenged by Neumann (1963), who observed that many of these cleft faces were formed below the low tide water line (Thomas, 1996). He contended that because most clefts were too deep to be cut by wind or wave action, bioerosion was the main force driving their formation. Species shown to be potent drivers of bioerosion in Harrington Sound include several bivalve mollusks and sponges found along the cliffs of the Sound (Acker and Risk, 1985; Thomas, 1996).

Harrington Sound is notable in the way it fills and empties with each tide. The Sound has a direct connection to the ocean through a single 26.4 m wide surface channel called Flatts Inlet (Fig. 1.3; Fig. 1.4). Morris et al. (1977) calculated that 50% of the tidal exchange received by Harrington Sound flows directly through this channel. This inflow and outflow of Harrington Sound is unbalanced as 63% of the Sound's volume flows in during a rising tide, but only 35% flows out during a falling tide (Morris et al., 1977). The remaining water is thought to enter and leave the Sound through the cave passageways surrounding it. This imbalance implies the system around the Sound acts as a pump, with a net inflow of water through Flatts Inlet and a net outflow through the island.

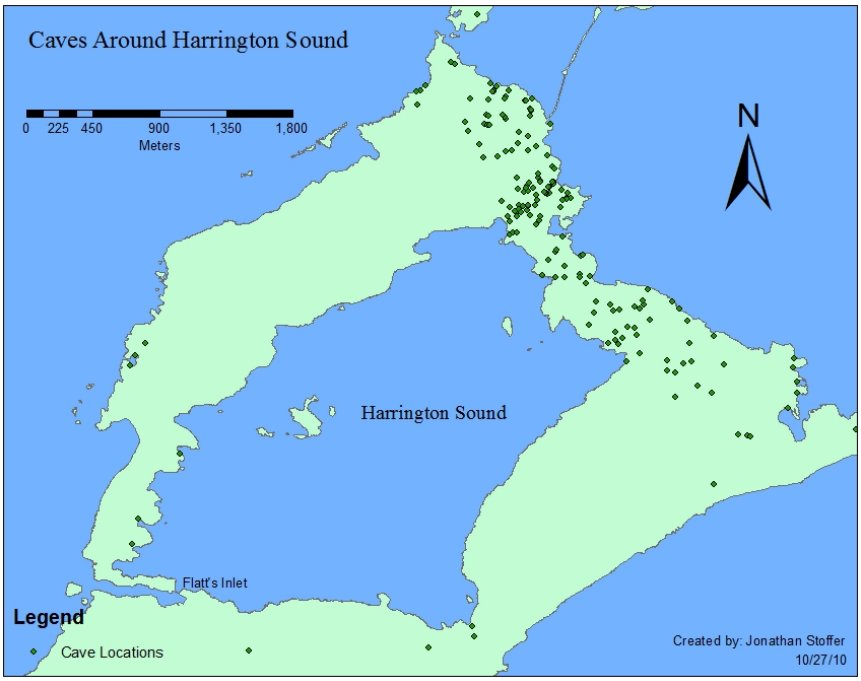

Fig. 1.3. Harrington Sound, Bermuda and its surrounding caves.

Fig. 1.4. Water flowing under Flatts bridge during a falling tide.

The restricted exchange between Harrington Sound and the ocean results in large tidal lag times and reduced tidal ranges. The oceanic tidal range of open waters around Bermuda varies from 0.45 to 1.2 m (Morris et al., 1977). However, restricted flow into Harrington Sound prevents full tidal exchange: the tidal range of the Sound is about 0.25 m with a tidal volume of 1.2×10^6 m^3. High and low tides for Harrington Sound, on average, lag about 2 hours and 53 minutes behind high and low tides in the ocean (Morris et al., 1977).

Residence time estimates can be calculated for the Sound based on its tidal exchange and volume using the relationship

$$R = \frac{V + T}{T} \tag{2.1}$$

where R = residence time (number of tidal exchanges), V = total volume of the basin (m^3), and T = tidal volume entering the basin (m^3) (Morris et al., 1977). This equation estimates Harrington Sound's residence time to be around 29.4 days (Morris et al. 1977). Not all factors are accounted for with such simple models, but if average values of mixing and stratification are used, residence time is still estimated to be around 177 days. More information on tidal exchange is needed to further refine the estimates on Harrington Sound's residence time. However, with such large residence time estimates, the Sound is likely to be sensitive to human influences, such as pollution (Morris et al., 1977).

1.4 Island Hydrology

The hydrology of islands typically consists of a fresh water lens sitting atop salt water with a transition zone or halocline between them (Anderson, 1976). Bermuda has five identifiable fresh water lenses including the St. Georges, Devonshire, Warwick, Southampton and Somerset lenses. These lenses formed as a result of variations in rock porosity, allowing fresh water to accumulate on top of the more dense salt water (Vacher, 1978). Due to the limited sizes and recharge rates of these lenses, special permits are required to extract water from them. The majority of the water feeding these lenses comes directly from rain water, but as much as 27% of their water is derived from cesspit effluent (Simmons et al., 1985).

Tides move through large islands and coastal aquifers with heights decaying exponentially with distance (White, 2009; Slooten et al., 2010). However, smaller karstic islands such as Bermuda do not follow this pattern; they are governed by more factors than distance-to-shore alone (Wheatcraft, 1981; Ayers and Vacher, 1986; White, 2009). The apparent reason for this unexpected tidal behavior is that the highly permeable karstic limestone propagates pressure signals through cracks and traversable passageways in the island rocks. Thus, tidal efficiency (defined as the percent ratio of tidal range in the cave compared to the surrounding ocean) is dependent on the medium through which it propagates. Finer sediments typically produce 5% tidal efficiency with lag times on the order of 2.5 hours. Coarser sediments have efficiencies on the order of 45% with 2 hour lags. Karstic limestones, such as that in Bermuda, usually have 50% efficiency with 1.5 hours lags (White, 2009). Measurements by Thomas Iliffe suggest

tidal lag times in these caves range from 10 minutes to 1.5 hours, with most caves being around 1 hour (Iliffe, 1980; Iliffe, 2000). This indicates that most Bermudian cave tides correspond to predictions by White (1980) that the geology and water flow within caves around the perimeter of Harrington Sound are in agreement with the caves acting as conduits for water exchange between the ocean and the Sound. Cracks, fissures and collapses provide additional connections (Iliffe, 1980). Within the Harrington Sound hydrological system, caves with longer lag times are expected to be supplied primarily by Harrington Sound and those with shorter lags by the ocean.

1.5 The Caves of Bermuda

The caves found in Bermuda formed due to the soluble nature of the island's limestone cap; there are at least 166 known caves in the island and possibly an equal number remaining to be discovered (Gibbons, 2003). Limestone cave formation occurs as rain water absorbs soil and atmospheric CO_2, causing the water to form a slightly acidic solution of carbonic acid (H_2CO_3). The limestone is dissolved by this acidic groundwater seeping through cracks in the stone. Over time, fissures in the rock continued to widen until a cave was formed (Palmer, 1991).

In order for Bermuda's caves to have formed, the island would have needed to be far less permeable or much larger to retain a large body of fresh groundwater (Land, 1967). All solution caves in Bermuda exist in older rocks which are denser and less permeable (Bretz, 1960), but these rocks cannot retain a freshwater body.

Pleistocene sea level records show that the reef-rimed lagoon around Bermuda was once emergent, providing approximately 648 square kilometers of land. This early Bermuda could have supported a large rain fed body of groundwater which could have extended well above sea level. This presence of an enlarged groundwater lens is evidenced by nearly horizontal solution chambers, the appearance of blind solution pockets in cave ceilings, the restriction of solution caves to lower stratigraphic layers, and the lack of evidence for solutional enlargement caused by free surface flow (Bretz, 1960). As this groundwater body worked toward the sea, solutional chambers developed into the Bermudian cave systems (Land, 1967).

The majority of Bermuda's limestone cave systems contain sea level anchialine pools. The term "anchialine" was originally coined by Holthuis (1973) to describe "pools with no surface connection to the sea, containing salt or brackish water, which fluctuates with the tides." These pools provide points of entry for divers and extend down to networks of submerged marine passageways, primarily at a depth of 18 meters below sea level (Iliffe, 1981). The existence of speleothems (stalactites and stalagmites) in submerged portions of the caves confirms their formation during low oceanic sea stands, since these cave formations can only be produced in dry caves (Iliffe et al., 1983). The use of $^{230}Th/^{234}U$ ratios in speleothems has allowed scientists to date the age of Bermuda's caves to the late Pleistocene era (~105 to ~85 kyr) (Harmon et al., 1981). During the last glacial period, in the late Pleistocene (~9 to ~115 kyr), low sea stands were as much as 127 m below current sea levels (Iliffe et al., 2011). The deepest Bermudian caves that have been explored reached depths of 26 m, a depth reached by

local sea levels ~9 kyr (Iliffe et al., 2011). The caves were formed to 26 m because at that depth the island's limestone cover meets non-carbonate base rock (Mylroie and Mylroie 2011). This explanation creates a problem because Bermuda's caves would have been exposed during most of the last glacial period, but the diversity of the endemic cave fauna inhabiting them suggests the islands caves have been colonized for far longer than ~9 kyr. Researchers suspect that deeper caves (>127 meters below sea level) must have harboured local cave fauna during glacial low sea stands (Iliffe et al., 2011).

There are four main cave areas around Bermuda. The first are reef caves occurring at 10 to 20 m depths along the seaward base of fringing reefs. The second area, called the Walsingham Tract, is northeast of Harrington Sound and has the largest concentration of caves on the island (Iliffe, 2009). The Walsingham Tract is also home to several cave systems investigated in this study. The Walsingham Cave System is 1300 m long (Iliffe, 2004) and has a maximum depth of 24 m (Iliffe, 2009). It has eight known entrances: Deep Blue, Vine, Old Horse, Walsingham, Fern Sink, Crystal, Fantasy and Blue Grotto. Most tidal exchange in the Walsingham System seems to pass through the northeast portion of the cave via Blue Grotto (Iliffe, 2003). The Palm Cave System, also in Walsingham Tract, is located southwest of the Walsingham System. It is about 500 m long (Iliffe, 2004) with five entrances: Cripplegate, Myrtle Bank, Palm, Sailor's Choice and Straw Market Caves (Iliffe, 2003). The Walsingham Tract has a number of other anchialine pools that have been investigated but that have not yet been connected to these two larger systems. The third area is the Green Bay Cave System, located on the

western side of the Sound (Iliffe, 2009). This is Bermuda's longest cave system, with a length greater than 2 km (Iliffe, 2003) and an average depth of 18 m (Iliffe, 2009). The Green Bay System has two known entrances, one at the end of Green Bay off Harrington Sound, and a second small anchialine pool near the Sound called Cliff Pool. The system itself extends submerged beyond the North Shore but becomes too low and narrow for farther exploration (Iliffe, 2003). The final area is at Devil's Hole, on the southern corner of Harrington Sound where only a few primarily submerged caves are known. For this investigation, samples were taken from the latter three cave areas mentioned above.

1.6 Groundwater and Cave Hydrology

Bermuda lacks any surface fresh water lakes or rivers. All hydrological exchange between water bodies around the island is either through direct marine connections or is subterranean. Water column profiles in Bermudian cave pools are similar to most external anchialine pools and ponds. At the surface, atmospheric precipitation contributes to a surface layer of brackish water (0-25 ppt salinity), which mixes with underlying saltwater (Martin, 2011). Between salt and brackish/fresh water, there is a halocline of variable thickness (Iliffe and Kornicker, 2009). The thickness depends on the size of the island and rock permeability. Interfacial regions, such as the halocline, can also drive mixing corrosion (Martin, 2011).

Differences in hydraulic head, temperature and density drive subsurface water flow in conduits and within the rock matrix (Whitaker and Smart, 1990). In the case of Bermuda, the primary driving force of subsurface flow is oceanic tides, as indicated by

the semi-diurnal reversal in flow direction observed in caves (Whitaker and Smart, 1997). As tides generate flow, bottom friction retards it, causing lag times and reducing the amplitude of the hydraulic head, i.e., the measure of depth and pressure at a specific point (Whitaker and Smart, 1990). Open conduits create paths of preferential flow during tidal exchange. This preferential flow results in smaller lag times and greater tidal ranges for conduits than for the surrounding matrix (Martin, 2011). Head differences between the ocean, conduits, and matrix porosity may establish gradients that facilitate exchange between conduits and matrix (Martin, 2011).

Flow rate and direction through a matrix are dictated by the density of the sediment the water passes through. For highly permeable sediment, flow tends to move horizontally through the island. For sediment with low permeability, flow tends to move vertically from below the island (Ritzi et al. 2001). Porosity for eogenetic carbonates, such as those in Bermuda, are commonly 30% or higher (Mylroie and Mylroie, 2011).

Above the marine layer and halocline, most islands have a fresh water lens. Lens thickness is highly influenced by the porosity of local sediment. The sediment in Bermuda is laterally partitioned into sectors of different ages. Areas of low density and high conductivity act as a drain, quickly partitioning off excess water horizontally with little vertical mixing. Areas of high density and low conductivity act as dams collecting the excess water from areas of high permeability and allowing for far more vertical mixing and a thicker lens (Fig. 1.5) (Vacher and Wallis, 1992; Ritzi et al., 2001).

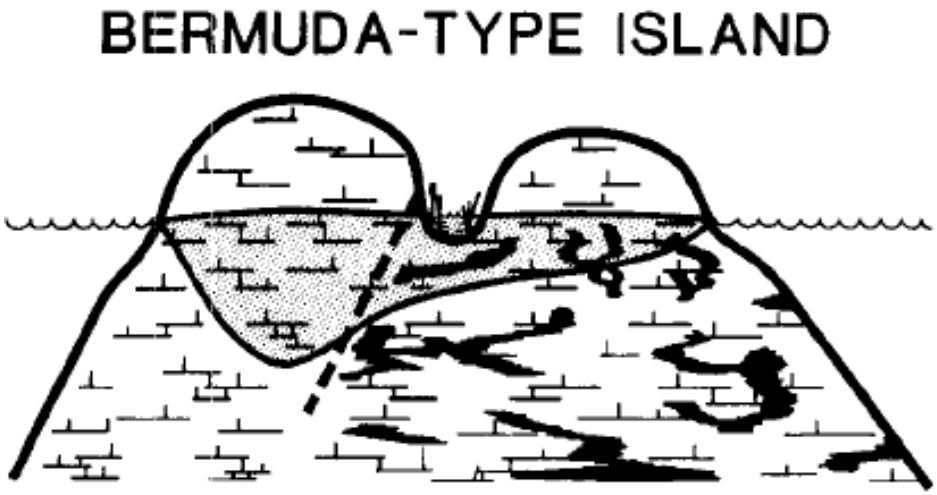

Fig. 1.5. Development of a fresh water lens on Bermuda type islands. These islands have variable sediment porosity. Image from Vacher and Wallis (1992).

The lens margin thins as the fresh water lens approaches the coastal discharge zone. As a result, the discharging water is forced through smaller cross sectional areas and discharge velocities increase near the shore. At this point, flack margin caves can quickly develop (Mylroie and Mylroie 2011). As water moves shoreward, saturation of unstable minerals such as aragonite can drive precipitation of more stable minerals such as calcite onto rock faces reducing permeability. Dissolution of rock results when the recharged water is under saturated (Martin, 2011).

1.7 Endemic Cave Biology

While the dry portions of Bermuda's caves are more readily accessible, it is the marine portions of these caves that support the richest biological diversity. Anchialine habitats require a mixed salinity water body as well as some kind of containment

structure (Mylroie and Mylroie 2011). The anchialine caves around Bermuda are home to a great variety of cave adapted life forms such as *Typhlatya iliffei* (Fig. 1.6). There have been over 250 identified species discovered in Bermudian caves (Oldfield, 1999) with at least 78 of those being endemic species including two new orders, one new family, and 15 new genera (Iliffe, 2004). Many of these animals are restricted to areas as small as a single cave. Limited habitat range and declining environmental quality has led to most cave fauna becoming classified as endangered (Glasspool, 2003). While the marine fauna and flora of Bermuda has direct connections with the Caribbean through the Gulf Stream, its cave fauna is considerably more isolated (Iliffe, 1983). The isolation of Bermudian caves have resulted in the majority of species being endemic to the island (Iliffe, 1983), an impressive value compared to the 2% endemic rate for littoral species (Manning et al., 1986). Due to the small size and vulnerability to disturbance faced by their habitats, 25 of these species have already been classified as critically endangered on the IUCN Red List (Iliffe et al., 2011). The survival of these species is directly linked to the environmental health of the caves in Bermuda.

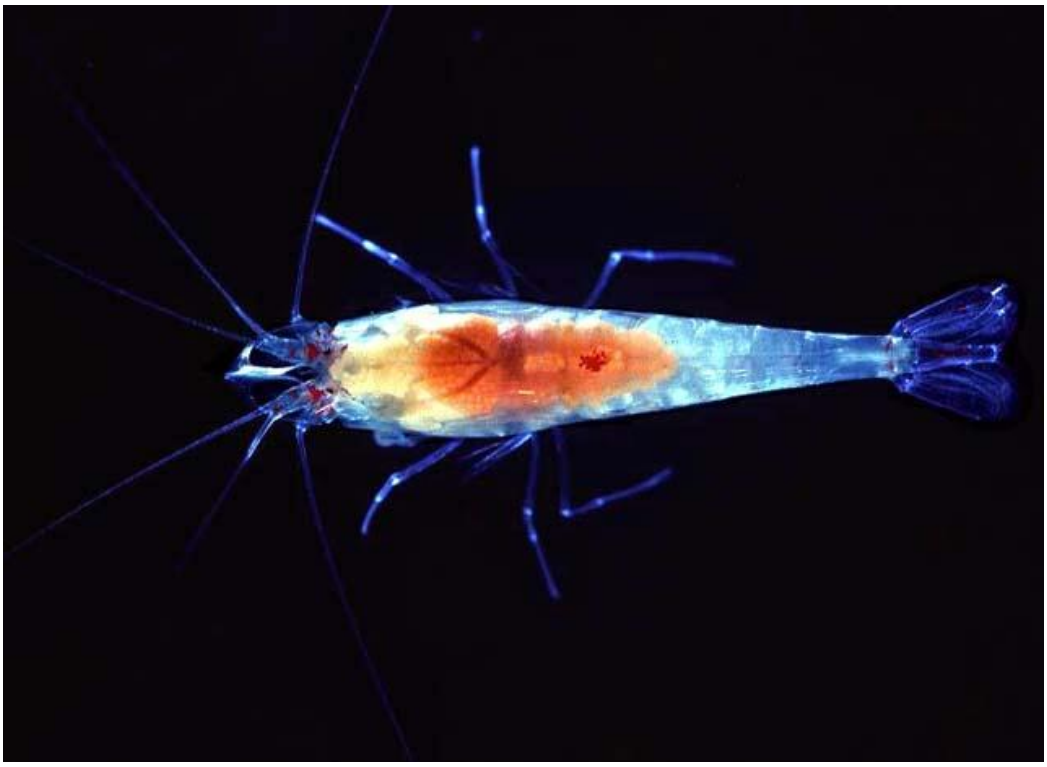

Fig. 1.6. *Typhlatya iliffei* Hart & Manning (1981) Discovered in Tucker's Town Cave, Bermuda. Image from CaveBiology.com

Pollution resulting from the use of unlined landfills, dumping of wastes into caves, deep well injection, and cesspit seepages can produce anoxic conditions in the groundwater. With so little understanding of the local cave hydrology, it is difficult to predict how pollution at one site may spread. Iliffe et al. (1984) conducted a study on Government Quarry Cave after a large amount of debris had been dumped into the cave. No life was observed at the cave entrances closest to the dump site. Biological Oxygen Demand (BOD) in the top 10 m of the water column in Government Quarry Cave was 10-60 times higher than in nearby and unpolluted Church Cave. This is believed to result from organic matter released from the debris. This study suggests that pollutants are

most likely to be transported to adjacent caves. In the years prior to 1995, a similar event occurred in Bassett's Cave when the United States Navy used it as a cesspit for disposal of raw sewage and fuel oil (Iliffe, 2004). Once the conditions governing an ecosystem have been altered, returning them to a productive state can be a long, difficult, expensive and sometimes impossible task (Gunderson and Holling, 2002).

1.8 Bermuda Cave and Karst Information System (BeCKIS)

In 1997, the Bermuda Aquarium, Museum and Zoo created the Bermuda Biodiversity Project (BBP) to gather environmental data from projects such as this one. BBP data includes terrestrial and marine inventories as well as aerial photographs**.** A component database, the Bermuda Cave and Karst Information System (BeCKIS), contains the data gathered during this study. BeCKIS allows for a variety of data sources, including cave maps, species distribution, hydrographic parameters, etc., to be integrated and visualized through the creation of maps for decision makers.

1.9 Thesis Research

Recent investigations in Bermuda have produced a wealth of knowledge about cave hydrology on the island. Previous hydrological studies have been short term, with supplementary data used to support other studies. In this research, cave hydrology has taken center stage and long term data (up to 2.5 months) have been collected from seven sites. Shorter two day profiles have been taken from 33 additional sites. Results from

this investigation have broadened understanding of local hydrology in Bermuda and how subterranean habitats exchange with open water.

1.10 Objectives

The goal of this research was to support the recovery plan for Bermuda's critically endangered cave fauna as well as investigate the questions first raised by Morris et al. (1977). The specific objectives of this study were to:

i. Choose suitable sites to collect water quality, current velocity, and tidal lag and range data.
ii. Collect short term water quality profile and tidal data from at least 75 sites.
iii. Gather longer term tide and current data in Red Bay, Green Bay, Walsingham East, Castle Grotto, Burchall's Cove and Leamington Caves.
iv. Compare the lag time and tidal range data collected over 48 hours from my 2011 study to similar data taken by Thomas Iliffe in 1980.
v. Use six week tidal and current data, as well as historical data, to create a water exchange budget for Harrington Sound.
vi. Use six week tidal and current data with historical tidal records to create a model capable of describing current and tidal behavior in caves as a function of tidal fluctuations in the ocean and Harrington Sound.

1.11 Statement of Hypotheses

Upon collection and analysis of data, the following null hypotheses were tested regarding tidal behavior:

- Ho: Water levels and currents in Bermudian caves are random.
- Ho: Water quality in cave pools across Bermuda is uniform.
- Ho: Tidal flow out of a Bermudian cave is always equal to the tidal flow into the cave.
- Ho: Directional cave flow does not stop and reverse the moment tidal heights in the ocean and Harrington Sound equalize.

CHAPTER II

WATER QUALITY PROFILES IN BERMUDIAN CAVES

2.1 Introduction

Profiles of water quality properties have been taken in Bermudian caverns as part of numerous past investigations. Profiles of salinity and temperature for the top meter of 36 anchialine pools were reported by Iliffe (1980). The daily monitoring of salinity and temperature over a 13 month period was described from the top meter of the water column in Walsingham and Crystal Caves (Iliffe, 2000). An investigation into the effects of large scale trash dumping into the pool of Government Quarry Cave showed evidence of contamination in nearby cave systems, including increases in nitrite, ammonia, phosphate and trace metals (Iliffe et al., 1984). Other investigations include those by Thomas et al. (1991), Gibbons (2003), and Maloney (2008).

The majority of the Bermuda's cave systems contain anchialine pools, having water with fresh to brackish salinity overlying fully marine water salinity (~37 ppt). The salinity of the surface layer decreases with distance from the coast. For caves with high exchange, salinity at 1m is typically around 34-35 ppt. More stagnant caves only reach salinities of 20 ppt at 1 m (Iliffe, 2009).

Salinity profiles of open inland ponds can be used to infer the types of connection sites have to the ocean. Higher salinity reflects greater exchange with coastal water. Sites close to the ocean can flush out fresh water inputs more readily, resulting in

minor stratification in salinity profiles. More remote locations have greater accumulation of fresh water (even with extensive flushing), resulting in a greater salinity stratification (Thomas et al., 1991).

The salinity and thickness of the brackish layer in caves can also be influenced by meteorological and geomorphological events such as storms, heavy rainfall, and the porosity of the limestone (Sket & Iliffe, 1980; Mylroie et al., 1995). Cave systems connect to the surface via percolation through the soil, and direct runoff into entrances throughout the island (von Bodungen, 1982). Tidal fluctuations show that Bermuda's caves also exchange water with the ocean, although most do not have passable connections (Iliffe, 2003).

Sheltering from external influences helps to maintain a more constant year round temperature in caves (Iliffe et al., 1983). Like salinity, temperature increases with depth below the surface in cave systems remote from the sea shore, possibly due to geothermal heating (Iliffe et al., 1983). Caves that have large water exchange rates with Castle Harbour have similar temperature profiles to that of the surrounding ocean. Temperatures for coastal water off Bermuda typically range from 17 to 29ºC (Morris et al., 1977). Inland cave temperatures range between 20-20.5ºC at the surface and about 22.2ºC at depth (~20m) year-round (Ford and Williams, 1989).

The pH of Bermuda's inshore water (including the coastal waters of Castle Harbour) is around 8.1 (BIOS, 2009). In caves, pH usually increases with salinity, with a pH minimum typically reached at the halocline (Iliffe, 2000). This may result from an accumulation of organic matter and its subsequent oxidation by microorganisms (Iliffe

and Kornicker, 2009). Fully marine portions of Bermudian caves (portions beneath the halocline) have a pH of around 7.68 (Iliffe, 2000).

Surface waters in caves have dissolved oxygen (DO) levels close to saturation (>90%) since air exchange and dripping water maintain the oxygen equilibrium (Iliffe, 1984). However, DO concentrations drop sharply with depth as biological oxygen consumption reaches a maximum near the halocline (Pohlman, 2011). As with the pH minimum, this is likely due to the trapping and oxidation of particulate material there. Below the halocline, DO remains low (Iliffe, 1984). Deep cave water have DO levels as low as 55% (< 3.75 mg O_2/liter), well below surface oceanic conditions (Iliffe, 2000).

2.2 Methods

Bermuda's anchaline pools (Fig. 1.3) were surveyed during a six week field study from July to August 2010. Caves were located using GPS coordinates recorded by Iliffe and with aid from local experts who had visited the sites before. One of the main goals of this research was to look at water exchange between cave systems, the ocean and Harrington Sound. This is why caves selected for study were chosen based on proximity to, and interconnectedness with, other sites of interest. Water profile measurements included five environmental parameters: pH, DO, temperature, salinity and water density (density was determined through calculation).

We were unable to collect from each cave initially chosen during this project. Some caves were never surveyed because the difficulty associated in accessing them.

Others were not surveyed due to time restraints. I was able to collect profile data from 73 sites.

2.2.1 Instruments

The YSI 600 XLM Multiparameter Water Quality Monitor (Fig 2.1) was used in conjunction with Eco-Watch Windows software to measure and analyze salinity, pH, temperature, dissolved oxygen, and depth as frequently as once every four seconds.

Fig. 2.1. YSI 600 XLM Multiparameter Water Quality Monitor.

2.2.2 Cave Surveys

Profile data were taken at each cave pool with the YSI 600 XLM Multiparameter Water Quality Monitor. The device was programmed to take readings at a rate of one reading every four seconds using the Eco-Watch software. At each site, the YSI 600 XLM was lowered at a rate of about 1.5 cm/s into the deepest accessible point in the cave pool (>1 m) until it approached the bottom (Fig. 2.1). Cave pool depths ranged from 1 to 10 meters. All profiles were at least 1 meter deep, but deeper profiles were taken when possible.

Water typically flows into coastal caves during a rising tide and out during a falling tide. The reverse is true for caves opening into Harrington Sound because the systems lag put it out of sync with the ocean. For cave pools in proximity to either the ocean or Harrington Sound, readings were taken during their respective tidal outflows, so that the data represented cave water.

After a day of data collection, consisting of readings from 8-10 caves, the data were downloaded to a laptop using Eco-Watch software, examined and graphed. After returning to Texas A&M, the profile data were displayed spatially using Arch GIS v9.1.

Fig. 2.2. Jonathan Stoffer conducting a water quality survey in Admirals Cave.

2.3 Results

The majority of the sites were within the Walsingham Tract. The most common pattern exhibited in profile graphs was an increase in temperature and salinity and a decline in pH and DO with depth. However, many sites did not follow this trend (Table 2.1).

Temperature profiles were relatively consistent in shape for the top meter of water at each site, but diverse in range from cave to cave. Temperature values ranged from 20.7 to 28.7°C, with higher temperature values found at sites with stronger connections to the ocean (Table 2.1). Oceanic surface temperatures ranged from 26.7 to 30.6°C during the time of this investigation (BF&M, 2010). Profiles for caves with no sun exposure usually had temperature increasing with depth (75% of 28 sites) (Fig. 2.2).

Most caves with sun exposure showed a decrease in temperature with depth (70% of 20 sites) (Fig. 2.3). Performing a statistical two-proportion Z-test (α=0.05) on caves with and without sunlight exposure produced a p-value of 0.0019. Exposure to sunlight does appear to have a significant influence on the top meter of the temperature profile.

Table 2.1. Water quality parameters. Given for sampled caves at the surface (Left Columns) and about one meter (Right Columns) or deepest accessible depths.

Location	Temperature	Salinity	pH	DO	Exact Depth	Temperature	Salinity	pH	DO
Admirals S. 1	20.75	1.75	7.64	8.86	0.518	20.93	18.94	6.71	2.02
Admirals S. 2	21.1	1.56	7.81	8.74	1.074	21.18	28.32	6.72	1.6
Admirals S. 3	21.14	3.34	8.04	8.71	1.008	21.19	27.69	6.74	.9
Admirals N. 4	20.37	20.71	7.5	7.95	1.017	20.68	26.61	7.39	7.07
Admirals N. 5	20.28	18.99	7.63	8.04	1.01	20.74	26.81	7.45	6.77
Chalk	21.84	23.81	7.43	5.9	1.011	22.37	28.73	7.19	4.9
Devils Hole	25.75	34.11	7.27	6.1	1.021	25.62	34.27	7.22	4.22
Grenadier	28.18	19.77	7.95	7.21	0.905	25.78	32.06	7.08	4.8
Whisky	24.77	26.78	----	----	0.967	25.2	31.08	----	----
Causeway	26.97	35.85	----	----	1.024	27.76	36.47	----	----
Castle Grotto	26.47	36.09	----	----	1.019	25.7	36.35	----	----
Blue Grotto	28.56	36.54	----	----	0.899	28.4	36.55	----	----
Bath Tub	28.38	36.68	----	----	0.832	28.4	36.54	----	----
Calabash	28.35	36.91	----	----	0.886	28.2	36.54	----	----
Harbour Pool	27.25	36.55	----	----	0.944	27.03	36.38	----	----
Walsingham Cave	27.67	36.38	----	----	1.024	27.49	36.47	----	----
Dead Horse	22.29	31.94	7.3	7.44	1.043	22.44	34.55	6.57	6.9
LeaningTower	28.64	37.18	7.65	5.9	0.998	27.87	37.43	7.57	5.68
Emerald	28.58	36.84	7.67	6.64	0.979	27.95	37.48	7.59	5.65
Leamington 1	26.77	35.32	7.59	6.14	0.668	27.94	37.16	7.58	5.04
Leamington 2	28.01	36.42	7.62	5.99	1.032	28.1	37.25	7.62	4.94
Leamington 3	27.42	33.26	7.74	6.2	0.995	28.65	37.47	7.78	5.11
Palm	29.49	37.68	7.68	8.15	1.024	29.49	37.78	7.93	7.73
Walsingham Sink	24.05	32.05	7.63	9.15	0.814	26.06	37.26	7.63	6.51
Cherry Pit	27.38	37.67	7.54	8.59	0.983	26.94	37.58	7.53	6.24
Angel	27.57	37.39	7.62	8.47	0.98	27.4	37.6	7.6	6.96

Table 2.1. Continued.

Small Crack	28.31	37.67	7.6	6.55	---------	----------	----------	----	----
Double South	29.44	37.92	7.89	9.44	0.889	29.45	37.96	7.66	13.44
Double North	29.33	37.65	7.93	9.51	1.01	29.11	37.79	7.78	11.69
Vine first	26.55	37.5	7.51	7.57	1.01	26.43	37.57	7.52	5.57
Vine mid	26.26	37.57	7.6	8.25	0.974	26.29	37.54	7.59	5.53
Vine back	26.69	37.6	7.59	7.55	1.044	26.69	37.58	7.6	5.58
Deep Blue	25.28	37.52	7.54	8.05	0.988	25.06	37.4	7.52	5.68
Cow	27.47	37.65	7.64	7.94	1.023	26.84	37.56	7.6	6.93
Walsingham Pond	29.85	37.78	7.63	7.49	0.995	29.67	37.76	7.61	7.23
Straw Market left	28.5	37.69	7.75	7.35	0.958	28.51	37.67	7.75	7.03
Straw Market right	27.86	37.72	7.73	7.49	0.975	27.95	37.65	7.73	6.34
Shrimp	25.82	37.59	7.33	7.22	0.99	25.49	37.55	7.31	5.83
Water Bottle	29.26	37.75	7.56	6.51	0.982	29.26	37.76	7.56	5.86
Coral	28.48	36.82	7.54	7.68	1.015	28.67	37.09	7.65	7.04
Walsingham Lodge	28.2	37.78	7.6	8.48	0.99	28.48	37.73	7.66	6.65
Fern	21.16	23.35	7.4	7.83	0.883	21.59	28.71	6.92	7.11
Road Side	23.32	32.89	7.37	6.88	0.972	25.48	34.83	7.35	5.58
Valley	26.45	30.19	7.6	6.78	0.702	26.91	36.57	7.58	4.76
Olive Wood	23.78	28.49	7.45	7.17	---------	----------	----------	----	-----
Bee Pit	25.64	35.49	7.49	6.57	0.973	25.1	36.87	7.51	4.28
Davis Pond	27.53	35.57	7.22	6.03	0.82	27.75	36.85	7.44	6.95
Park Pond	26.56	36.75	7.14	5.01	0.367	26.03	37.11	7.12	2.21
Park Puddle	27.09	6.03	7.05	3.15	---------	----------	----------	----	----
Crystal	21.41	33.75	7.58	7.21	0.975	21.49	26.47	7.3	6.65
Fantasy	21.88	18.44	7.4	5.91	0.99	21.68	24.64	7.25	5.78
Grotto Sign	24.15	6.85	7.56	5.88	1.049	23.02	26.54	7.13	2.5
Island	26.08	33.49	7.62	4.79	1.051	27.48	36.74	7.76	4.2
Cathedral	24.27	27.87	7.53	5.04	0.99	25.32	30.68	7.58	4.22

Presence of a subsurface temperature maxima was a fairly common occurrence in pools with sun exposure (Fig. 2.3). Sun exposed pools which also had a subsurface maxima included: Devils Hole, Grenadier, Blue Grotto, Calabash Sink, Double South

and Walsingham Pond. Partially exposed, yet heavily shaded caves with similar behavior include: Walsingham Sink, Causeway and Whiskey.

Warmer profiles were observed at sites in the Walsingham Tract and surface exposed sites such as Walsingham Pond (Table 2.1). The coldest sites included Chalk, Church and Christies Caves as well as sites near Grotto Bay, north of the Walsingham Tract (Table 2.1).

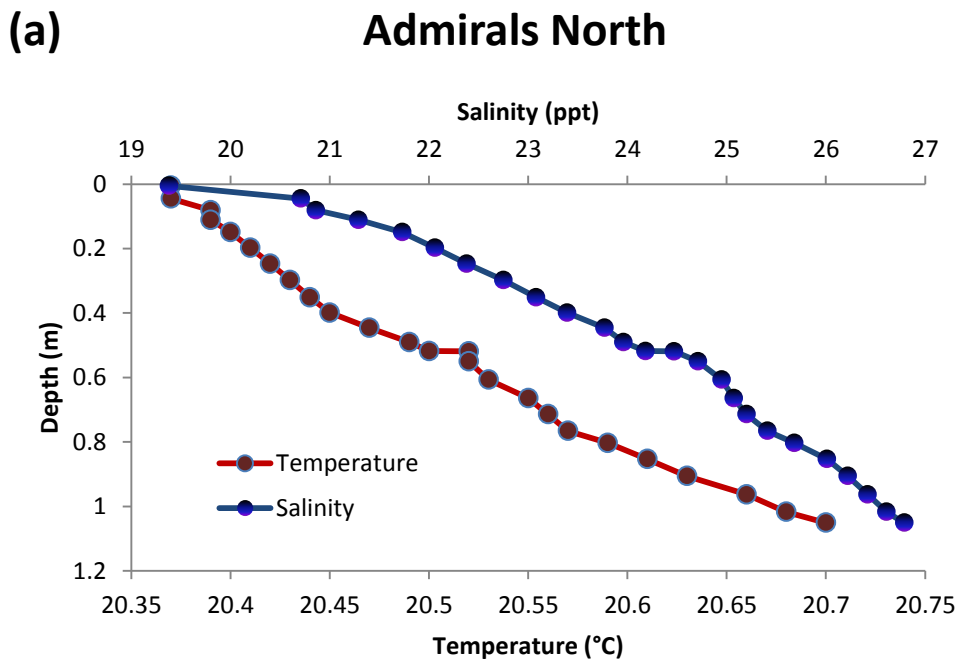

Fig. 2.3. Temperature profiles for two cave pools. (a) No sun exposure (Admirals North): A steady increase in temperature with depth is typical of most pools without sun exposure. (b) Sun exposed (Grenadier Pool): These sites tended to have warmer surface waters.

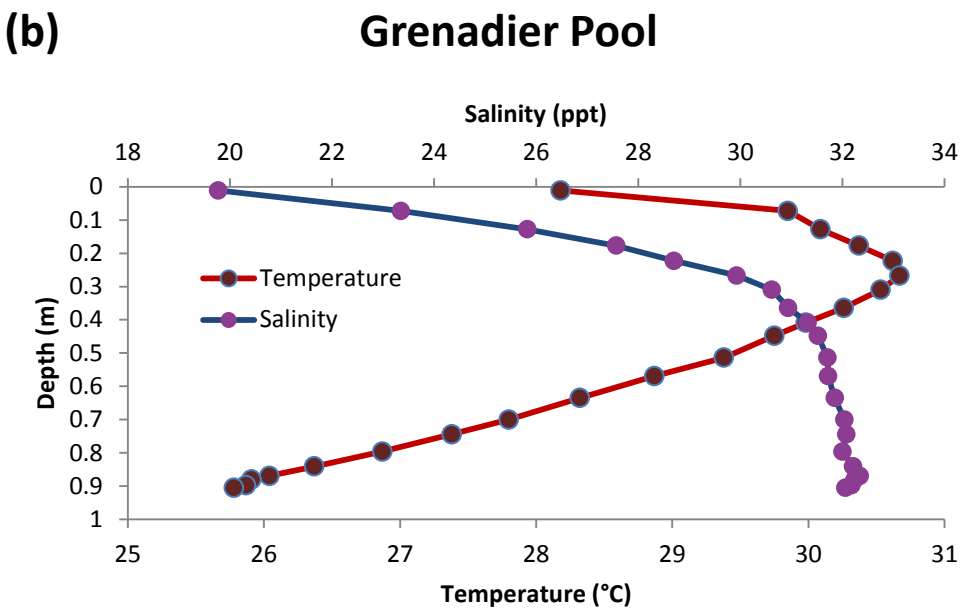

Fig. 2.3. Continued

Salinity profile values ranged from 7 to 37 ppt with salinity increasing with depth (Fig. 2.3). Higher salinities (34-37 ppt) were found in the isthmus between Castle Harbour and Harrington Sound (Fig. 2.4). Lower salinities (7-28 ppt) were found in sites near Grotto Bay (Fig. 2.3).

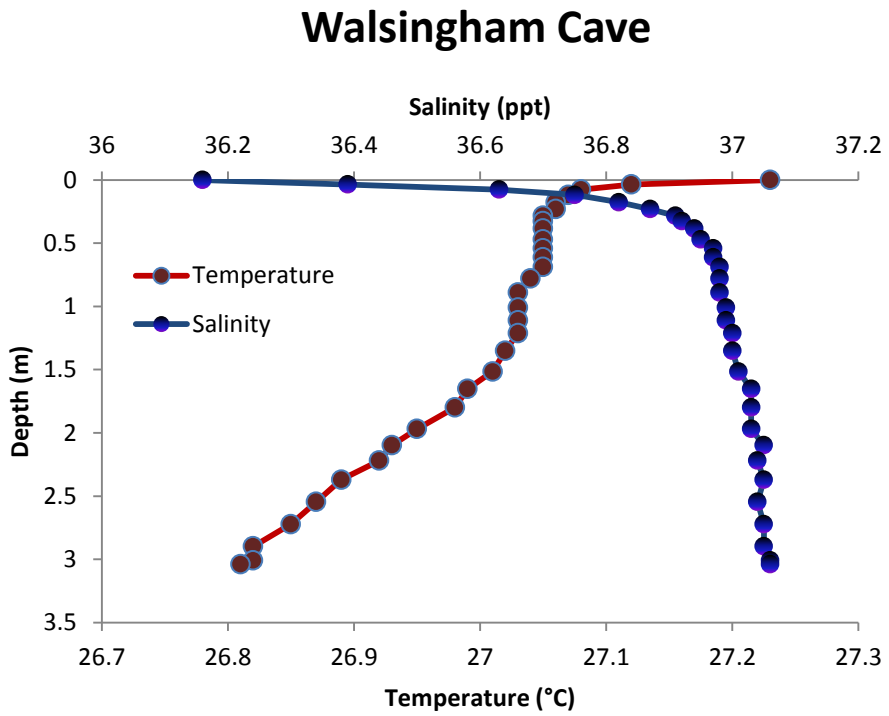

Fig. 2.4. Salinity profile for Walsingham Cave. At sites like this one, water was close to marine salinities even at the surface.

For most sites, surface DO values were 6-7 mg O_2/l and had a steady decline to about 5-6 mg O_2/l at roughly 1 meter depth (Fig. 2.5). Sites that differed from this pattern, such as Walsingham, Angel, Grenadier and Double Ponds, tended to have exposure to sun light and the presence of algae. With the exception of Double Pond, these sites also had a decrease in DO with depth. However, their decreases were much more irregular. DO values for Double Pond North and South reached super saturated levels, ranging from 9 to 13 mg O_2/l with DO maxima reached below the surface (Fig. 2.5).

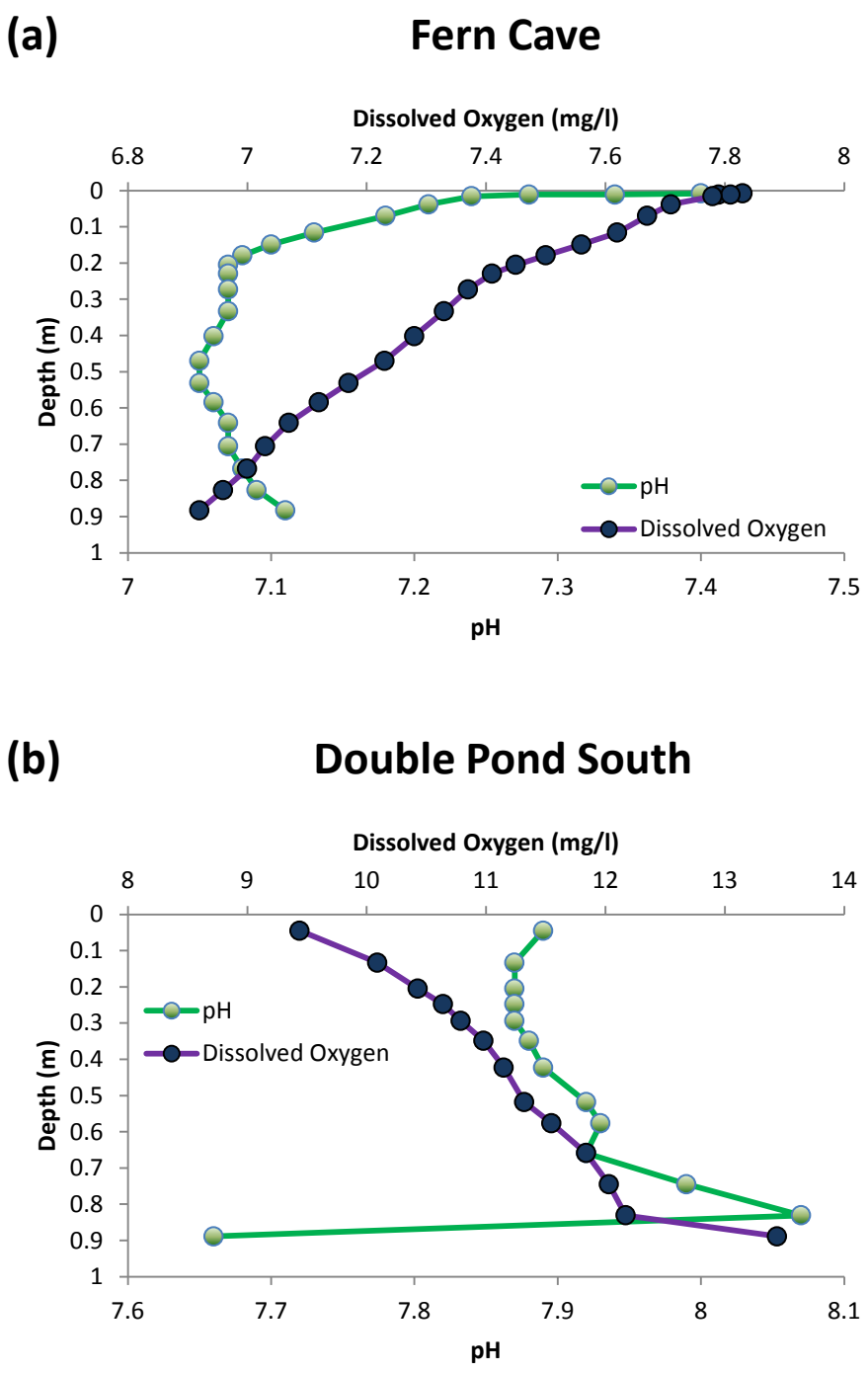

Fig. 2.5. DO profile for Fern Cave and Double Pond.(a) The steady decline in dissolved oxygen with depth recorded at Fern Cave is representative of the readings found at most pools surveyed. (b) Some sun exposed sites such as Double Pond South showed an increase in DO with depth.

Values for pH mirrored DO concentrations in many sites. Surface and one meter DO and pH data were compiled for all sites. The correlation between the two came out to R^2=0.399 (pH = 0.4381ln (DO) + 6.7077). Thus, it would be a mistake to assume that DO levels direct pH readings in any way. However, salinity can have an influence on both pH and DO, so some of my readings may reflect variation in salinity. Correlation for salinity vs pH and DO came to R^2=0.016 and R^2=0.004 respectively.

Typical surface pH values were around 7 to 7.7 with only minor variation and usually staying within that same range as the sensors moved to one meter depth (Fig. 2.5). The only sites to break from this pattern were the three polluted sample sites located at the southern end of Admirals Cave. In all three sites, pH values at the surface were around 7.8 and then dropped to about 6.7 at one meter depths (Fig. 2.6). These pH values were slightly above normal for Bermudian caves. This is likely due to calibration issues. After entering the field, I discovered that I had no additional calibration fluid. So all calibrations made during this study were based on an approximation using distilled water. The pH values in this research should not be compared to other studies, but can still be useful by comparing pH level between sites within this study.

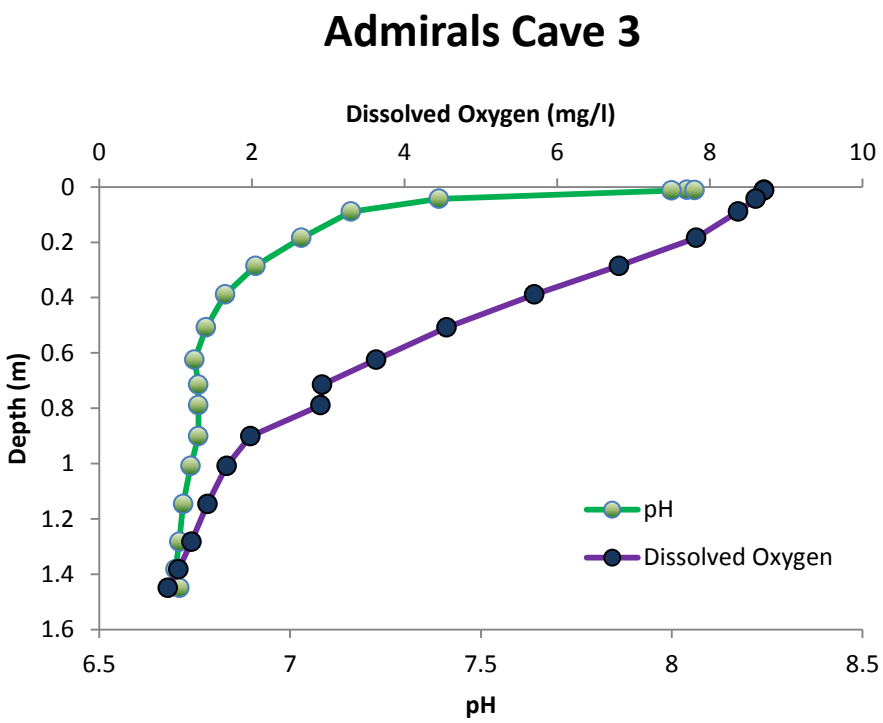

Fig. 2.6. The pH profile for a southern pool in Admirals Cave. All three sites on the south side of Admirals Cave showed a large drop in pH and DO over the top meter of water.

2.4 Discussion

Salinity increased and DO decreased with depth at most sites. The increase in salinity is a reflection of denser marine water sitting beneath a lens of brackish water (Iliffe, 2000). DO levels are highest near the surface due to air exchange and drip waters maintaining the oxygen supply (Iliffe, 1984). Sites that broke from the pattern of steadily declining DO had sun exposure and algae growing on their sediment, allowing for photosynthesis to produce additional oxygen below the surface. Fluctuations in pH and temperature were usually minor in the top meter of water. This observation is consistent

with the expectation that temperature profiles in the top meter of water rarely fluctuate more than one degree for most of the year (Iliffe, 2000). Sites with sun light were exposed to constant daytime heating. Less exposed caves were cooler near the surface, but became warmer with depth. This could result from geothermal heating (Iliffe et al., 1983). The hypothesis that water quality in Bermuda's caves would be uniform is not supported by these results.

2.4.1. GIS

Water property distributions allow us to distinguish between groups of caves through observation and statistical comparison of variation in water parameters. The first group includes sites near Grotto Bay and extends down the Walsingham System as far as Dead Horse Cave. The second group includes the remaining sites south of Grotto Bay, in the isthmus between Harrington Sound and Castle Harbour. Sites in the isthmus had temperatures ranging from 24 to 28°C. Temperatures at sites near Grotto Bay ranged from 20 to 22°C (Fig. 2.7). A similar spatial pattern is apparent for the distribution of both salinity and pH values. Salinity readings show that water around the isthmus is more saline, with values ranging from 34 to 37 ppt.

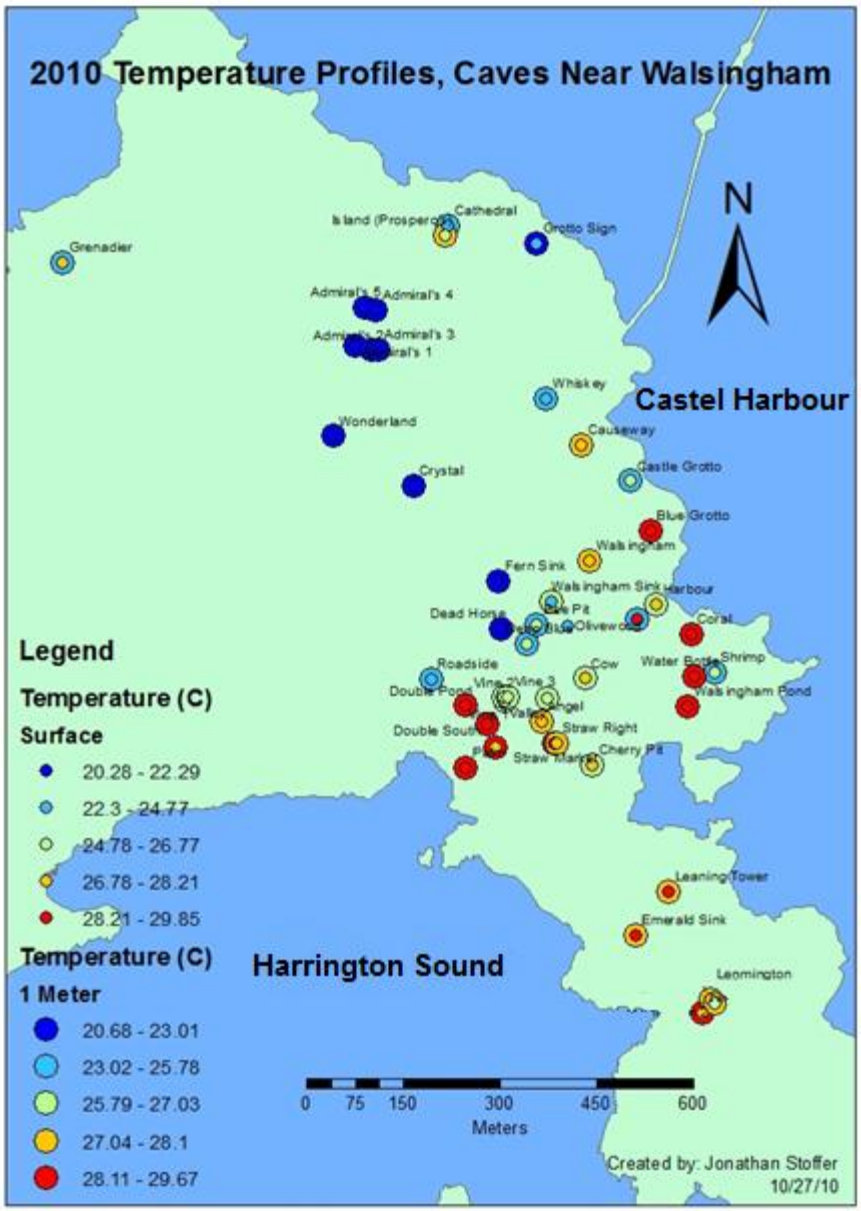

Fig. 2.7. Temperature profiles of the top meter of water in the Walsingham Tract.

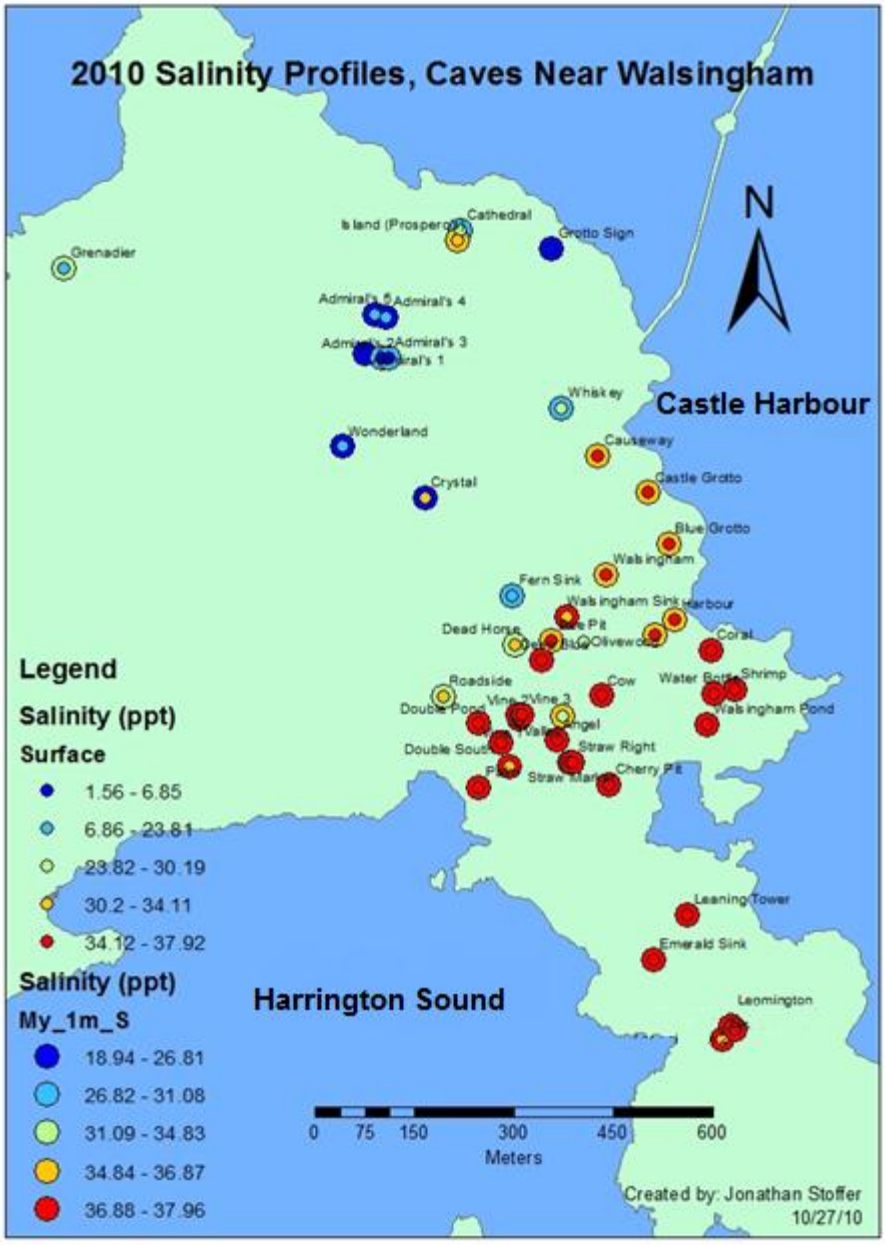

Fig. 2.8. Salinity profiles of the top meter of water in the Walsingham Tract.

The waters around Grotto Bay were fresher and had salinities ranging from 6 to 28 ppt (Fig. 2.8). The pH values in the isthmus were slightly basic and ranged from 7.4

to 7.9. For pools around Grotto Bay, pH tended to be more acidic, ranging from 6.6 to 7.4 (Fig. 2.9).

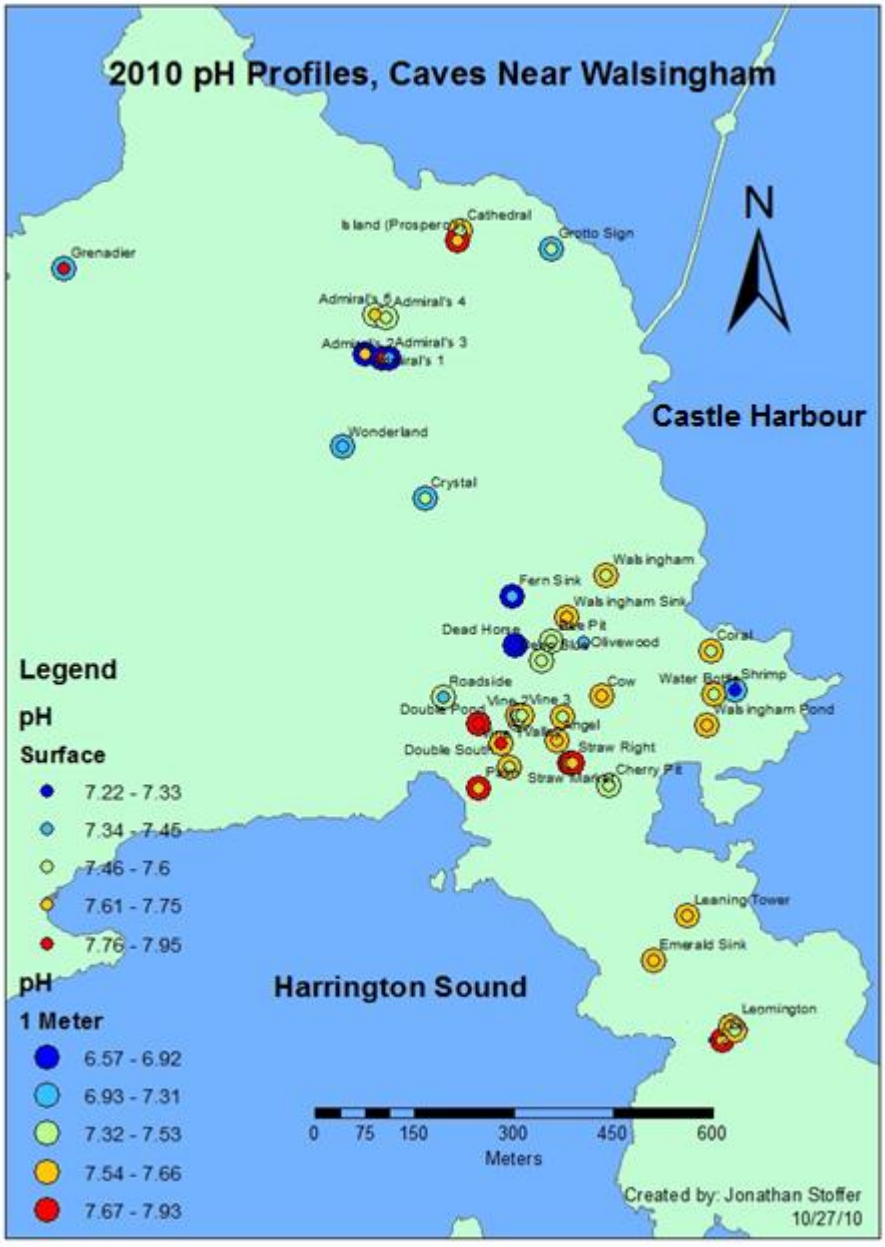

Fig. 2.9. pH profiles of the top meter of water in the Walsingham Tract.

A 2 sample t-test (α=.05) was performed on the temperature, salinity and pH values measured for these two regions to show statistical differences (Table 2.2). Potential bias in these tests could come from how the caves were grouped. To minimize bias, groups were separated with a straight line division. A line was drawn from just above Castle Grotto to just above Double Pond north. All caves north of this line were grouped with Grotto Bay and all caves south were grouped with Walsingham. Several other lines were drawn to slightly change distribution of the two groups, but these changes did not alter the significance in the t-test.

Table 2.2. Statistical results of a two sample t-test. Given for caves near Grotto Bay and Walsingham Park. Mean values are for all data. (α=.05)

	Mean ± St Dev (GB)	Mean ± St Dev (WP)	All data	Surface data	1 Meter data
df	-------	--------	51	19	19
Temperature	23.4 ± 2.3	27.4 ± 1.7	<.00001	<.00001	<.00001
Salinity	27.9 ± 6.7	36.5 ± 2.5	<.00001	<.00001	0.0006
pH	7.3 ± 3.4	7.6 ±.15	0.01	0.04	0.012

The inshore waters of Bermuda, including Castle Harbour, have summer salinity values around 36.9 ppt, temperatures of about 28°C, and a pH around 8.1 (BIOS, 2009). Harrington Sound values typically only differ from other inshore waters by about 1-2°C warmer, 0.05 pH units more acidic and 0.4 ppt fresher (Morris et al., 1977). The spatial patterns of water quality across all sites show that caves in the isthmus have water quality values closer to coastal waters. These caves probably exchange water between Harrington Sound and Castle Harbour more often and likely have shorter residence times

since their water properties are closer to typical coastal values in Bermuda. Conversely, caves near Grotto Bay likely have longer residence times with lower turnover rates, a thicker brackish layer and possibly deeper connections to the ocean, as evidenced by their water properties. This can be further displayed by overlaying temperature, salinity and pH profiles with partial transparency onto one map using the same color scheme (Fig. 2.10). In this fig., areas with lighter shading have water properties more similar to coastal levels while those with darker shading are less similar to coastal water

A simple explanation for this variation in water properties is the geology of Bermuda. The Walsingham region may be more karstic than the area around Grotto Bay. Caves in the isthmus are also much closer to a shoreline than caves in Grotto Bay. Fresh water inputs in Grotto Bay may have a longer residence time since they are further from the coast. Being pinched between Harrington Sound and Castle Harbour may lead to higher exchange rates. To test for a correlation between location and water quality in caves, temperature, salinity and pH were graphed against distance to the nearest shoreline. The strongest correlation was for temperature (R^2=0.43), followed by salinity (R^2=0.34), and finally pH (R^2=0.26).Dissolved oxygen concentrations had no spatial tendencies. Closely situated water bodies such as those in Admirals Cave had similar DO values, but there were no large scale tendencies over the entire area (Fig. 2.11).

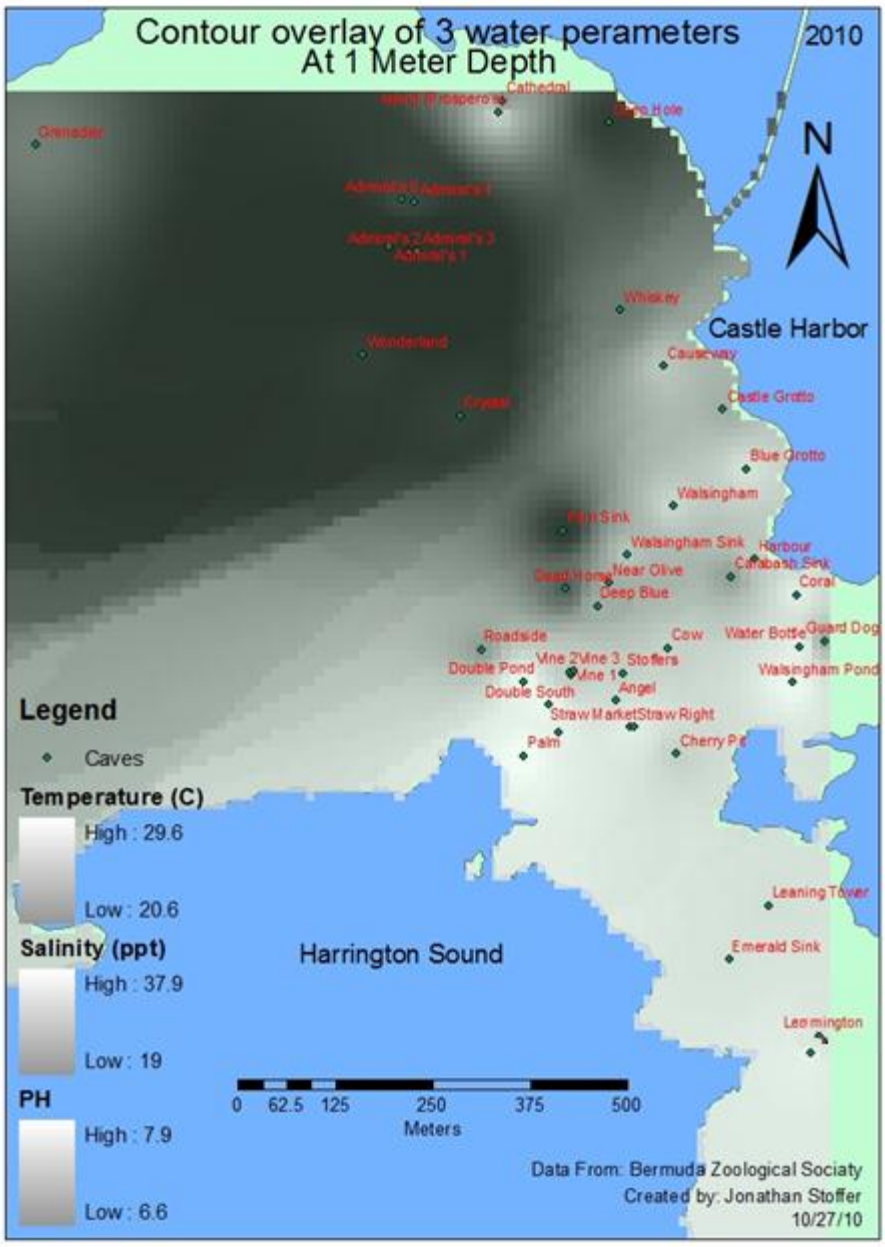

Fig. 2.10. Temperature, salinity and pH values measured at 1 meter depth. The transparencies have been overlaid onto a single map.

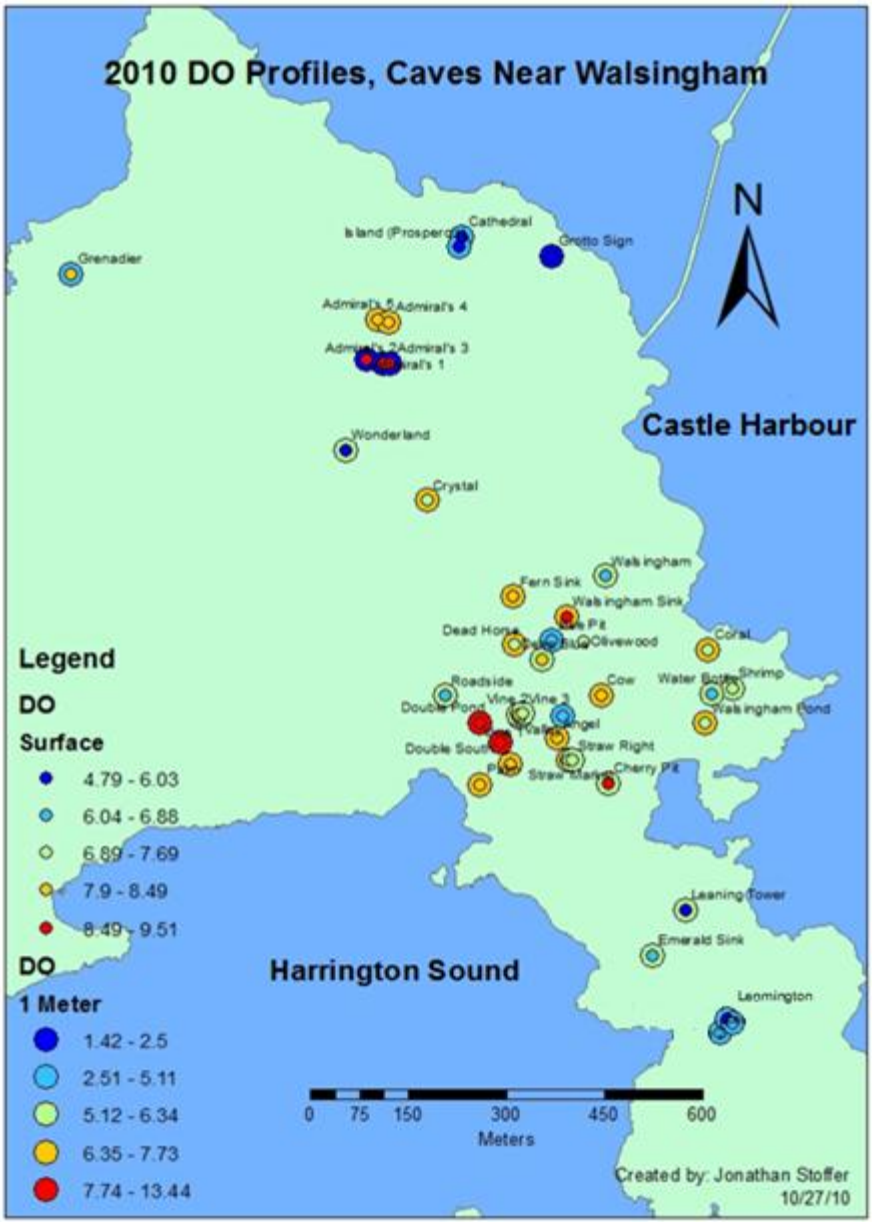

Fig. 2.11. Dissolved oxygen levels for surface waters of anchaline caves. Given for caves around the Walsingham Tract.

Within the Walsingham Cave System, there is a clear difference in water quality values for sites within the main flow path (Fig. 2.12). Starting with Wonderland Cave, locations on the northern side of the Walsingham System, outside of the main flow path, tend to have water quality similar to sites found in Grotto Bay. Warmer, saltier and more basic water is found at the southern end of the system, in the main flow path of Walsingham. The caves in the main flow path of Walsingham System were more similar to other caves in the isthmus.

Water quality samples in the Palm Cave System were more consistent, although the only caves in the system sampled were: Straw Market, Walsingham Lodge and Palm Cave. Temperature readings were relatively warm, ranging from 27.8 to 29.5°C. Salinity readings were also high, ranging from 37.68 to 37.78 ppt. The pH values ranged from 7.6 to 7.75 and DO from 7.35 to 8.48 mg/l. At 1 meter depth, the Palm caves only had minor fluctuations in their values; ±0.2°C, ± 0.1 ppt, ±0.25 pH and ±1 mg/l. Water quality values in the Palm System were closer to oceanic values than caves in the Walsingham System.

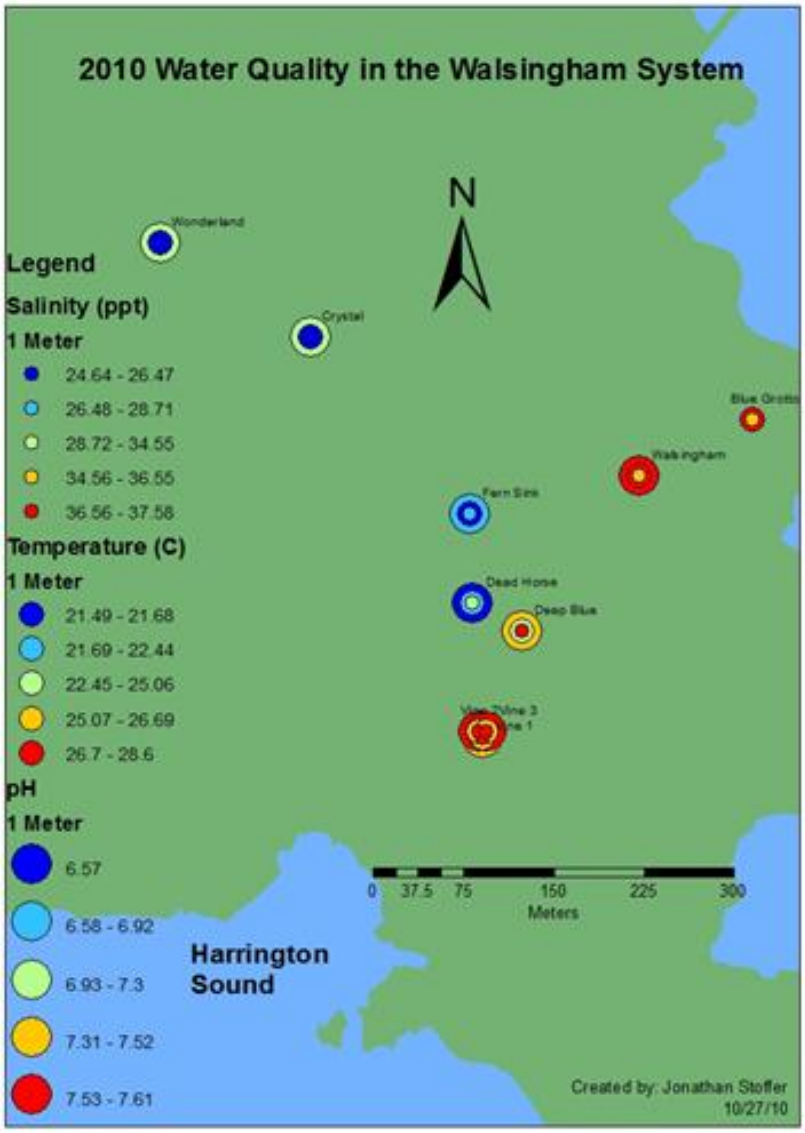

Fig. 2.12. Water quality in the Walsingham System. Caves in the main flow path of the cave have distinctly more marine water quality profiles.

There was also a distinct profile signature in the three sites at the southern end of Admirals Cave. All three sites had a large decrease in pH (7.6-8 to 6.7) and DO (8.7-8.8 to 1-2 mg O_2/l), and an increase in salinity (1.5-3.3 to 18-27 ppt) in the top meter of water. The water clarity in these three sites was cloudy despite being undisturbed and

there was a grayish to black precipitate in the zone just below the surface where hydrogen sulfide seemed to be present, as evidenced from the distinct sulfide smell that was absent from all other sites investigated. These data from the three pools at southern end of Admirals suggests the presence of large organic matter inputs into the cave, depleting the dissolved oxygen and producing hydrogen sulfide. Large amounts of organic matter in an anchailine environment can enhance biogeochemical activity that may deplete dissolved oxygen and lower the pH (Pohlman, 2011). As dissolved oxygen is consumed, alternative electron accepters, such as the sulfate (SO_4^{2-}) in sea water is used and converted into sulfide gas (H_2S) (Fairfield et al., 2009; Pohlman 2011). The staff quarters of a large hotel sits above parts of Admirals Cave and its cesspit may be this source of this additional organic input.

2.4.2. 1980 – 2010 Comparison

Our salinity and temperature data and those results collected by Iliffe in 1980 shows temperatures are lower around Grotto Bay (Fig. 2.13; Fig. 2.14). The caves surveyed in 2010 were generally warmer than in 1980, averaging 26°C. The average temperature in 1980 was 22.75°C. A two sample t-test (α=.05) revealed that the 2010 data was significantly warmer than the 1980 data (Table 2.3). This difference in temperature could reflect seasonal variation, since the 1980 survey was performed during the fall (October to November) and the 2010 survey was carried out in the summer (June to August). Bermuda's inshore waters reach their maximum temperature in August (Morris et al., 1977).

Both data sets show an increase in salinity south of Grotto Bay. However, the 2010 values were more saline than then those collected in 1980 (Table 2.3). A two sample t-test showed that this difference was significant (Table 2.3). The differences in salinity were primarily in caves south of Grotto Bay. The 2010 readings north of and including Crystal Cave had salinities which were not significantly different to the readings taken in 1980.

Table 2.3. A statistical comparison of temperature and salinity. Data taken in 1980 and 2010 (α=.05).

	2010 mean±sd	1980 mean±sd	df	p
Temperature (Surface)	25.95 ± 2.9	22.5 ± 1.6	57	<.00001
Temperature (1 Meter)	26.07 ± 2.78	23.49 ± 1.4	51	<.00001
Salinity (Surface)	31.08 ± 10.3	24.59 ± 9.8	72	0.006
Salinity (1 Meter)	34.22 ± 4.8	31.77 ± 5.2	71	0.038
Grotto Salinity (Surface)	20.31 ± 12.1	15.22 ± 8.2	19	0.24
Grotto Salinity (1 Meter)	28.9 ± 4.7	25.45 ± 3.6	20	0.059

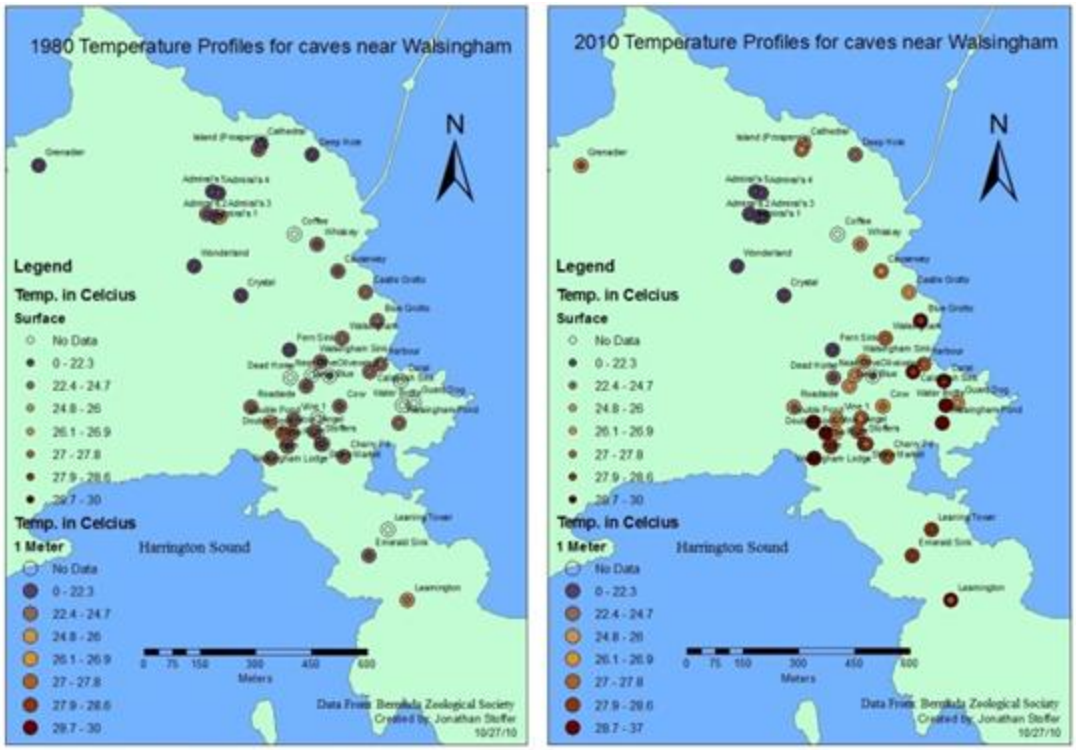

Fig. 2.13. Temperature levels for caves in the Walsingham Tract. (a): Data taken by Iliffe in 1980 (b): Data taken by J. Stoffer in 2010.

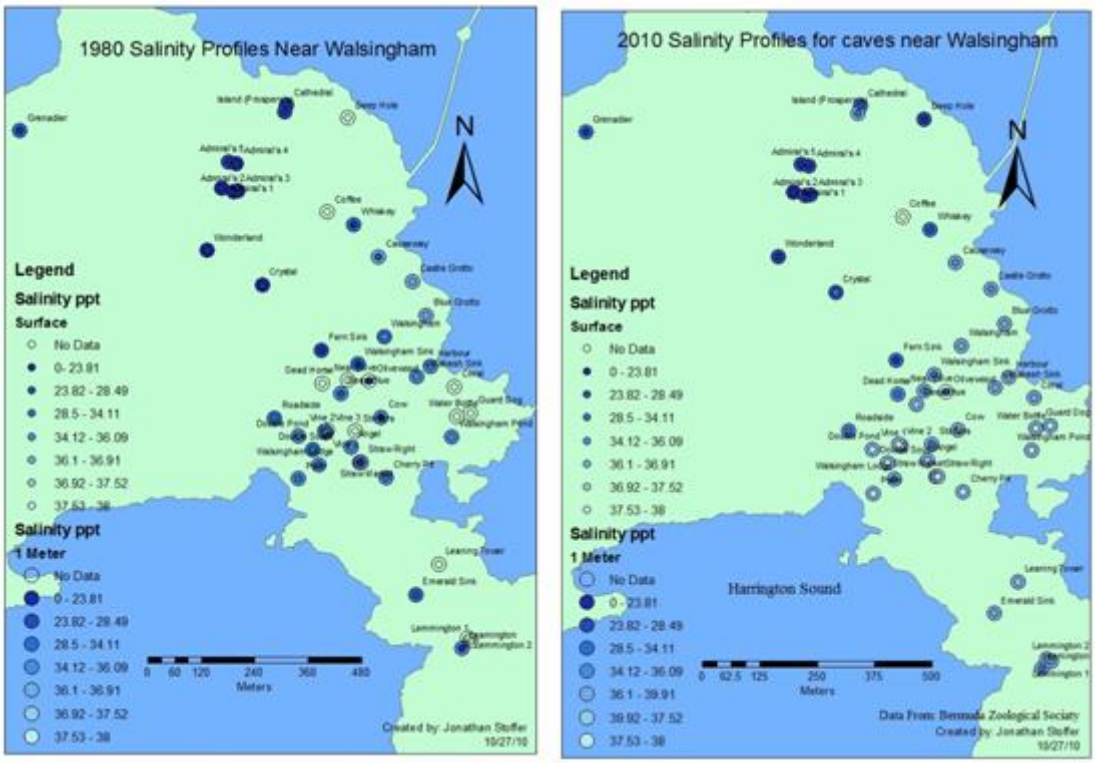

Fig. 2.14. Salinity levels for caves in the Walsingham Track. (a): Data taken by T. Iliffe in 1980 (b): Data taken by J. Stoffer in 2010

In Iliffe's (1980) survey, salinity levels in cave surface water never exceeded 35 ppt. However, in the 2010 survey, many caves south of Crystal Cave reached salinity levels close to 37 ppt (Fig. 2.14). The salinity and thickness of the brackish layer in caves are heavily influenced by meteorological and geomorphological events such as storms and rainfall (Sket & Iliffe 1980; Mylroie & Carew 1995). Prior to this investigation in April-June 2010, Bermuda was experiencing the driest three months in the last 50 years. During this period, 7.9 cm of rain fell. This is 20.7 cm below the average rainfall from April to June (Bermuda Weather Service, 2011). The dry spell would have also led to an increased use of reverse osmosis throughout the island since

the only other major source for drinking water in Bermuda is through roof top collection of precipitation (Gil Nolan personal communication). Reverse osmosis in Bermuda primarily uses water extracted from wells (Atlantic Water Development, 2012).

No freshwater inputs and constant pressure on the brackish layer by mixing, evaporation and the increased use of reverse osmosis may have led to the increased salinity readings in some parts of the island. Bermuda's three month dry spell finished at the end of July. That month had 13.6 cm of rain, with 8.3 cm falling in the last three days (Bermuda Weather Service, 2011). At that time, the Aqua Troll was deployed at Coral Cave, a coastal site which experiences a large outflow from caves during low tides. The impact of this precipitation can be seen on Coral Cave's salinity readings on 7/30/2010 (Fig. 2.15).

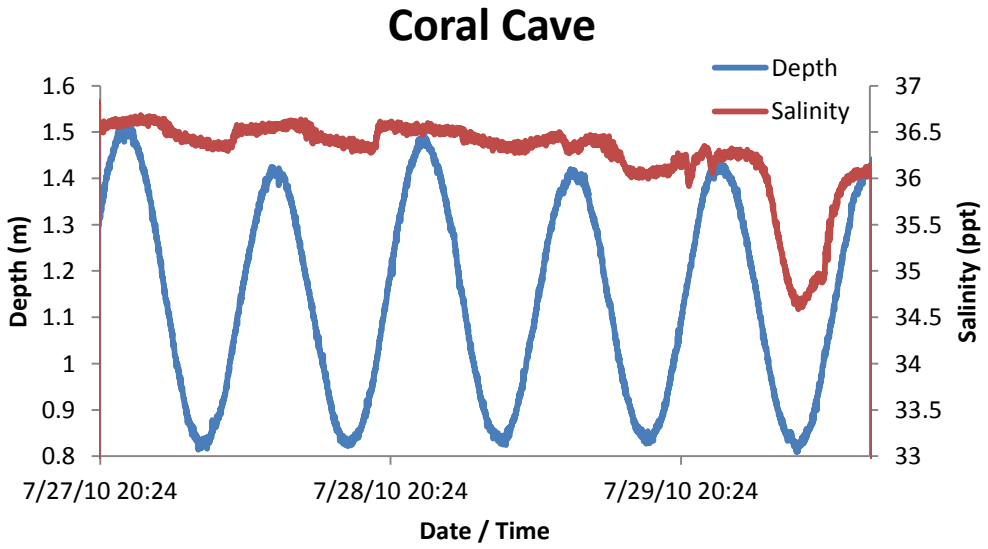

Fig. 2.15. Salinity level in Coral Cave over several tidal cycles. Data taken at the end of Bermuda's 50 year dry spell. The drop in salinity on 7/30/2010 indicates the impact of a large storm.

CHAPTER III

TIDAL SIGNATURES IN BERMUDIAN CAVES

3.1 Introduction

Tidal predictions were once made by hand, however the first machine built to calculate and predict tides was designed by Sir William Thomson in 1873. Calculations for this machine were based on 10 different tidal constituents. Tide-predicting machines now use over 35 different constituents, although some constituents are more significant than others depending on where the test is being conducted (NOAA, 2006).

Bermudian tides fall within the WNAT (Western North Atlantic Tidal) Domain. Within this domain, the O_1, K_1, Q_1, M_2, S_2, N_2, and K_2 astronomical as well as the M_4 and M_6 overtides, tend to be the most important tidal constituents for predicting tidal fluctuations (Mukai et al., 2002) (Table 3.1)

Table 3.1. Tidal constituents significant in Bermuda caves (Defant, 1961).

	Symbol	Period
Name		
Principal lunar diurnal	O_1	25.82
Luni-solar semidiurnal	K_1	11.97
Large lunar eliptic	Q_1	26.87
Principal Lunar	M_2	12.42
Principal Solar	S_2	12
Large lunar eliptic	N_2	12.66
Luni-solar semidiurnal	K_2	11.97
Principal Lunar	M_4	6.21
Principal Lunar	M_6	4.14

For most of the world, tides moving through large islands and coastal aquifers with tidal heads decay exponentially with distance (White, 2009; Slooten et al., 2010). In this study, I was able to determine head fluctuations and lag times through direct measurements rather than calculation. Tidal efficiency was determined as

$$TE = \frac{Cave\ water\ level\ change}{Ocean\ water\ level\ change} \tag{3.1}$$

where *TE* is tidal efficiency (Martin, 2011).

Tidal signals for islands like Bermuda are governed by more factors than distance-to-shore (Wheatcraft, 1981; Ayers and Vacher, 1986; White, 2009). The reason for this unexpected tidal behavior is that the non-uniform density of highly permeable karstic limestone propagates pressure signals across the island at different rates. Thus, true tidal efficiency (defined as the percent ratio of tidal range in the cave compared to

the surrounding ocean (Carr and Van Der Kamp, 1969) is highly dependent on the medium through which it propagates. Finer sediments typically have a 5% tidal efficiency with lag times on the order of 2.5 hours for 1000 m. Courser sediments will have efficiencies on the order of 45% with 2 hour lags. Karstic limestone, such as in Bermuda, has 50% efficiency with 1.5 hours lags (White, 2009).

Bermuda's oceanic tides are predominantly semi-diurnal, with high or low amplitudes occurring every 6.21 hours. The average tidal range for Bermudian water is around 0.75 meters with yearly ranges from 0.45 to 1.2 meters (Morris et al. 1977). Tidal data for many of Bermuda's caves were collected by Thomas Iliffe in 1980. Some of these data can be found in Iliffe (2000). Those readings suggested tidal lag times in Bermuda caves ranged from 10 minutes to 1.5 hours, with most having around 1 hour lags. Tidal efficiency ranged from 30-83% with most caves being around 60% (Iliffe unpublished results, 1980). Iliffe's data suggest that within the Walsingham Track, the longest tidal lag times (<90 minutes) are found in caves south of the isthmus, between Harrington Sound and Castle Harbour (Fig. 3.1). Grotto Bay caves tended to have the second longest lag times (60-70 minutes). The shortest lag times (10-60 minutes) tended to be found in the isthmus. Within this isthmus, the shortest lag times were in caves closest to Castle Harbour (Iliffe unpublished results, 1980). While there is variation, Iliffe's data indicate that many cave tides correspond to predictions made by White (2009).

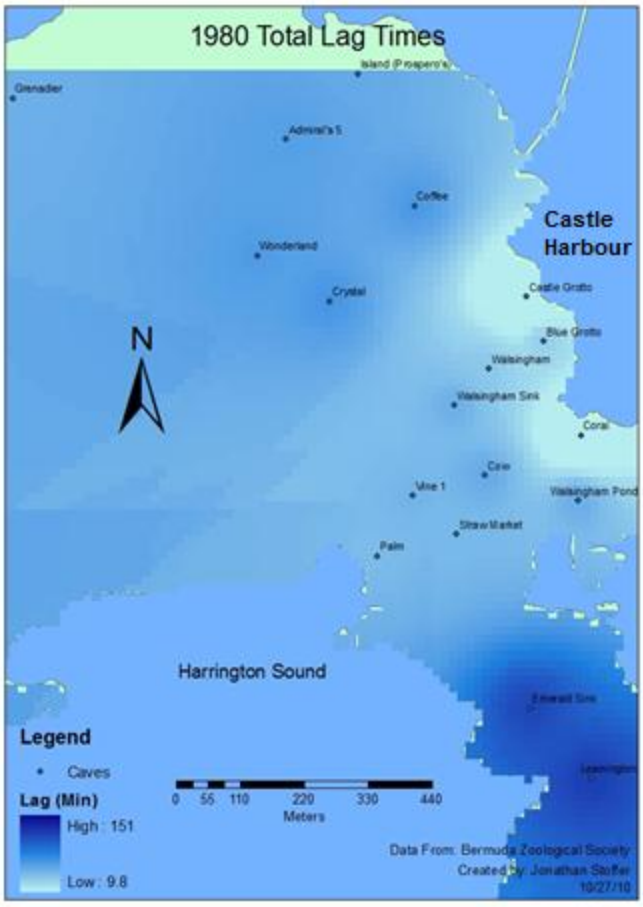

Fig. 3.1. Tidal lag times for Bermudian caves in 1980. Data taken by T. Iliffe in unpublished research.

The geology and water flow within caves around the perimeter of Harrington Sound are consistent with to the caves acting as conduits for water exchange between the ocean and the Sound, with additional connections through cracks, fissures and collapses (Iliffe unpublished results, 1980). Within the Harrington Sound hydrological system, those caves with longer lag times are most likely supplied by Harrington Sound, while those with shorter lags are likely supplied by the ocean.

3.2 Methods

Water elevation and associated tidal signatures in Bermuda's caves were collected and analyzed for a six week period, spanning July to August 2010. Additional collection of long term tidal data was also performed by a local cave diver, Gil Nolan, during and after this period. The survey included four environmental parameters: water quality pH, dissolved oxygen (DO), temperature, salinity, tidal range and tidal lag times. This collection was chosen to be comparable to tidal and water quality data collected by Thomas Iliffe in 1980.

3.2.1 Instruments

The study used a GPS unit and two water monitoring devices: a YSI 600 XLM Multiparameter Water Quality Monitor and an In-Situ Level Aqua TROLL.

Fig. 3.2. Water Quality Monitor deployed at Church Cave.

The YSI 600 XLM Multiparameter Water Quality Monitor (Fig. 3.2) was used in conjunction with Eco-Watch Windows software to determine salinity, pH, temperature, dissolved oxygen and depth once every minute. This instrument was used to collect water level data for 48 hours in a number of caves as well as in Harrington Sound.

The In-Situ Level Aqua TROLL water quality monitor was used in conjunction with Win-Situ 5 software to measure conductivity, temperature, and depth. Salinity was computed from temperature, conductivity and pressure. The Win-Situ 5 software can program the Aqua TROLL to take readings as often as once per minute. This instrument was used to collect data over both 48 hour and six week periods for cave lag time and water height analysis.

The Garmin GPSMAP 76CSx GPS unit is a basic hand held GPS used to obtain locations of study sites. The instrument is accurate to within a 3 meter radius when able to receive signals from at least 5 to 6 satellites (Garmin 2011). I also used Microsoft Excel, SAS, and ArcGIS v9.1.3 software for data processing.

The Aqua TROLL and YSI 600 XLM were recalibrated at least once per week or between deployments. Additional calibrations were performed based on the performance of the unit. Calibration can be performed by connecting the instrument to a computer running either YSI Eco-Watch or Aqua TROLL Win-Situ 5 software. The sensors are then placed in specific calibration fluids and the software is instructed to run the specified calibration. For both the YSI and Aqua TROLL, conductivity is calibrated with a 10 mS/cm fluid at 25°C. For the YSI, pH calibration is set with a 2 point calibration. The manufacturer recommends using calibration fluids with a pH of 7 and 10.

Calibration should be performed at 25° C. I ran out of calibration fluid in the field, as such my pH sensor was not calibrated to this standard. I was forced to calibrate using fresh water rather than salt water. Thus, the pH readings in my research are not comparable to other studies. Dissolved oxygen is calibrated as needed by cleaning the sensors, replacing the KCl solution and the membrane covering. The sensor is then wrapped in a wet towel while allowing it to run for several minutes. The final step for calibrating the new membrane is to set air pressure levels for the device. Calibrating pressure is performed by ensuring that the depth sensor module is in air and not immersed in any solution. This zeros the sensor relative to current barometric pressure. Temperature sensors were not calibrated in the field as the manufacturer recommends that the device be returned for recalibration.

3.2.2 Cave Surveys

I collected water depth data from 39 caves. These sites were located using GPS coordinates recorded by Thomas Iliffe and with the aid of local experts who have visited sites before. Caves selected for study were chosen based on proximity to Harrington Sound and interconnection with surrounding caves. Local divers experienced in exploring these caves and cave maps including those of the Walsingham, Palm Cave and Green Bay Cave Systems provided this information. Cave pools situated at various distances from the shore line were chosen. In this way, I was able to compare tidal data within and between cave systems as well as variation based on distance to shoreline.

Fig. 3.3. The line for the Water Quality Monitor deployed at Church Cave.

Water depth data were collected for 48 hours at most sites. These readings were used to track tidal fluctuations in salinity, DO and pH. They were also used to calculate lag times and depth ranges of the water in each cave. Since tides in Bermuda are semidiurnal, 48 hour runs were used to capture eight tidal peaks (four neap and four spring tides). These data were collected with either the YSI 600 XLM Multiparameter Instrument or the In-Situ Level Aqua TROLL programmed to take readings at a rate of once every minute.

To place either device in the cave, the instrument was tied with diving line at about one meter depth (Fig. 3.3). Instruments were hidden to avoid being disturbed by visitors of the caves. After completing a run, tidal charts were consulted and the device was removed about 1-2 hours after the last change in tide during the 48 hour run. After

retrieval, the data were downloaded to a laptop using the EcoWatch or Win-Situ software. The instruments were then re-deployed at new sites.

Additional depth data were collected for six weeks at sites where current magnitude and direction were also being recorded. These data were used for the same purposes as the shorter runs, but were also used to run time series analysis and test for correlation with depth data obtained simultaneously from Harrington Sound and the ocean. Ocean data came from tidal records being collected in St. George, Bermuda, while depth data in Harrington Sound were collected from the aquarium dock near Flatts Inlet (Fig. 1.3) for one of the six week runs using the YSI 600 XL Multiparameter instrument. The YSI 600 XL was only available to collect depth data from Harrington Sound for one of the six week periods.

3.2.3 Data Processing

The collected data were converted to Microsoft Excel, SAS and ArcGIS formats using either Eco-Watch or Win-Situ 5 software. Excel graphs of sea level and water quality fluctuations were created. Excel was used to calculate total and average tidal lag time and tidal range for each site. Lag time at each site was calculated by taking the time difference for high/low tides between the caves vs. oceanic records taken at St. Georges Harbour. Tidal range was calculated by determining the depth difference between each consecutive tide. Since the tidal gauges took readings once per minute, there were slight fluctuations in the depth data around each tidal peak. To remove these fluctuations and to determine the true time of each tidal peak, the depth reading were smoothed with a 21

point running average. True high/low tides were recorded as the time with the highest/lowest average depth. Readings used to determine tidal range were those with the highest/lowest recorded depth within 10 minutes of the high/low tidal peak in the running average. Tidal efficiency was calculated using equation 3.1 (Gregg 2006).

A time series analysis was performed in MATLAB using the supplementary program T_Tide. Data was organized into a series of columns for date, time, and water level. The data file was then uploaded with MATLAB and processed using the T_Tide program. In the final readout, constituents with an SNR (signal to noise ratio) value > 1 are considered significant.

When analyzing oceanic tidal or current data, tidal and non-tidal components must be separated. This can be accomplished by time series analysis using the MATLAB program "T_Tide" (Pawlowicz et al. 2001). T_Tide analyzes the time series using tidal constituents that have potential influence on the data. The program offers 45 astronomical and 101 shallow-water constituents to choose from. After analyzing each time series, the twenty four most important constituents are listed in order of importance. Importance is determined by the size of the Rayleigh resolution limit (Pawlowicz et al. 2001). A large limit means the influence of the constituent was significant. A small limit means the influence of the constituent was difficult to resolve from other constituents. T_Tide also gives error estimates for the phase and amplitude of tidal constituents. Finally, the program shows the variation in data that does not appear to be related to the tides.

3.3 Results

Lag time is primarily dictated by how well a site is connected to the ocean vs. Harrington Sound. The Sound has a two and a half hour lag time relative to Bermuda's other inshore water bodies. Lag times for all sites ranged from five minutes to two and a half hours. Average lag time for all sites was 72 minutes. Many sites with small lag times were located, as expected, nearer to the ocean, but some coastal sites, such as Dark Room in Green Bay Cave, actually behaved more like Harrington Sound (Table 3.2). Tidal Efficiency for all caves ranged from 21 to 86%. Average tidal efficiency for all sites was 50%. Sites closer to the ocean were usually more efficient, but as with lag time, some sites broke from that pattern (Table 3.2).

Table 3.2. Lag times and tidal efficiency results for all caves tested.

Caves	Lag Time (min)	Low Lag (min)	High Lag (min)	Tidal Efficiency
Walsingham				
Angel	71.1	84.2	58	0.488
Castle Grotto	13.3	20.4	6.2	0.799
Cherry Pit	75.44	82.2	67	0.488
Coffee	69.86	55.33	80.75	0.577
Cripple Gate	73.33	73.5	73.14	0.469
Coral Cave	5.1	8.8	1.4	0.859
Blue Grotto	47	69	29.4	0.61
Causeway	49.75	59.25	40.25	0.621
Calabash	54	55.4	52.6	0.64
Walsingham Pond	74.75	81.75	67.75	0.37
Walsingham Cave	64.25	75.25	53.25	0.594
Stoffers	73.38	80.75	66	0.58
Walsingham Sink	68	79.5	56.5	0.566
Straw Market	79	71	85	0.496

Table 3.2. Continued.

Cow	68.25	71	65.5	0.572
Vine	59	57.2	60.8	0.577
Deep Blue	62.29	65	60.25	0.596
Palm	63.88	67.25	60.5	0.484
Fern	69.6	77.2	62	0.63
Road Side	64.13	70	58.25	0.364
Fantasy	69.36	78.33	58.6	0.585
Myrtle Bank	56.57	61	50.67	0.509
Red Bay	78.13	82.09	74.22	0.314
South of Walsingham				
Leaning Tower	77.75	81	74.5	0.376
Christies	98.5	103.5	93.5	0.32
Emerald Sink	87.82	88.6	87.17	0.403
Leamington	118.88	127.5	110.25	0.319
Church	99.63	110.75	88.5	0.301
Grotto Bay				
Island	61.44	66.5	57.4	0.604
Cathedral	64.11	70	59.4	0.61
Swizzle	68.88	54	83.75	0.58
Admirals N.	56.25	47.5	65	0.639
Admirals S.	57.25	58.25	56.25	0.647
South Harrington				
Chalk	65.11	68.4	61	0.301
Devils Hole	67.71	61	76.67	0.465
Flatts Inlet	159.29	147	175.67	0.259
North Harrington				
Cliff Pool	154.22	159	148.25	0.213
Davis Pond	15.6	17.2	14	0.596
Dark Room	153	162	144	0.286
Average	72.17718	75.57949	68.80359	0.505308

Similar tidal behavior is found in sites around Grotto Bay and East of Harrington Sound. Tidal efficiency for all caves around Grotto Bay were similar, ranging from 58 to 64.7%. Caves lying south of Walsingham, such as Church and Leamington Caves, ranged from 30.1 to 40.3% efficiency. Lag times for the two areas ranged from 56 to 69 min. and 78 to 119 min. respectively. Lag times and tidal efficiencies in other locations were far more variable.

Caves tested within the Walsingham System include Walsingham, Deep Blue, Vine, Fern, Blue Grotto and Fantasy Caves. Lag times and tidal efficiencies for these sites were fairly consistent. Lag times ranged from 47 to 70 minutes with an average time of 62. Tidal efficiency in the system ranged from 58 to 63% with an average of 60%. Within the Palm System, data were taken from Palm, Myrtle Bank, Straw Market, and Cripple Gate Caves. Lag times were variable within the Palm Cave System ranging from 57 to 79 minutes with an average of 70 minutes. However, tidal efficiency within the system was still consistent, ranging from 47 to 51% and averaging 46% (Table 3.1).

3.3.1 Graphing Water Quality as a Function of Tidal Influence

Generally, the behavior of the different types of water properties tested can be described as direct, indirect, skipping and erratic. An example of direct tidal influence is given in Fig. 3.4 a. In this figure, the salinity in Admirals Cave tracked the water level during each tidal cycle. Indirect fluctuations, shown in Fig. 3.4 b, are 180° out of phase with the tide. The temperature levels around the instrument in Fantasy Cave rose as the tide fell and fell as the tide rose. A skipping tidal influence is in Fig. 3.4 c. Here, pH

around the instrument in Cliff Pool rose and fell every other tide. Since Bermudian tides are semi-diurnal, skipping behavior may reflect a site influenced by exposure to the sun. Finally, an example of erratic behavior is in Fig. 3.4 d. The salinity in Palm Cave did not have a clear reaction to tidal fluctuations. Table 3.3 compiles tidal fluctuations in temperature, salinity, DO and pH for each cave according to what category of behavior the water property most closely resembled over eight tidal cycles.

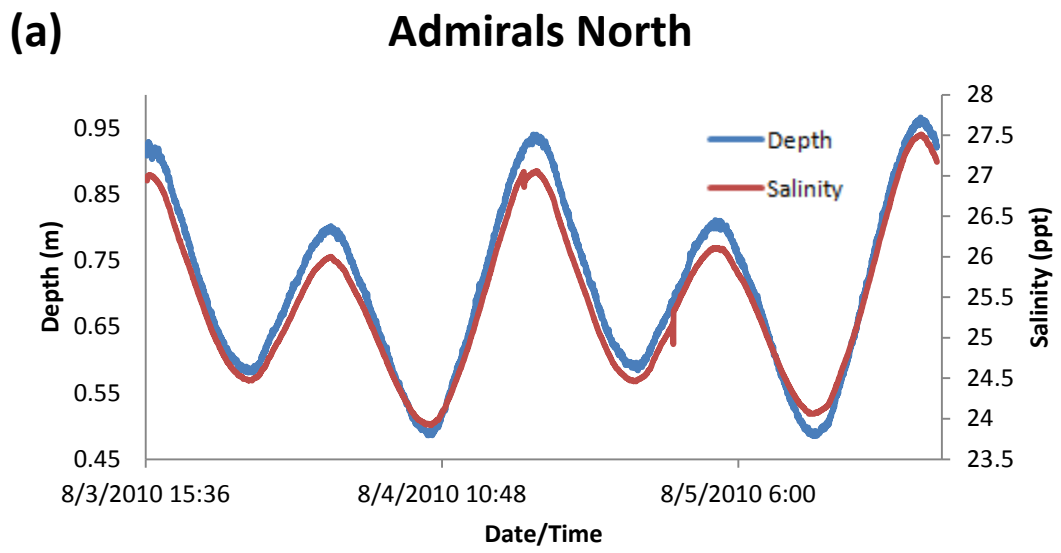

Fig. 3.4. Tidal fluctuations in water quality. (a): Direct fluctuations in salinity for Admirals North. (b): Indirect fluctuations in temperature for Fantasy Cave. (c): Skipping fluctuations in pH for Cliff Pool. (d): Erratic fluctuations in salinity for Palm Cave.

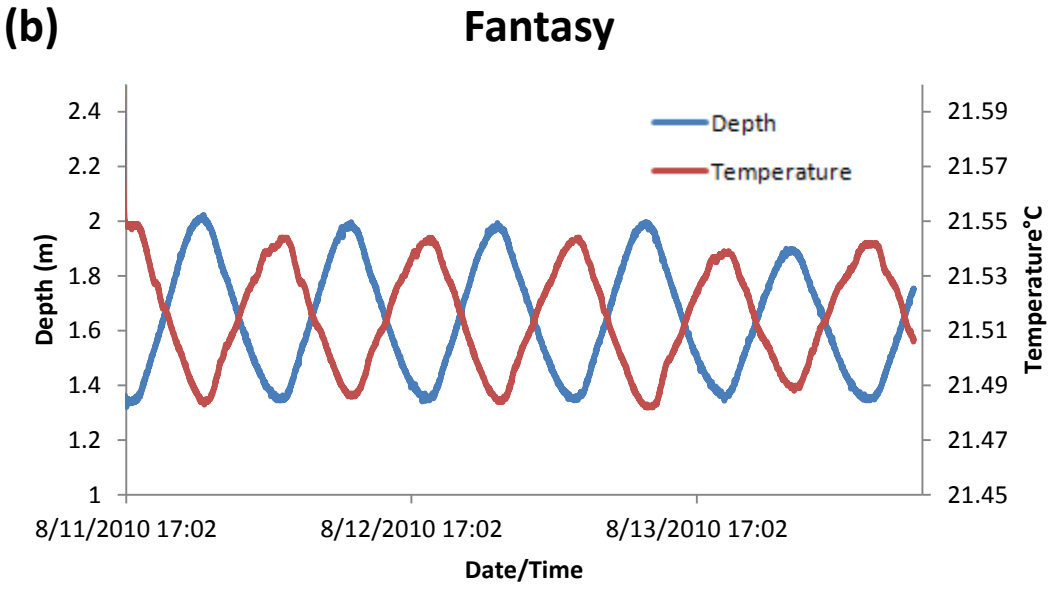

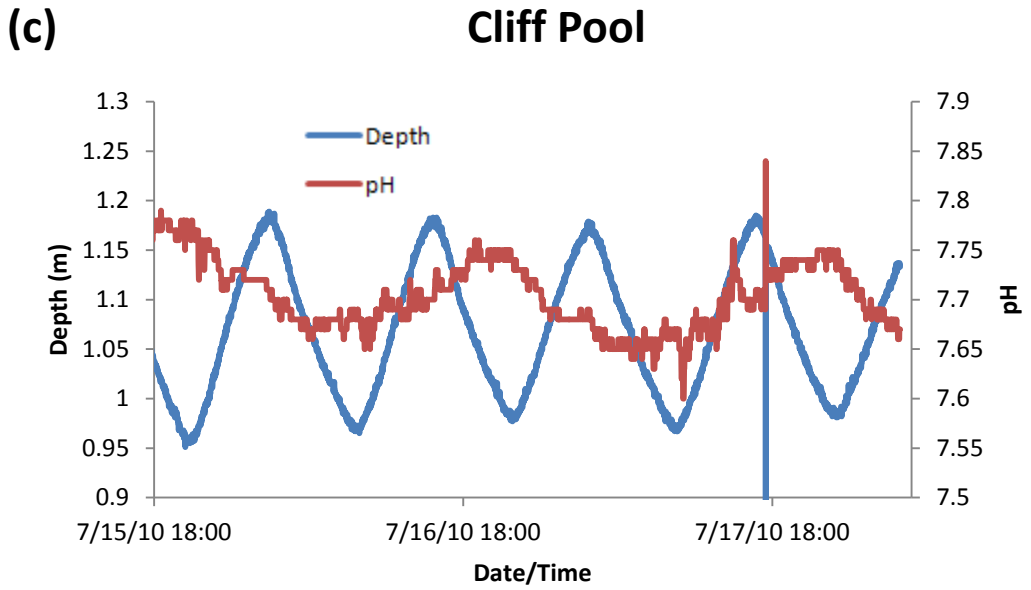

Fig. 3.4. continued

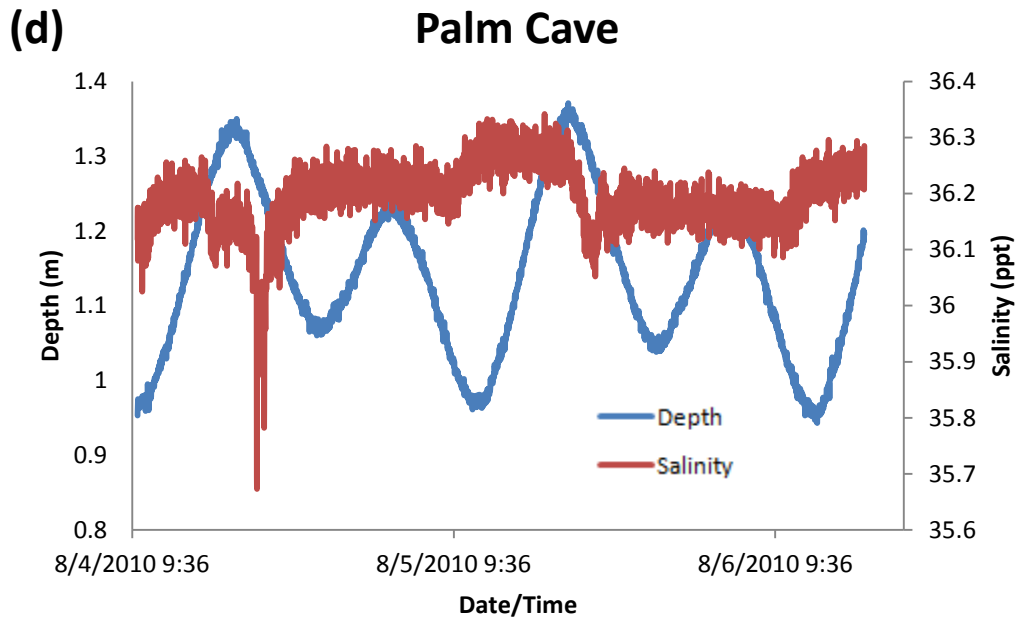

Fig. 3.4. continued

Table 3.3. Fluctuations in water quality with tidal cycles in Bermudian caves. Descriptors followed with the term "Leading" indicate the water property peaks slightly ahead of tide changes. Descriptors followed with the term "Trailing" indicate the water property peaks slightly behind of tide changes.

Caves	Temperature	Salinity	DO	pH
Walsingham				
Angel	Direct	Indirect	Direct	Indirect
Castle Grotto	Direct	Direct	Direct	Direct
Cherry Pit	Direct	Direct	Declining	Direct
Coffee	Direct	Direct	Direct/Indirect	Direct
Coral Cave	Direct	Direct		
Blue Grotto	Indirect	Direct	Direct (Leading)	Direct
Causeway	Direct/Skipping	Direct (Trailing)		
Calabash	Direct/Skipping	Erratic	Direct	Direct
Walsingham Pond	Indirect/Skipping	Indirect/Skipping	Indirect/Erratic	Indirect
Walsingham Cave	Direct/Skipping	Increasing		
Stoffers	Direct (leading)	Erratic		

Table 3.3. Continued.

Walsingham Sink	Erratic/Direct	Erratic	Erratic	Erratic
Straw Market	Direct	Erratic /Indirect	Erratic	Erratic
Cow	Direct	Direct		
Vine	Declines	Direct		
Deep Blue	Direct (Leading)	Direct (leading)		Indirect
Palm	Direct/Indirect	Erratic		
Fern	Direct	Direct		
Road Side	Direct	Direct		
Crystal	Erratic	Indirect	Direct (Trailing)	Erratic (Direct)
Fantasy	Indirect	Direct		
Myrtle Bank	Erratic	Erratic	Erratic	Indirect
Red Bay	Direct	Erratic		
South of Walsingham				
Leaning Tower	Erratic	Direct	Indirect	Direct
Christies	Direct	Direct		
Emerald Sink	Direct	Direct		
Leamington	Direct/Indirect	Direct/Indirect	Indirect/Skipping	Erratic
Church	Direct	Direct	Indirect	Direct(Leading)
Grotto Bay				
Island	Indirect/Erratic	Direct/Indirect	Direct/Skipping	Indirect/Erratic
Cathedral	Direct	Direct		
Swizzle	Direct	Direct	Indirect	Indirect
Admirals N.	Direct	Direct	Direct	Indirect
Admirals S.	Direct	Direct	Direct (Leading)	Stable
South Harrington				
Chalk	Direct	Direct		
Devils Hole	Direct (Leading)	Direct	Direct (Leading)	Direct(Leading)
North Harrington				
Cliff Pool	Indirect	Direct		Skipping

3.3.2 Time Series Analysis

Long term data were used to run time series analyses using MATLAB with the add-on program T_Tide. A time series was calculated for Red Bay, Green Bay, Castle Grotto, Walsingham East, Burchalls Cove, and Leamington Caves. Each time series compared the influence of common tidal constituents against my measured depth data to produce a predictive tidal graph (Fig. 3.5). In each time series graph, the blue line represents actual data, the green line represents predicted tides based on the data, and the red line represents variation in data that is not explained by the time series analysis. Twenty five constituents were significant to at least one site. Significant tidal constituents ($p > .95$), common to all sites included; O1, K1, N2, M2, L2, and S2.

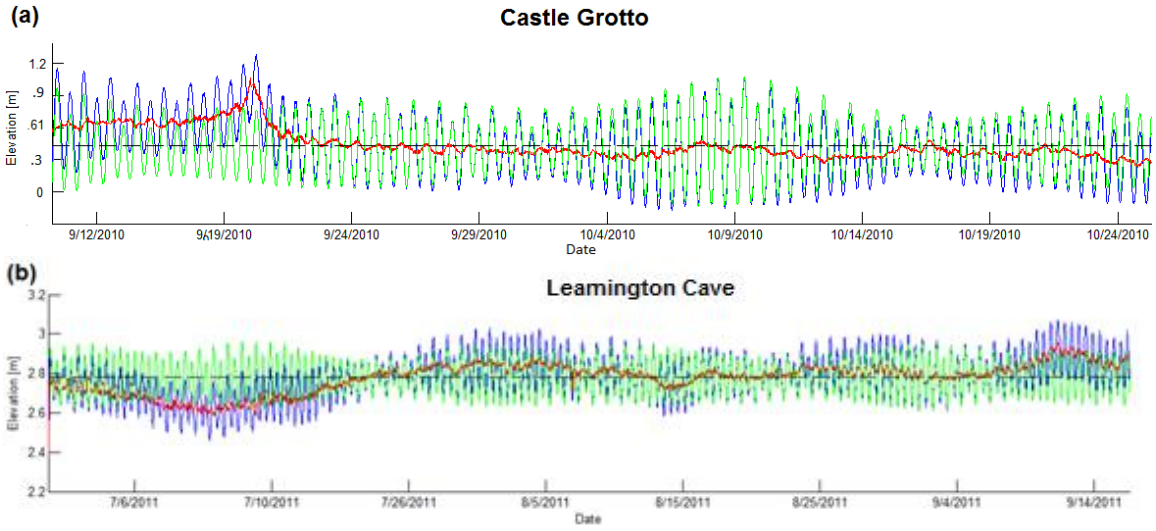

Fig. 3.5. Time series plots for two caves used in this study. The blue line represents measured data, the green line represents predicted tides, and the red line represents non-tidal variation, i.e. measured – predicted tides.

3.4 Discussion

Lag time and tidal efficiency are thought to depend on distance to shoreline and the geology of the sediment that tides propagate through. My results matched the expectation set by White (2009) that the average tidal efficiency for sea water propagating through karstic limestone would be about 50%. I expected tidal efficiency to be distributed in a similar manner to tidal lag times since the same factors impact both. To test this, a regression chart was created (Fig. 3.6). Distance to shore was measured using sampling locations with the measuring tool in Google Earth. Correlation between both readings were $R^2 = .64$. Since these readings were only taken for 48 hours, the oceanic tidal ranges while testing at each site would have been different. Regression charts were constructed to see if variation in oceanic tidal range influenced the variation in lag time or tidal efficiency readings of caves, but no correlation was found.

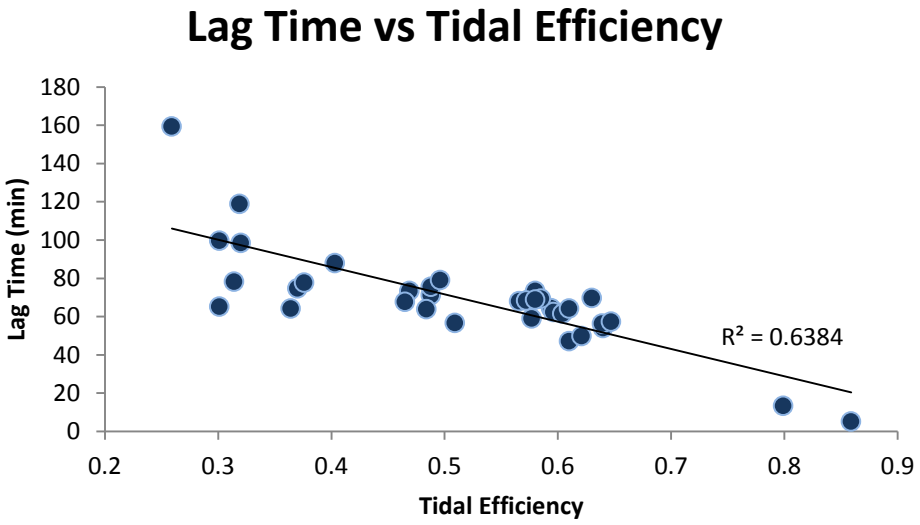

Fig. 3.6. Correlation of tidal efficiency and lag time in Bermudian caves.

3.4.1 Influences of Distance to Shoreline

The sites with the smallest lag times and highest tidal efficiencies were located, as expected, adjacent to the ocean. These sites are most likely supplied by the ocean as they reach high tide shortly after the corresponding tide in the ocean. Sites with the longest lag times and lowest tidal efficiencies were Cliff Pool and Leamington Cave. These sites were close to and had an open conduit with Harrington Sound. However, a few sites, like Dark Room in Green Bay Cave behaved contrary to expectations.

The Dark Room is a site located under the coastline to the ocean but is linked directly to Harrington Sound through the Green Bay Cave System. The Dark Room's lag time (143 minutes) and tidal efficiency (28.6%) is more reminiscent of Harrington Sound, despite its close proximity to the ocean. This site serves as an example of how influential Bermuda's caves are at directing the flow of water beneath the island. The presence of an open conduit between Dark Room and Harrington Sound has a greater impact on the site's tidal signature than its close proximity to the ocean.

I had expected distance to shoreline to have a larger impact on lag times and tidal efficiencies. Regression charts illustrating the conventional idea of a logarithmic relationship of distance to shore vs. lag time ($R^2 = 0.29$) and tidal efficiency ($R^2 = 0.24$) show that this concept cannot be applied to Bermuda's cave systems (Fig. 3.7). This is consistent with the claim by White (2009), that on small karstic island, lag time does not follow the typical logarithmic relationship with distance to shore.

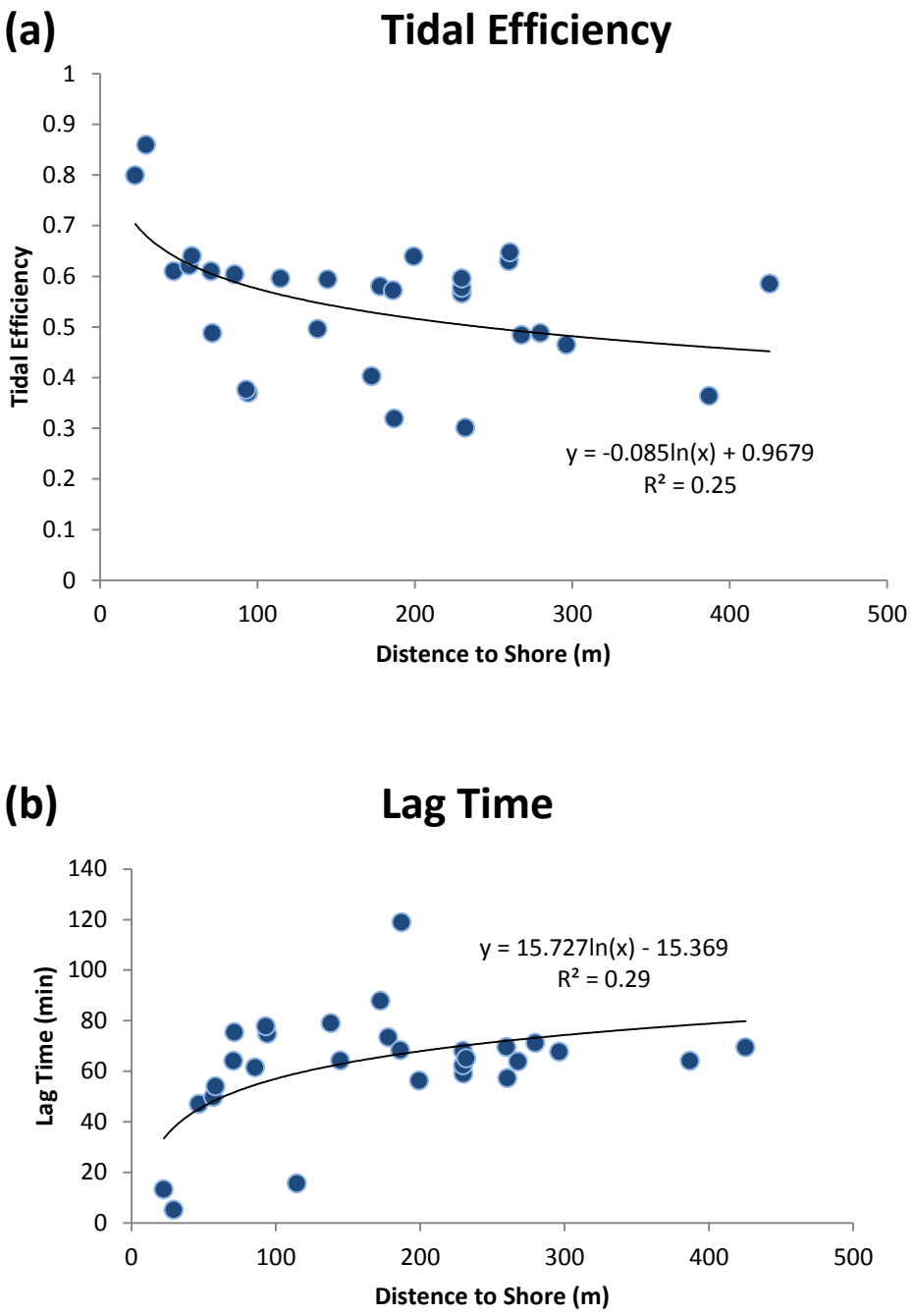

Fig. 3.7. Correlation graphs for distance to shore. (a) Correlation between tidal efficiency and distance to the ocean. (b) Correlation between lag time and distance to the ocean.

3.4.2 GIS – Tidal Variation Across the Walsingham Tract

Looking at spatial distribution shows that starting near Grotto Bay and moving southward, beyond the isthmus between Harrington Sound and Castle Harbour, there appears to be a trend toward increasing lag time and decreasing tidal efficiency (Fig. 3.8-9). Lag times were highest in caves south of Myrtle Bank (Fig. 3.8). The same is true of tidal efficiency. Sites south of Myrtle Bank were less efficient than sites tested in other areas.

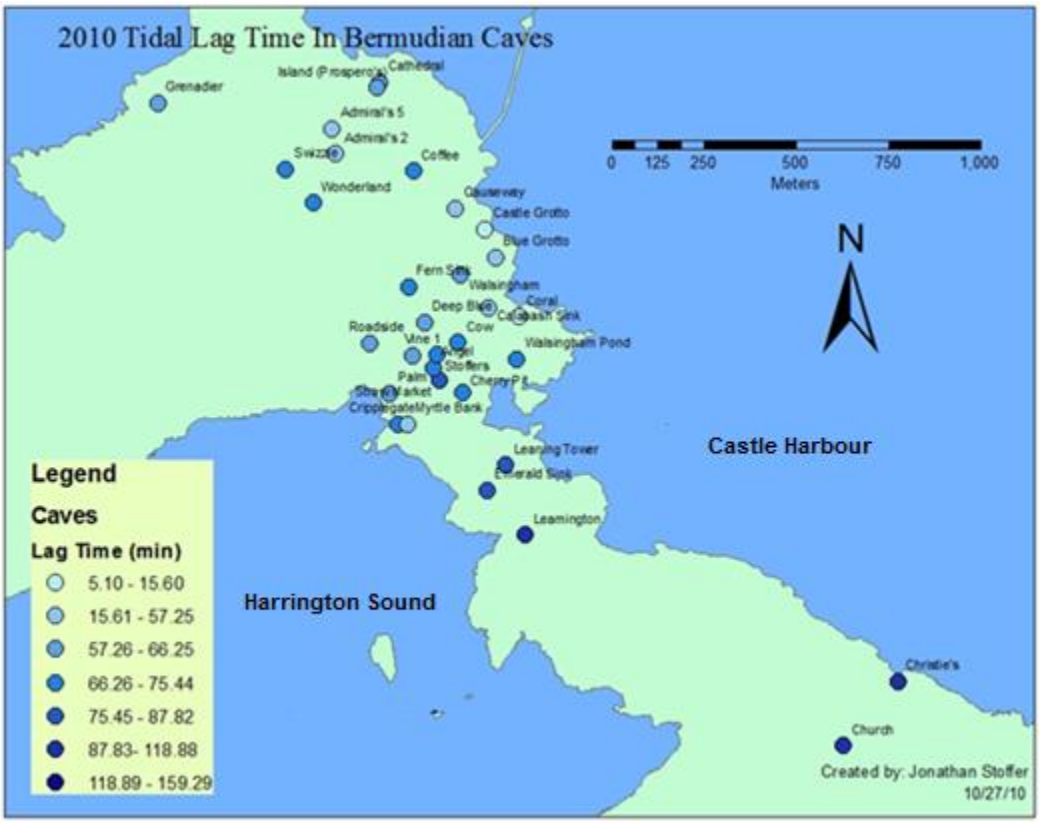

Fig. 3.8. Tidal lag times for all Bermudian caves surveyed in 2010.

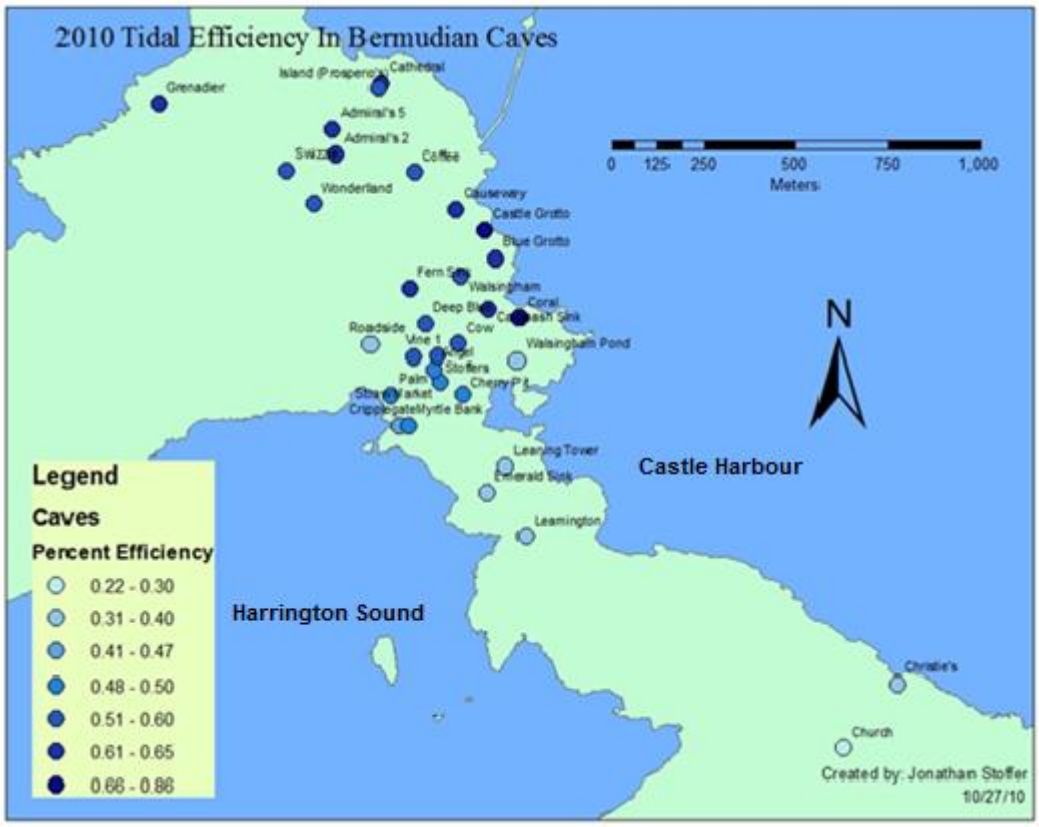

Fig. 3.9. Tidal efficiency for caves during a survey in the summer of 2010.

Table 3.4. Two sample t-test comparing the lag times and tidal efficiencies. Given for caves found in different areas of Bermuda (α=.05).

	Mean	St. Dev.	df	Grotto Bay	Walsingham	S. Walsingham
Lag Time						
Grotto Bay	61.59	5.1689	26	**********	0.9466	0.0084
C. Walsingham	61.28	18.55	26	0.9466	**********	0.0042
S. Walsingham	96.52	15.343	26	0.0084	0.0042	**********
Tidal Efficiency						
Grotto Bay	0.616	0.0272	26	**********	0.0448	< .00001
C. Walsingham	0.556	0.1232	26	0.0448	**********	< .00001
S. Walsingham	0.344	0.0435	26	< .00001	< .00001	**********

Significant differences in lag times were found between caves south of Myrtle Bank and caves in central Walsingham as well as Grotto Bay (Table 3.4). Significant differences in tidal efficiency were also found for the same areas. Differences between central Walsingham and Grotto Bay were not significant for lag time, but did show significance for tidal efficiency. These results suggest that the caves south of Myrtle Bank are not connected as strongly to the ocean as other caves in the Walsingham Tract. The results also further support the notion that tidal propagation in Bermuda is influenced by local geology.

When comparing lag times for high tides vs. low tides, there was some variation on a site by site basis, but generally the patterns of distribution for high and low tides were very similar (Fig. 3.10). The mean lag time for high tides in the Walsingham Tract was 62.53 minutes, while the mean lag time for low tides was about 8 minutes longer at 70.69 minutes. Running a test to compare mean values failed to find a significant difference in lag time for high and low tides.

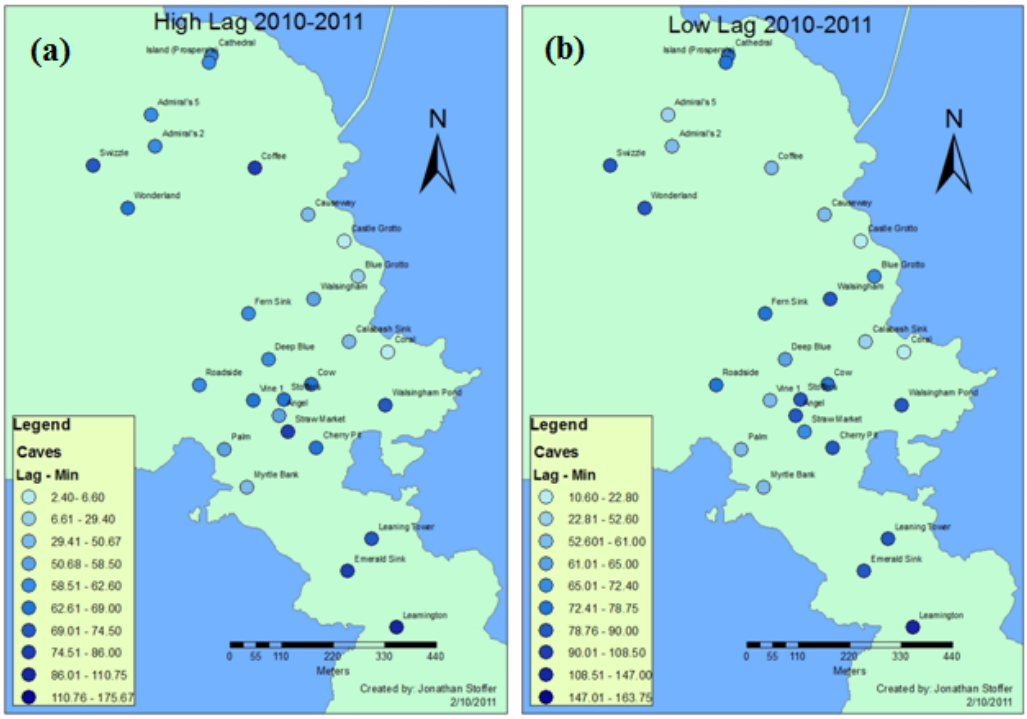

Fig. 3.10. A side by side comparison of the tidal lag time in caves. Given for high and low tides. (a): High tide lag times (b): Low tide lag times

3.4.3 The Influences of Connectivity

If local geography does help drive tidal propagation through islands, it should be expected that within cave systems, where all sites are connected by open conduits, lag times and tidal efficiencies should be more consistent than for other caves in the same area.

Within the Walsingham Tract, there were two major caves systems that I took multiple readings from - the Walsingham System and the Palm System. The standard deviation in lag time for all caves in the Walsingham formation is about 20 minutes and the standard deviation in tidal efficiency about 14%.

Looking only at caves in the Walsingham System, the standard deviation of lag times drops to 9.2 minutes and the standard deviation from mean tidal efficiency fell to 1.8%. Blue Grotto was the outlier in the Walsingham System with a lag time of 47 minutes (14 minutes below the mean). Without Blue Grotto, the standard deviation in lag times was 3.7 minutes. Blue Grotto is closer to the ocean then the other caves in Walsingham System so it is not surprising to see it has a smaller lag time.

In the Palm System, the standard deviation in lag time was 8.61 minutes and the standard deviation of tidal efficiency was 3.73%. The greatest difference between caves in Palm System was between Myrtle Bank and Cripple Gate Caves. Lag time for these sites differed by 16.76 minutes and tidal efficiency differed by 4%. These differences were a surprising discovery considering how close the two sites are spatially (Fig. 3.10) and the fact that they are directly linked with a conduit. It is unclear why readings for these two sites were so different, but Cripple Gate does have a direct connection to Harrington Sound.

To determine if lag times and tidal efficiencies were significantly more uniform between sites in the Walsingham and Palm Systems than for other caves in the isthmus between Harrington Sound and Castle Harbour, a comparison of standard deviation F-test (α=.05) was performed (Table 3.5).

Table 3.5. Comparison of standard deviation (F-test). Given for lag times and tidal efficiencies in the Walsingham and Palm Systems against other caves in the Walsingham Tract (α=.05). The final column excludes Castle Grotto and Coral Caves from the test.

	Mean	St. Dev.	df	With Crl/Cstl	Without Crl/Cstl
Lag Time					
Walsingham System	62.5	9.23	21	$0.04 < p < 0.05$	$0.3 < p < 0.4$
Palm System	68.2	8.61	21	$0.03 < p < 0.04$	$0.3 < p < 0.4$
Tidal Efficiency					
Walsingham System	0.603	0.0175	21	$0.001 < p < 0.01$	$0.01 < p < 0.02$
Palm System	0.505	0.0373	21	$p < 0.001$	$p < 0.001$

These results show that when all data are included in the analysis, there is a significant difference in the standard deviations of lag time and tidal efficiency between both cave systems and the remaining caves in the Walsingham Tract (Table 3.5). However, due to their proximity with the ocean, Coral and Castle Grotto Caves potentially skew the results. When removing these two sites from the test, differences in the standard deviation of lag times are no longer significant for either system but differences in the standard deviation of tidal efficiency remain significant (Table 3.5). It appears that the presence of an open conduit connecting sites does not necessarily homogenize lag time between cave entrances in Bermuda. However, open conduits do appear to homogenize the tidal efficiency between sites.

Our results also show that the caves in Walsingham System have slightly lower lag times and a higher tidal efficiency then the caves in Palm System. The average lag time for Walsingham caves was 5.7 minutes shorter than caves in the Palm System and the average tidal efficiency was 9.8% higher. Running a test to compare mean, a

significant difference in time lag was not noted. The difference in tidal efficiency between Walsingham and Palm Systems showed the Walsingham System to be more efficient with a p-value of 0.0032. This result suggests that the Walsingham System has a stronger connection to the ocean than the Palm System.

3.4.4 Comparing 2010 and 1980 Data

Tidal data in Bermudian caves were measured by T. Iliffe in 1980. At the time, the gauge used for data collection was mechanical. The data for this experiment were collected using electronic instruments. To determine if there was a significant difference between the results gathered by either method, a two sample t-test was performed (α=.05) (Table 3.6).

Table 3.6. A comparison of tidal lag times and efficiencies. Given for data collected by T. Iliffe in 1980 and J. Stoffer in 2010 (α=.05).

	1980		2010			
	Mean	St. Dev.	Mean	St. Dev.	df	p-value
Lag Time	66.6	30.62	69.94	31.79	19	0.737
Tidal Efficiency	0.526	0.1571	0.571	0.1458	19	0.3536

We failed to reject Ho. It appears that there is no significant difference between the data obtained by the testing methods employed by T. Iliffe in 1980 and the methods employed by J. Stoffer in 2010.

3.4.5 Time Series Analysis

In the time series graphs, there was a certain amount of variation not explained by the tidal constituents. The largest variations occurred in Castle Grotto, Leamington and Red Bay Caves. Oceanic tidal ranges are influenced by changes in atmospheric pressure. Much of the unexplained variation found in the time series could be attributed to changes in air pressure. Graphs were constructed to compare unexplained variation in the time series with changes in air pressure for each site (Fig. 3.11).

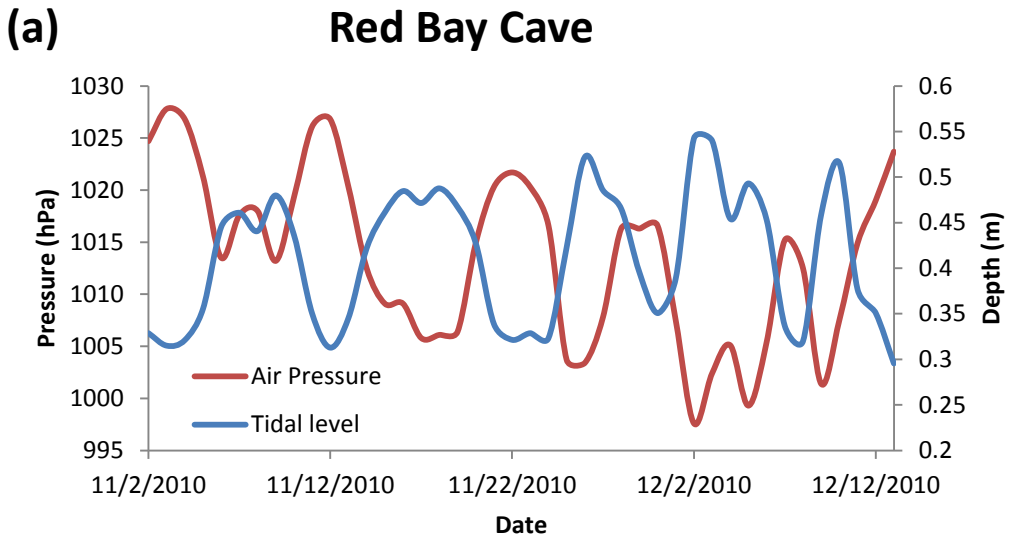

Fig. 3.11. Changes in atmospheric pressure and unexplained tidal variation. Given for Red Bay (a) and Walsingham East (b) caves. Air pressure data comes from www.weather.bm.

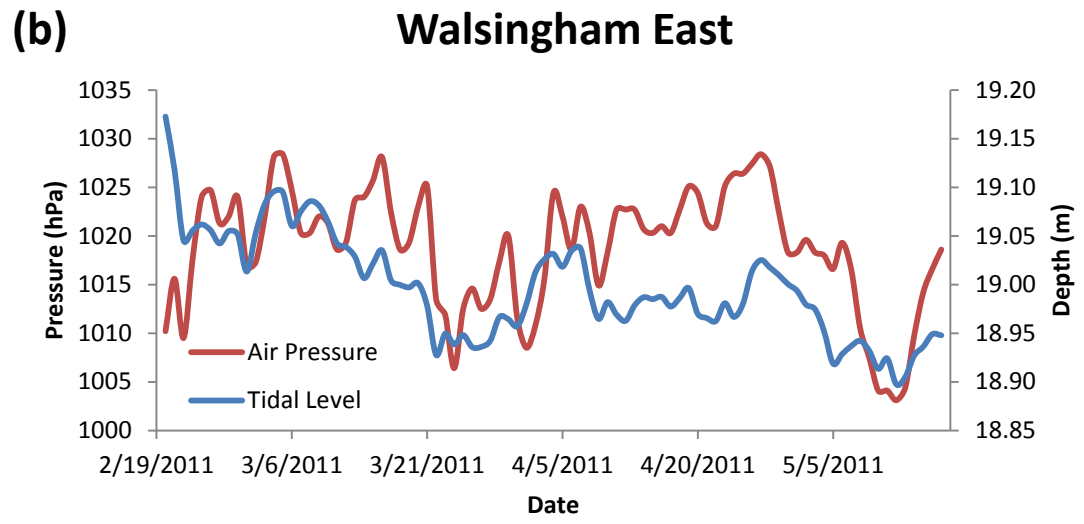

Fig. 3.11. Continued

These charts show that variations in air pressure do line up with non-tidal variations fairly well in sites like Red Bay. As atmospheric pressure drops, water level begins to rise and vise versa. However, in other sites such as Walsingham East, non-tidal variation behaved opposite to expectations by rising and falling in sync with atmospheric pressure. Regression plots were constructed to determine the correlation between unexplained tidal variation and changes in atmospheric pressure (Table 3.7).

Table 3.7. The results of six regression plots. These plots are comparing unexplained tidal variation with changes in atmospheric pressure.

Caves	Slope	R^2
Green Bay	-0.0125	0.6524
Castle Grotto	-0.0115	0.2911
Leamington	-0.0014	0.0040
Red Bay	-0.0073	0.6593
Walsingham East	0.0041	0.2197
Burchall's Cove	0.0010	0.1054

Green Bay, Castle Grotto and Red Bay Caves behaved as expected. They had negative tidal responses to rises in air pressure. Walsingham East behaved contrary to expectations with a positive tidal response to rises in air pressure. Correlations for Burchall's Cove and Leamington Caves were very weak. Since the strongest correlations were found at Red and Green Bay (~.65), it appears that Bermuda's cave systems respond differently to changes in air pressure.

There was a large spike in water level in the time series for Grotto Bay Cave. This spike was associated with a drop in atmospheric pressure at the beginning of the testing run for that site. Weather reports for Bermuda during this time showed that the large drop in atmospheric pressure was associated with hurricane Igor moving over Bermuda. Hurricane Igor passed over Bermuda as a category 1 storm and the eye passed 64 kilometers to the west of the island.

Atmospheric pressure can influence tidal changes in caves, but it is not the only factor affecting them. The angle of ocean current and wind around Bermuda can cause water to pile up around or drain away from Harrington Sound and the coast line (Morris

et al., 1977). I did not collect the kind of data that would be needed to test that possibility but it is an additional factor influencing my unexplained variation.

CHAPTER IV

A HYDROLOGICAL MODEL AND BUDGET SUMMARY

4.1 Introduction

Determining the water budget in any hydrological system is a matter of balancing inputs with outputs (Ritter, 2011). Typical inputs include tides, wind (as an influence on currents and evaporation), currents, river water and rainfall. Typical outputs include evaporation, tides, wind and currents.

Within the Harrington Sound hydrological system, inputs include atmospheric precipitation, tidal flow through Flatt's Inlet and tidal flow through the island's karstic limestone. Outputs include evaporation, tidal flow through Flatt's Inlet and tidal flow through the island's karstic limestone. Due to the porous nature of the limestone, Bermuda lacks surface rivers. The average annual precipitation for Bermuda is 1.39 meters. Annual evaporation rates for Harrington Sound are between 3.8×10^6 m^3/yr and 5.7×10^6 m^3/yr, while annual rainfall entering the Sound averages 7.2×10^6 m^3/yr (Morris et al., 1977). Morris et al. (1977) calculated that only 50% of the tidal water received by Harrington Sound during a single tide actually flows directly from the ocean through Flatt's Inlet. The inflow and outflow through this channel is also disproportionate, with 63% of the Sound's volume flowing in during a rising tide and 35% flowing out during a falling tide (Morris et al., 1977).

Since Harrington Sound only exchanges about half of its water through Flatt's Inlet, the remaining water exchange must occur through the island itself, either by diffusion or being channeled through the island's many cave systems. Because water will preferentially flow through areas of lower resistance, the majority of water that passes into Harrington Sound through Bermuda's limestone cap is thought to flow through the many cave passages throughout it (Morris et al., 1977). Some studies have taken tidal flow readings in these cave passageways (see Cate, 2009; Iliffe, 2008). However, these studies only ran flow data for a few days. To get an accurate picture of how tidal water flows through these cave systems over complete lunar cycles, flow data needs to be taken for longer. Short of a full year, several weeks of data can cover the major tidal constituents for a site sufficiently well (Ayal personal communication). The majority of tidal constituents are less than 6 weeks long (Defant, 1961).

Fig. 4.1. Castle Grotto Cave. A site with significant flow during tidal cycling.

Numerous studies have modeled subterranean hydrology, particularly the drainage and storage capacity of karstic aquifers. Barrett and Charbeneau (1997) modeled the Edwards Aquifer around Austin, TX using local water levels to describe water flow and elevation among portions of the large aquifer as well as aquifer recharge and spring discharge. A small scale flow study by Campbell and Sullivan (2002) used the EPA developed storm water management model (SWMM) to determine the level of flow that would be created in Gap Cave, Jackson County, Alabama, due to runoff under storm conditions. Models describing the propagation of tides in coastal aquifers have been used by Carr and Van Der Kamp (1969), Townley (1995), Trefry (1999), Li and Jiao (2001) and Slooten et al. (2010). Rotzoll et al. (2008) modeled dual tidal fluctuations in Maui. They attempted to describe piezometric head fluctuations in an

island aquifer that was subject to asynchronous dual-tidal propagation based on hydraulic diffusion. Rotzoll et al. (2008) estimated diffusivity of the land mass using

$$D_{amp\,j} = x^2\omega_j/2(\ln A_j)^2 \quad (4.1)$$

where D_{amp} is hydraulic diffusivity for amplitude of the j^{th} tide (m^2/day), Aj is the ratio of the tidal amplitude in the study site and the amplitude in the ocean, x is the distance to the shoreline and ω_j is the angular frequency of the j^{th} tide (/day).

Because the two main impacts on water level and current flow in Bermudian caves are the water levels in Harrington Sound and the ocean, it is reasonable to assume a model for water level in those caves will be best described using these two inputs.

4.2 Methods

A survey of long term flows for six of Bermuda's caves was performed for approximately six weeks each, spanning July 2010 to August 2011. Gil Nolan assisted in data collection, throughout this period. The survey consisted of measurements of salinity, temperature, and depth determined by an electronic water quality analyzer. As well as current magnitude and direction data from an electronic current meter. This information was used to create a water budget for Harrington Sound and calculate correlation with the simultaneously obtained tidal data from Harrington Sound and the ocean.

4.2.2 Instruments

This study used two different water monitoring devices: an In-Situ Level Aqua TROLL, and a Nortek Vector Current Meter. Additional equipment included software for my final analysis as well as a GPS unit.

The In-Situ Level Aqua TROLL water quality monitor was used in conjunction with Win-Situ 5 software to measure conductivity, temperature, and depth. Salinity was then computed from temperature, conductivity and pressure. The Win-Situ 5 software can program the Aqua TROLL to take readings as frequently as once per minute. This instrument was set up to take a reading once every ten minutes for the six week surveys.

The Vector Current Meter was used with WinADV software to measure temperature, current velocity and direction. Current velocity and direction was measured by bouncing sound waves off suspended particles in the water. While deployed, the Vector Current Meter took a single "burst reading" consisting of 100 successive readings every 10 minutes. The Vector can burst sample velocity, temperature and pressure at up to 64 Hz. The instrument was used to collect data on current velocity and direction for each cave over a six week period.

The Garmin GPSMAP 76CSx GPS unit is a basic hand held GPS used to obtain locations of study sites. The instrument is accurate to within a 3 meter radius when it can communicate with at least 5 to 6 satellites (Garmin 2011). Microsoft Excel, SAS, and ArcGIS v9.1.3 software was used for data processing.

The Aqua TROLL was recalibrated between each run. Calibration was performed by connecting the instrument to a computer running Aqua TROLL Win-Situ 5 software.

The sensor is then placed in specific calibration fluids and the software is instructed to run the specified calibration. Conductivity is calibrated with a 10 mS/cm fluid at 25°C. Calibrating pressure is performed by ensuring that the depth sensor module is in air and not immersed in any solution. This zeros the sensor with regard to current barometric pressure. The manufacturers recommend that temperature sensors not be recalibrated in the field and that the device should be sent back for recalibration so this was not performed. The Vector Current Meter was also recalibrated after every run. Recalibrations require linking the device to a computer running the Vector PC software and running recalibration tests. These tests include recalibrations of the temperature, pressure and compass sensors. Temperature calibration is performed by submerging the device in a container of water with a known temperature. Calibration proceeds until the sensor's temperature reading has stabilized (about 5 minutes). The pressure sensor is calibrated by placing the instrument in water and entering the actual depth of the pressure sensor. If in air, zero should be entered. To perform a compass calibration, the calibration is started and the devise is rotated 360°. Any magnetic fields stemming from the mounting frame will be spotted and compensated for.

4.2.3 Cave Surveys

We collected data from six sites. These sites were located using GPS coordinates recorded by Dr. Iliffe and with the aid of local experts who have visited sites before. Caves selected for study were chosen with the aid of local experts familiar with caves having larger flow passing through them. Local divers experienced in exploring these

caves also provided information on where the best points for deployment of the Vector Current Meter would be. Priority was given to locations containing a point of constriction near the cave mouth with higher flow rates where the majority of water in the system passes through (typically constrictions will have a cross sectional area of no more than 10-20 m^2). The deployment sites needed to be relatively symmetrical and to allow the instrument to be in a horizontal position.

The Vector Current Meter (VCM) was deployed for six weeks in each cave. This allowed the data to cover a full lunar cycle with enough overlap to determine if cycles repeated themselves. The VCM was programmed for each run before being deployed.

4.2.4 Data Processing

4.2.4.1 Calculating Flow

The Vector Current Meter measures current velocity as three dimensional X, Y and Z vector data in 100 reading bursts. Excel was used to average each burst and convert the three sets of vector data to total current magnitude for each site. The magnitude readings calculated represented water velocity exactly 27 cm above the sensor positioned at the center of the cave passage. However, this magnitude reading cannot represent flow across the entire cave passage because it does not take water friction with the cave walls into account. Due to the effects of friction, the velocity profile of each cave will be like that of a pipe. The average velocity of water moving through a pipe is normally interpreted as half the velocity of water moving through the center of the conduit (Recktenwald, 2002). However, this assumption is for circular

conduits with laminar flow. Most caves are not circular and there is no way to justify such a simplistic assumption. From the sketches taken, the caves in this study more closely resemble a rectangle in shape. The flow in a rectangular conduit will resemble the profile shown in Fig. 4.2 (Shah, 1978).

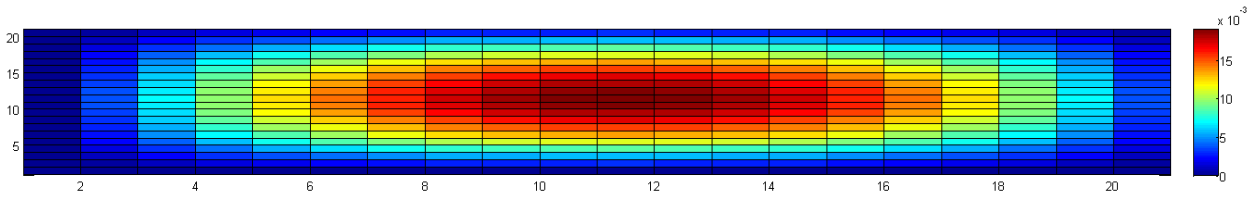

Fig. 4.2. Flow velocity profile for rectangular conduits.

To determine total flow in each cave, the cross sectional area where the current meter was placed was divided into a 100x100 matrix (larger matrixes = better resolution). In each cell of the matrix, I inserted the rectangular boundary condition for flow. This equation predicts flow ratio at any point in the cave based on its coordinates in relation to the center of flow (Berker, 1963; Poiseuille, 1840).

$$\mathrm{u(y,z)} = \frac{16a^2}{\mu\pi^3}\left(-\frac{dp}{dx}\right)\sum_{i=1,3,5\ldots}^{\infty}\left(-1^{\frac{i-1}{2}}\right)\left(1-\frac{\cosh\left(\frac{i\pi z}{2a}\right)}{\cosh\left(\frac{i\pi b}{2a}\right)}\right)\frac{\cos\left(\frac{i\pi y}{2a}\right)}{i^3} \qquad (4.2)$$

Where *y* and *z* are the cells coordinates for length and height respectively, u(y,z) is the velocity of water moving through the cell, a is the width of the cave and b is the height

of the cave. The first term in equation 4.2 is a constant for all cells so it can be ignored in the final solution leaving us with

$$u(y,z) = \sum_{i=1,3,5\ldots}^{\infty} \left(-1^{\frac{i-1}{2}}\right)\left(1 - \frac{\cosh\left(\frac{i\pi z}{2a}\right)}{\cosh\left(\frac{i\pi b}{2a}\right)}\right)\frac{\cos\left(\frac{i\pi y}{2a}\right)}{i^3} \qquad (4.3)$$

in each cell. Solving for each cell in the matrix will produce a velocity ratio profile for each site (Fig. 4.3) (Berker, 1963; Poiseuille, 1840).

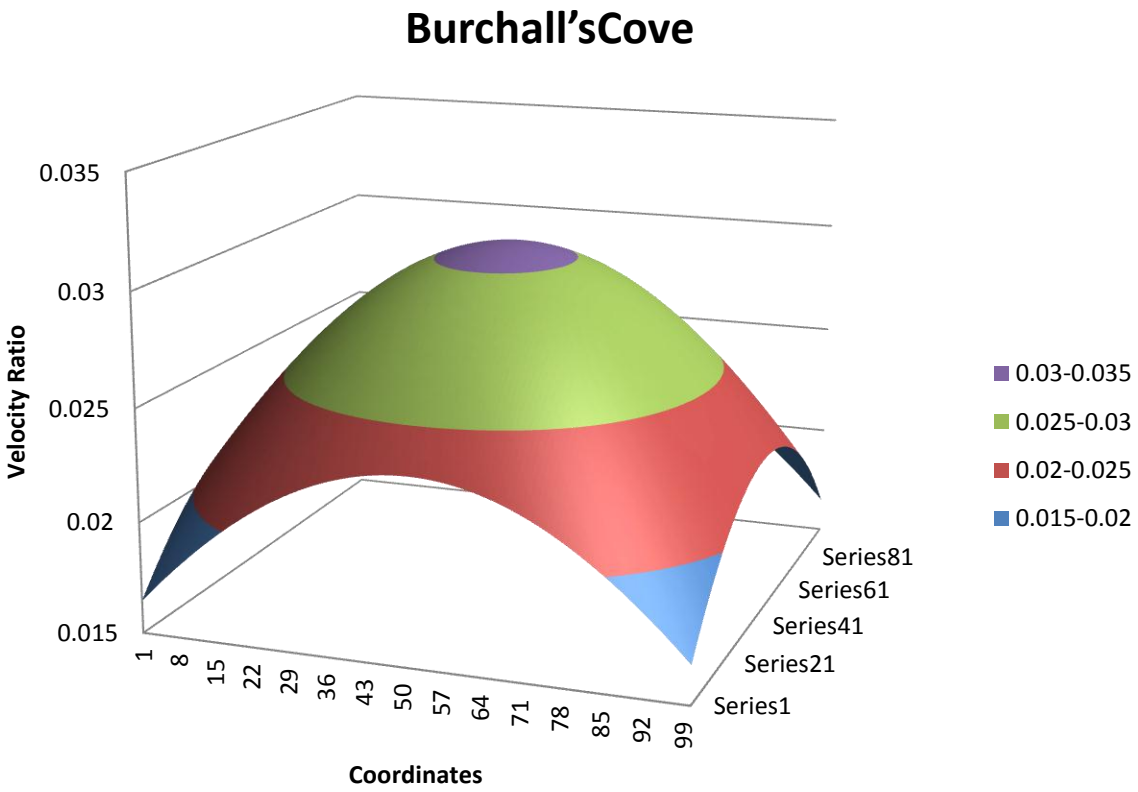

Fig. 4.3. Flow velocity profile for Burchall's Cove Bermuda.

The value in the peak of the curve in 4.3 represents the 100% velocity ratio or *Vmax*. The average value for all cells can be interpreted as the average velocity ratio of all cells or *Vave*.

$$Vave\ as\ a\ \%\ of\ Vmax = \frac{Peak\ ratio\ value}{Average\ Ratio\ value} \tag{4.4}$$

The final step before calculating flow was to determine water velocity where each measurement was taken. The vector was always placed in the center of flow for each cave and the device takes readings 27 cm above its point where it is placed. Returning to the matrix, I simply needed to pick out the ratio value for the cell that covered that point. So measured velocity values can be determined by equation 4.5.

$$Measured\ velocity\ as\ a\ \%\ of\ Vmax = \frac{Peak\ ratio\ value}{Ratio\ value\ at\ point\ of\ measurment} \tag{4.5}$$

With the values obtained in equations 4.4 and 4.5 flow at any site can be determined as

$$F = m * \frac{1}{m_p} * Vave_p \tag{4.6}$$

Where F is total flow, m is measured velocity, m_p is measured velocity as a percent of $Vmax$ and $Vave_p$ is $Vave$ as a percent of $Vmax$. Volumetric flow is simply F multiplied by the cross sectional area of the site.

Note that there are at least 3 assumptions for eq. 4.2 that are not met here. First, the equation is for laminar flow. This is a turbulent system, in which the boundary effects of the walls affect the flow differently. Second, the equation assumes pipe flow, in which there are walls on top. Flow in a cave where the flow was measured, at least, had a free surface at the top and was closer to channel flow. Since the flow in the cave was assumed to be a pipe flow to convert a velocity measurement to total flow, this introduces a second error. Third, the cross-section of a conduit is not a constant rectangle, even if the free surface disappears. All these unmet assumptions introduce errors in the use of Eq. 4.2 to describe the flow in the caves. As a result, the results should be viewed as very approximate.

4.2.4.2 Water Budget

For a balanced water budget, inputs should equal outputs (Ritter, 2011). Harder et al. (2007) created a water budget for a South Carolina watershed using the following equation,

$$P - ET - Q = \pm \Delta S, \tag{4.7}$$

where P is precipitation, ET is actual evapotranspiration, Q is stream outflow, and ΔS is the change in water storage. Methods similar to those employed by Harder et al. (2007) were used to create a water budget for Harrington Sound. First, since Bermuda lacks surface rivers, rather than looking at stream outflow (Q), I looked at tidal inflow/outflow at the six main caves in my study ($C_1 - C_6$) as well as Flatt's Inlet (I). Second, ΔS was placed on the left side of my equation since it can be measured with the Sound's tidal range and surface area. Finally, my budget solved for the amount of in/out flow in the Sound that remains unaccounted for (U). My water budget equation is,

$$\Delta S - (C_1 \pm C_2 \pm C_3 \pm C_4 \pm C_5 \pm C_6 \pm I + P - E) = U, \quad (4.8)$$

where P is precipitation, E is actual evaporation, $C_1 - C_6$ is inflow/outflow at each of the six cave I collected current data from, I is mean inflow/outflow from Flatt's Inlet, ΔS is the change in water stored in Harrington and U is the remaining amount of water exchange still unaccounted for. Values used for P come from Bermuda's historical weather records accessed at www.weather.bm. Values used for E and I come from Morris et al. (1977). This water budget is able to describe Harrington Sound at scales as small as a single tidal cycle or as large as a full lunar cycle.

4.2.4.3 Water Level Model

This study uses simultaneous tidal and current data taken from Harrington Sound, the ocean and Leamington Cave for 6 weeks to create a model describing the

relationship of the three tidal systems. The relationship for tidal level in caves is almost completely dependent on tidal level outside caves. So this model is based upon the tidal data collected in chapter 3.

$$T_{L(i)} = C_1 * T_{S(i-(\Delta LS))} + C_2 * T_{O(i-(\Delta LO))} + C_3 \quad (4.9)$$

Where $T_{L(i)}$ is the tidal level in Leamington Cave at time i, T_S is the tidal level of Harrington Sound, T_O is the tidal level of the ocean, ΔLS and ΔLO represent the average lag time between tidal peaks in Leamington Cave and Harrington Sound and the ocean respectively (min) and C are constants.

The next step was to add actual data to the model and solve for the constants using the Excel add-on "Solver". Solver is a program that attempts to find the best fitting values in an equation. For this model, "Solver" was able to find the constants that would result in the model having the smallest sum of squared differences (SSD) between the predicted and actual tidal data for Leamington Cave.

4.3 Results

4.3.1 Water Budget

Based on my measurements, 9.3% of inflow and 7.6% of outflow from the Sound passes though the six caves in this study. Adding data from all available sources, a water budget was created for Harrington Sound. This budget was able to account for 75.5% of all tidal inflow and 48% of all tidal outflow. Mean water flow for all sites ranged from

0.044 to 0.33 m^3/sec. The remaining 24.5% and 52% of unaccounted exchange is likely due to both diffusion and channeling through some smaller cave systems not examined in my study. Data from Illife (2008) was only taken for two tidal cycles so the measured flow values are likely not as accurate as the six week data in this study. The exact measurements for each site are listed in Table 4.1.

Table 4.1. Inflow and outflow contributions to Harrington Sound. Contributions by surrounding cave systems during a single tide.
* Data comes from Illife (2008).
** Data comes from Morris et al. (1977). Morris gives a range of evaporation (80-120 cm/yr) values are calculated from those two extremes.

	Inflow (1000 m^3/tide)	Outflow (1000 m^3/tide)	Net Flow (1000 m^3/tide)	Pos %	Neg %
Harrington Sound**	1200	1200	0	100	100
Flatt's Inlet**	756	420	336	63	35
Burchall'sCove	37.55	22.02	15.54	3.12	1.83
Castle Grotto	19.85	11.12	8.74	1.65	0.92
Red Bay	15.36	0.53	14.84	1.28	0.04
Green Bay	13.21	13.47	-0.26	1.10	1.12
Walsingham East	20.91	42.26	-21.35	1.74	3.52
Leamington	5.04	1.94	3.11	0.42	0.16
Cripple Gate*	0.5	0.2	0.3	0.04	0.01
Joyce's Dock North*	5.5	25.5	-20	0.45	2.12
Tucker's Town Dock*	3.35	3.05	0.3	0.27	0.25
Tucker's Town Bay*	28.5	27.5	1	2.37	2.29
Evaporation 120**		7.87	-7.87		0.65
Evaporation 80**		5.25	-5.25		0.43
Total (120*)	905.78	575.45	330.33	75.48	47.95

The site with the greatest inflow was Burchall's Cove, while the site with the greatest outflow was Walsingham East (Fig 4.1). The actual inflow budget based on the six sites in this study can be written as

$$1{,}200 - (37.55 + 19.85 + 15.36 + 13.21 + 20.91 + 5.04 + 756 + P) = U \qquad (4.10)$$

With values given as 1,000 m^3/tide. Assuming $P = 0$, U totals a volume of 332,000 m^3 during inflow. The actual outflow budget for the six sites in this study can be written as

$$1{,}200 - (22.02 + 11.12 + 0.53 + 13.47 + 42.26 + 1.94 + 420 + 7.87) = U \qquad (4.11)$$

Under this budget, U totals 689,000 m^3.

4.3.2 Tidal Model

Inputting lag time and water level data and solving for the constants using solver produced equation 4.12 for Leamington Cave.

$$T_{L(i)} = .803*T_{S(i-50)} + .0747*T_{O(i-180)} + 1.851 \qquad (4.12)$$

The averaged sum of squared differences (SSD) between the predicted data and the 6900+ actual measured data points for Leamington Cave was 5.2×10^{-4}. Equation 4.12

can be slightly improved by adding a factor to account for the slope of tidal change as well as depth measurements.

$$T_{L(i)} = C_1 * T_{S(i-(\Delta LS))} + C_2 * T_{O(i-(\Delta OS))} - C_3 * (T_{O(i-(\Delta LO))} - T_{O(i-(\Delta LO-1))}) - C_4 * (T_{S(i-(\Delta LS))} - T_{S(i-(\Delta LS-1))}) + C_5 \quad (4.13)$$

$$T_{L(i)} = 0.787*T_{S(i-(50))} + 0.0846*T_{O(i-(180))} - 0.0526*(T_{O(i-(180))} - T_{O(i-(170))}) - -0.358 * (T_{S(i-(50))} - T_{S(i-(40))}) - 1.86 \quad (4.14)$$

The average SSD for equation 4.15 (5.1×10^{-4}) is an improvement, but only a minor one (<.05). In most situations, the predictions made by equation 4.12 should be sufficient.

An alternative model developed which uses the instantaneous water levels in both Harrington Sound and the ocean was reasonably accurate as well.

$$T_L = 14.669 * \text{Log}(13.323 * T_s - 1.285 * T_o) \quad (4.15)$$

Where T_L represents the water level prediction for Leamington Cave, T_s represents the current water level in Harrington Sound and T_o represents the current water level of the ocean. Under this model, the average SSD was 8.4×10^{-4}.

4.3.3 Current Model

The best current model had an average SSD of 3.8×10^{-3}. In the model, current estimates are based on the combined height of the closest high and low tidal ranges.

Current flow seems unaffected by high/low tide variation so building a model that groups high and low tidal levels into one reading removes that effect. The model can be written out as

$$F_{L(i)} = C_1*(T_{S(i-\Delta P)} + T_{S(i+\Delta F)}) + C_2*(T_{O(i-\Delta P)} + T_{S(i+\Delta F)}) + C_3 \quad (4.16)$$

Where $F_{L(i)}$ is flow in Leamington Cave at time "i", T_S is the tidal level of the Sound, T_O is the tidal level of the ocean, ΔP is the average lag time (min) between peak flow and the preceding tide, ΔF is the average lag time (min) between peak flow and the following tide and the C terms are constants. Solving for the constants, the full model can be written out as, $T_{s(i-34)}$

$$F_{L(i)} = -0.206*(T_{S(i-34)} + T_{S(i+40)}) + 0.237*(T_{O(i-47)} + T_{S(i+23)}) + 0.0687 \quad (4.17)$$

4.4 Discussion

4.4.1 Water Budget

Morris et. al. (1977) calculated that 63% of tidal inflow and 35% tidal outflow for Harrington Sound went through Flatt's Inlet. I was able to account for ~10% additional flow in this study leaving 24.5% of inflowing water and 52% of outflowing water still unaccounted for. My data does not encompass all potential cave flow around Harrington Sound. There were several sites where flow was not tested, but these measurements do cover the majority of known cave flow.

It is clear that Bermuda's caves play a large role in water exchange throughout the area surrounding Harrington Sound. However, the exchange rates I measured were still smaller than expected. More curious though is the direction of cave flow. Morris et. al. (1977) showed that the inflow through Flatt's Inlet was much greater than the outflow. They suggested that the missing outflow may be accounted for by looking at flow in cave systems. After analyzing my data, it is clear that while each individual cave has different levels of net flow, the average net flow for all caves in table 4.1 does not show a preference toward either inflow or outflow. It is still unclear why Flatt's inlet would show such a strong preference toward inflow.

4.4.2 Evidence of Flow Through

Whitaker & Smart (1990) used natural tracers as an indicator of ground water flowing through North Andros Island on the Great Bahama Bank. They were able to show evidence of flow from one side of the island to the other by measuring salinity and temperature changes in blue holes along the island's banks and comparing those values to the salinity and temperature for the ocean on either side of the island.

We can use the same methodology to detect flow from Harrington Sound to Castle Harbour and North Lagoon. Temperatures in the Sound and Castle Harbour are similar throughout the year (17-28°C) but the Sound is slightly cooler than other inshore waters in the spring/summer months and slightly warmer in the fall/winter months. The Sound usually has a lower salinity than other inshore waters (~0.2-1 ppt lower) but this is highly influenced by evaporation and precipitation rates (Morris et al. 1977).

For current magnitude readings, a negative flow indicated water moving out of the Sound, toward the opposite shore. So, based on the water quality information provided in Morris et al. (1977), it appears that if flow through exists in a given cave, then a direct relationship between salinity and flow should be observed. There should also be a direct relationship between temperature and flow during spring/summer, and an inverse relationship during fall/winter (Table 4.2).

Table 4.2. Salinity and temperature fluxes in relation to changes in current flow.

	Salinity	Temp	Dates
Burchall'sCove	Direct	Inverse	1/4 - 2/21
Green Bay	--------	Direct	7/16 - 8/28
Red Bay	Direct	Inverse	11/20 - 1/4
Walsingham East	Inverse	Direct->Inverse	2/20 - 5/18
Castle Grotto	--------	Direct->Inverse	9/11 - 10/25
Leamington	Direct	Direct	6/30 - 9/16

Table 4.2 shows that Burchall'sCove, Green Bay, Red Bay, Castle Grotto and Leamington Caves all behaved as would be expected if exchange between the Sound and other inshore waters were present at each site. Only Walsingham East behaved opposite to expectation. This may be due to Walsingham East's location or it may be due to the sites inverse flow pattern. Except for Green Bay and Walsingham East, all other caves had a positive net flow (Table 4.2). Green Bay had a net flow close to 0 but Walsingham East had a large and distinctive negative net flow. In either case, these natural tracers in the data show good evidence that the cave systems in Bermuda do experience flow through from Harrington Sound to other inshore waters.

4.4.3 Tide and Current Models

A side by side comparison of the results from equation 4.14 with the actual measured tidal data for Leamington Cave is presented in Fig. 4.4. From Fig. 4.4, the model appears relatively accurate at predicting the water depth in Leamington Cave during falling tides. However, the model prediction seems to lag slightly behind the true depth in the cave during a rising tide. The instantaneous model seems to predict water depths during rising and falling tides more accurately, but predicts the final depth of each tidal peak slightly less accurately (Fig. 4.5). The graphical result for equation 4.16 is almost identical to Fig. 4.4 so it is not shown.

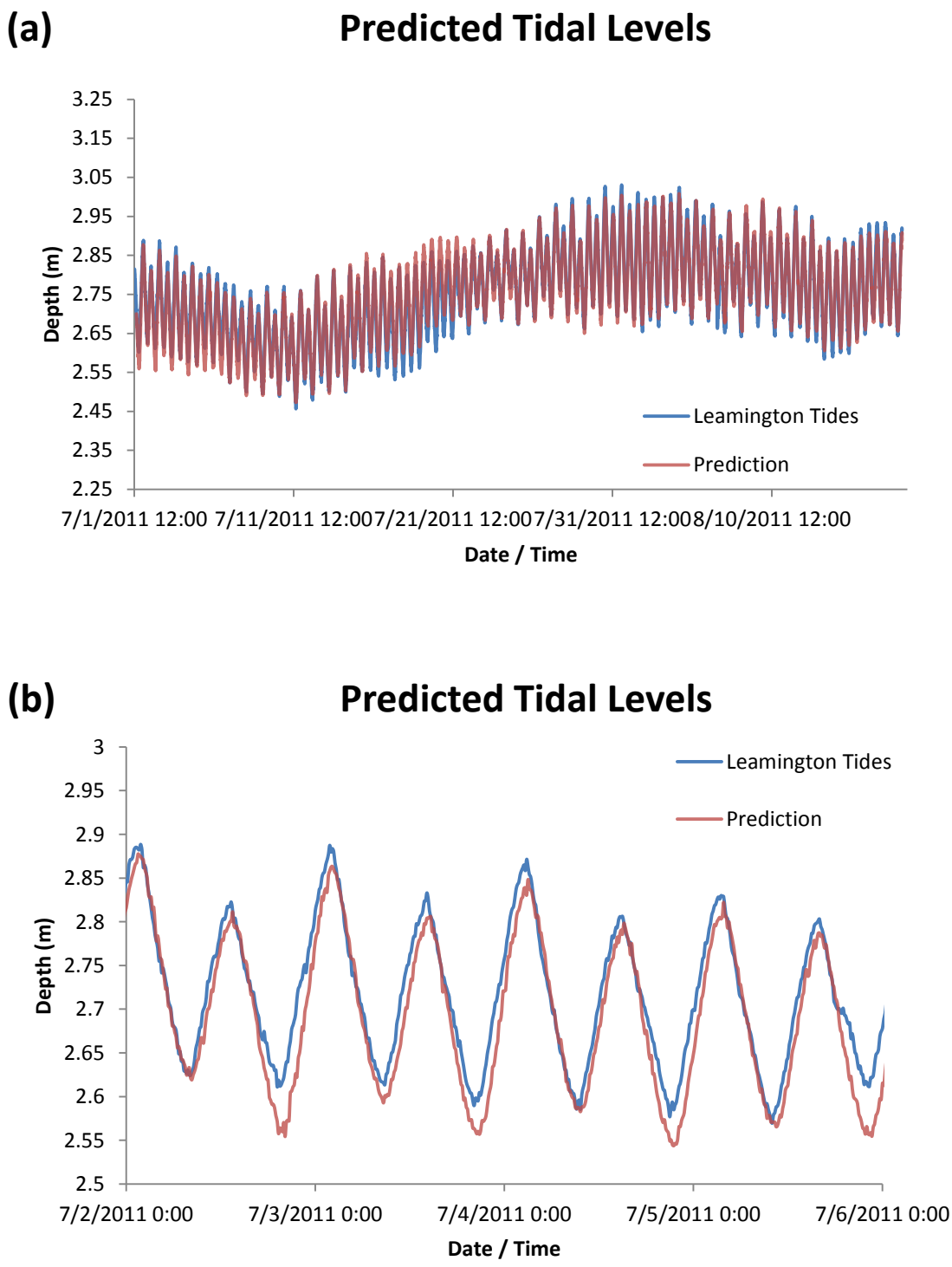

Fig 4.4. Actual tidal levels in Leamington Cave overlaid with model prediction. Prediction line generated by equation 4.14. (a) Full scale (b) Close scale

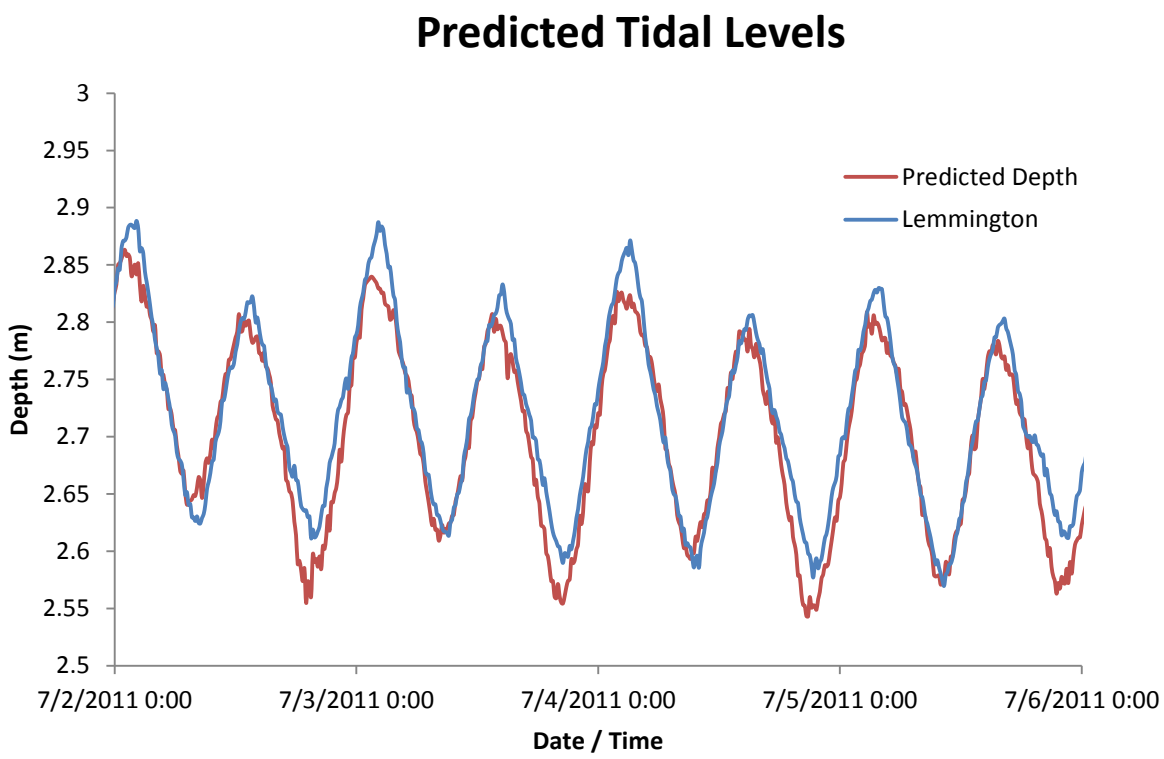

Fig 4.5. Results of my instantaneous model. Actual tidal levels in Leamington Cave overlaid with those predicted by equation 4.16.

For the current model, predictions were not as accurate as the tidal model. One of the major reasons for this was turbulence. While conducting flow tests in this study, I found each cave had different levels of turbulence. Leamington was a site that had higher levels. It is not realistic to predict turbulence using a model so it caused a lot of unaccountable variation (Fig. 4.6). Beyond turbulence, a second weakness of the model is how well it predicts the shape of each peak.

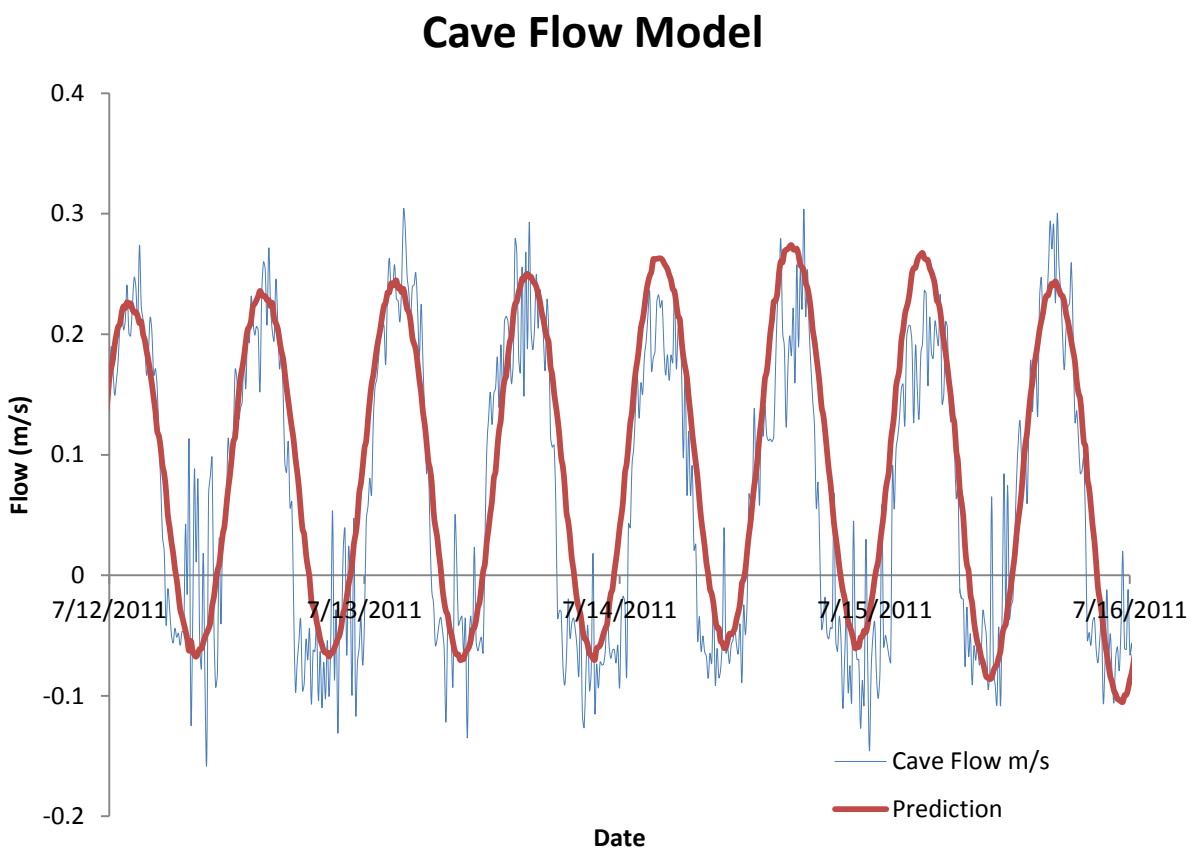

Fig. 4.6. Actual flow in Leamington Cave overlaid with model prediction. Prediction line generated by equation 4.17.

It is important to recognize that I do not have an independent array of data to test this model against so I am forced to compare it against the same data used to create it. This is not ideal. It should also be noted that this equation is based on the position of each sensor. Moving sensors in the water column will result in changing values for the constants.

4.4.4 The Green Bay Anomaly

For six weeks, depth and flow followed a solid pattern of flow rate increasing with rising tides, and reversing with falling tides. That is, until Sept. 18, 2010, when flow did not fully reverse, essentially skipping its positive flow cycle (Fig. 4.7).

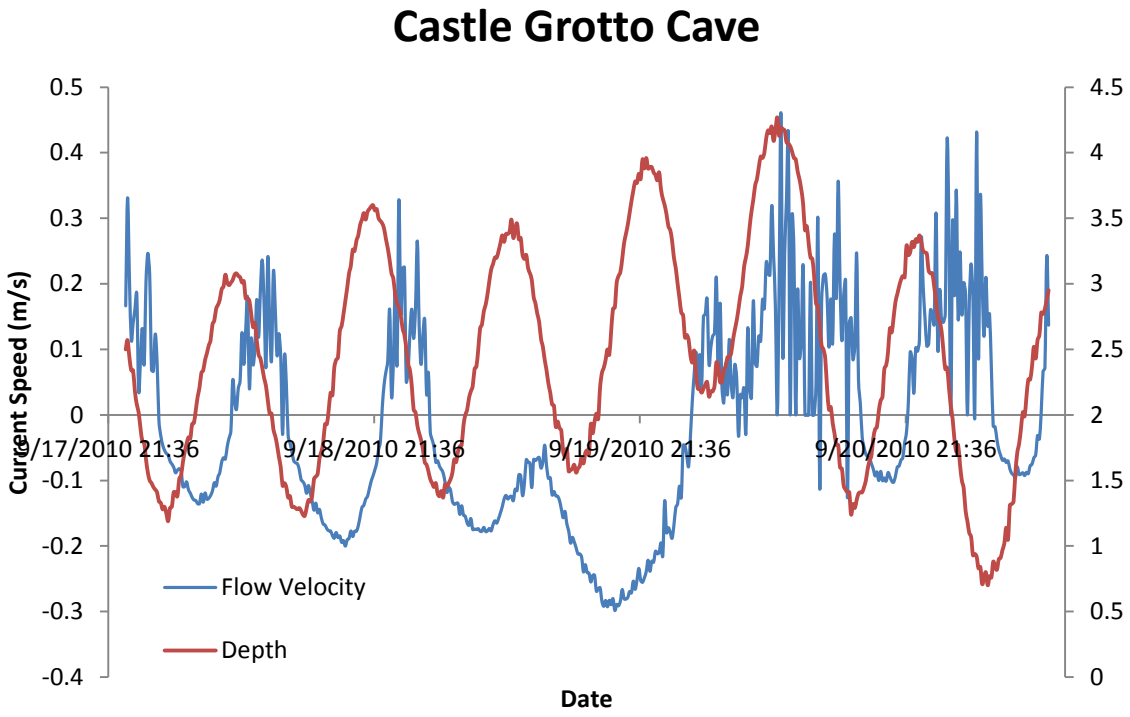

Fig. 4.7. Flow velocity in Castle Grotto Cave set against tidal variation. On Sept. 18 flow remained outward toward the ocean rather than reversing back into the Sound.

A similar event was reported by Morris et al. (1977) during their survey of Harrington Sound. They found that during low pressure fronts, Harrington Sound remained at high tide essentially skipping a low tide cycle (Fig. 4.8). We can imagine that if this were to happen, the pressure gradient across a cave along the perimeter of

Harrington Sound would remain high on the side of the Sound, thus causing flow to remain in the oceanic direction.

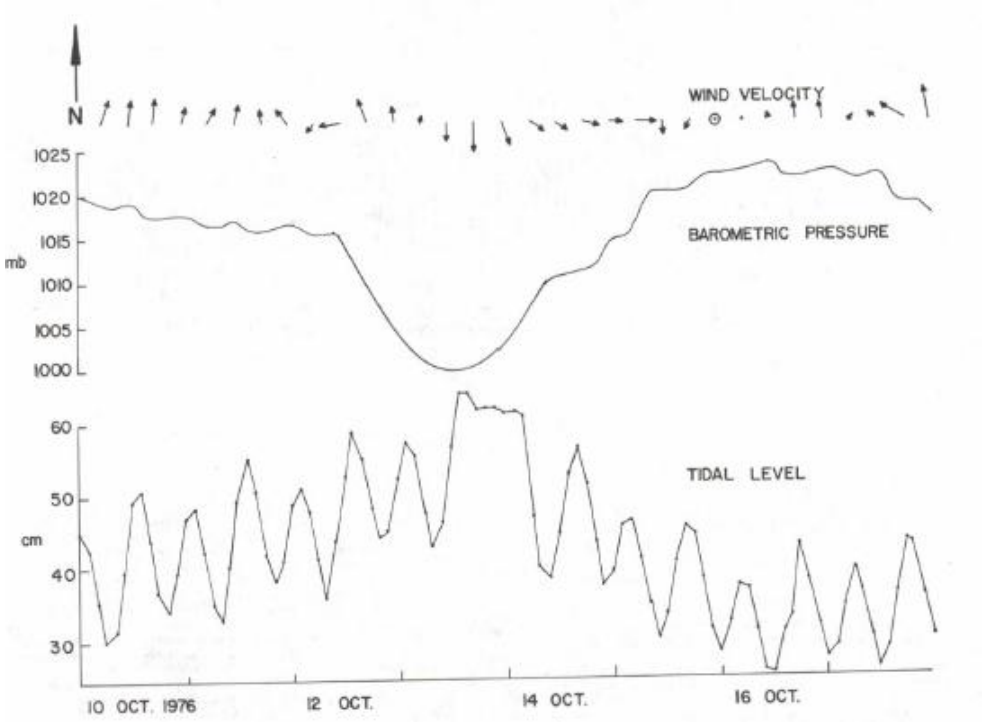

Fig. 4.8. Scanned image of the event recorded by Morris et.al. (1977). Note the tidal range in Harrington Sound remained high when air pressure dropped.

We examined past weather reports for Bermuda during this time and discovered that there was a large drop in atmospheric pressure at the time of the anomaly associated with Hurricane Igor moving over Bermuda. Hurricane Igor passed over Bermuda on September 20th as a category 1 storm with the eye located 64 kilometers to the west of the island. By graphing out flow magnitude against Bermuda's atmospheric pressure

over this time period, the data show a large pressure drop just as the anomaly in the caves flow cycle occurs.

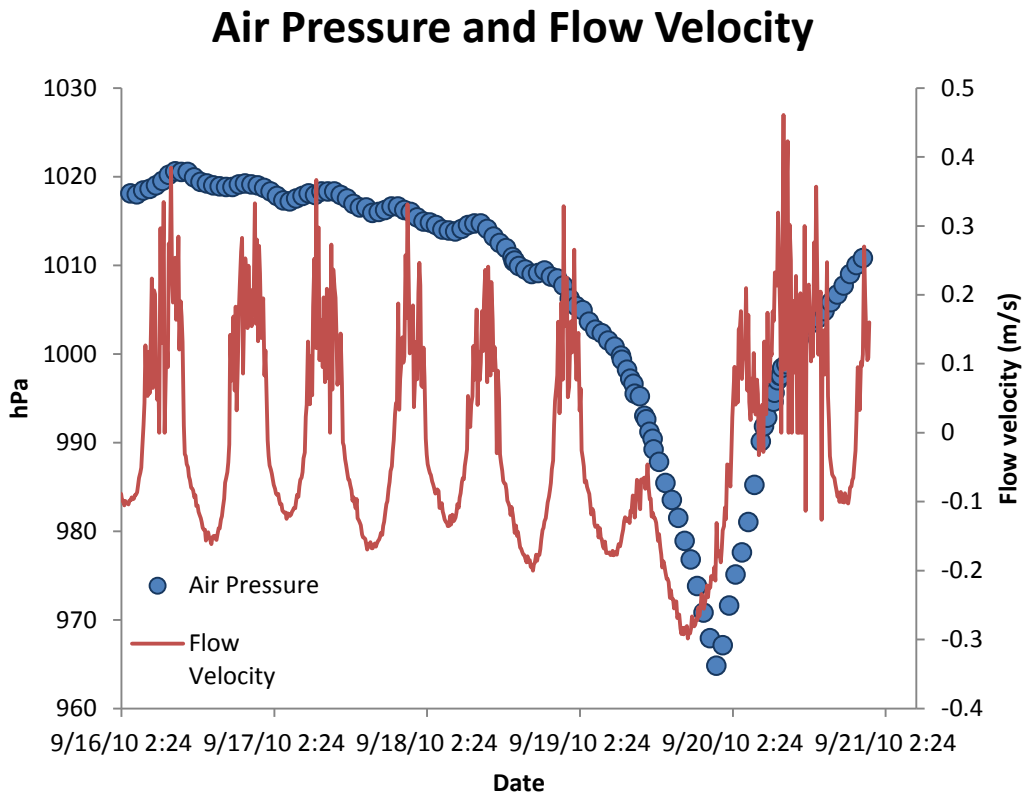

Fig. 4.9. A large drop in air pressure during flow anomaly. The passing of Hurricane Igor occurred just as the flow velocity anomaly in Castle Grotto Cave was recorded.

LITERATURE CITED

Acker, K.L., Risk, M.J., 1985. Substrate destruction and sediment production by the boring sponge *Cliona carribaea* on Grand Cayman Island, Journal of Sediment Petrology., 55, 705-711.

Anderson, M.P., 1976. Unsteady groundwater flow beneath strip oceanic islands, Water Resources Research, 12(4), 640-644.

Ayers, J.F., Vacher H.L., 1986. Hydrogeology of an atoll island, a conceptual model from a detailed study of a Micronesian example, Ground Water, 24, 185–198.

Barrett, M.E., Charbeneau, R.J., 1997. A parsimonious model for simulating flow in a karst aquifer, Journal of Hydrology, 197, 47-65.

Berker, A. R. 1963. Integration des equations du movement du movement d'un fluide visqueux incompressible. In: S. Flugge (Eds), Encyclopedia of Physics, Springer, Berlin, 9, 1-384

Bermuda Weather Service 2011. "Climate Data". Hourly Observations. Web. 16 June. 2011 < http://www.weather.bm/climate.asp>.

BIOS 2009. "Time Series BATS". Sea Water. Web. 30 November. 2012 <www.bios.edu>

Bretz, J.H., 1960. Bermuda: A partially drowned, late mature, Pleistocene karst, Bulletin of the Geological Society of America, 71, 1729-1764.

Campbell, C.W., Sullivan, S.M., 2002. Simulating time-varying cave flow and water levels using the storm water management model, Engineering Geology, 65, 133-139.

Carr, P.A., Van Der Kamp, G.S., 1969. Determining aquifer characteristics by the tidal method, Water Resources Research, 5, 1023-1031.

Cate, J.R., 2009. An assessing the impact of ground water pollution from marine caves on nearsshore seagrass beds in Bermuda. MS Thesis, Office of Graduate Studies of Texas A&M University.

Defant, A., 1961. Physical Oceanography, vol. 2, Pergamon, New York.

Fairfield, N., Kantor, G., Jonak, D., Wettergreen, D., 2010. Autonomous exploration and mapping of flooded sinkholes, The International Journal of Robotics Research, 29, 748-774.

Ford, D.C., Williams, P.W., 1989. Karst Geomorphology and Hydrology, Unwin Hyman, London.

Garmin 2011. "What is WAAS". Garmin. Web. 16 June. 2011 <http://www8.garmin.com/aboutGPS/waas.html>.

Gibbons, D.A., 2003. An Environmental Assessment of Bermuda's Caves. MS Thesis, Office of Graduate Studies of Texas A&M University.

Glasspool, A.F., 2003. Recovery Plan for Bermuda's Critically Endangered Cave Fauna. Department of Conservation Services Ministry of the Environment Bermuda.

Gregg, D.O., 2006. An analysis of ground-water fluctuations caused by ocean tides in Glynn County, GA, Ground Water, 4(3), 24-32.

Gunderson, Holling, 2002. Panarchy: Understanding transformations in human and natural systems, Island Press, Washington D.C, Chapter 15, 395-417.

Harder, S.V., Amatya, D.M., Callahan, T.J., Trettin, C.C., Hakkila, J., 2007. Hydrology and water budget for a forested Atlantic coastal plain watershed, South Carolina, Journal of the American Water Resources Association, 43(3), 563-575.

Harmon, R.S., Land L.S., Mitterer, R.M., Garrett, P., Schwarcz, H.P., Larson, G.J., 1981. Bermuda sea level during the last interglacial, Nature, 5, 481-483.

Hart, C.W., Manning, R.B., 1981. The cavernicolous caridean shrimps of Bermuda (Alpheidea, Hippolytidae, and Atyidae), Journal of Crustacean Biology, 1(5), 441-456.

Hearty, P. J., Vacher, H. L., 1994. Quaternary stratigraphy of Bermuda: a high-resolution pre-sangamonian rock record, Quaternary Science Reviews, 13, 685-697.

Holthuis, L.B., 1973. Caridean shrimp found in land locked saltwater pools at four Indo-West Pacific localities (Sinai Peninsula, Funafuti Atoll, Maui and Hawaii Islands), with the description of one new genus and four new species, Zoologishe Verhandelingen 128, 1-48.

Iliffe, T.M., 1980. Bermuda Field Notebook, Texas A&M University, Galveston TX, Unpublished results.

Iliffe, T.M., 1981. The submarine caves of Bermuda. In: Proceedings of the Eighth International Congress of Speleology, Bowling Green, KY, 161-163.

Iliffe, T.M., Hart, C.W., Manning, R.B., 1983. Biography and the caves of Bermuda, Nature, 302, 141 – 142.

Iliffe, T.M., Jickells, T. D., Brewer, M.S., 1984. Organic pollution of an inland marine cave from Bermuda, Marine Environmental Research, 12, 173-189.

Iliffe, T.M., 2000. Anchialine cave ecology. In: Wilkens H, Culver DC, Humphreys W.F. (Eds), Ecosystems of the World, Subterranean Ecosystems, Elsevier, Amsterdam. 30, 53–76.

Iliffe, T.M., 2003. Submarine caves and cave biology of Bermuda. NSS News. 217-224.

Iliffe, T.M., 2004. Walsingham Caves, Bermuda: Biospeleology. In: J. Gunn (Eds), Encyclopedia of Caves and Karst Science: New York, Fitzroy Dearborn, 767-769.

Iliffe, T.M., 2008. Groundwater pollution and its impact on Bermuda's reefs and inshore waters, NOAA Coral Reef Conservation Grant – Final Report, 1-22.

Iliffe, T.M., 2009. Bermuda. In: A.N. Palmer and M.V. Palmer (Eds), Caves and karst of the USA, National Speleological Society, Huntsville, AL, 353-357.

Iliffe, T.M., Kornicker, L. S., 2009. Worldwide diving discoveries of living fossil animals from the depths of anchialine and marine caves. Smithsonian Contributions to the Marine Sciences, 38, 269-280.

Iliffe, T.M., Kvitek, R., Blasco, S., Blasco, K., Covill, R., 2011. Search for Bermuda's deep water caves, Hydrobiologia, 677, 156-168.

Land, L.S., Mackenzie, F.T., Gould, S.J., 1967. Pleistocene history of Bermuda, Bulletin of the Geological Society of America, 78, 993-1006.

Leung, P., 2012. Personal Communication

Li, H.L., Jiao, J.J., 2001. Tide-induced groundwater fluctuation in a coastal leaky confined aquifer system extending under the sea, Water Resources Research, 37, 1165–1171.

Maloney, B.M., 2008. The role of macro algal species as bioindicators in Bermudian karstic cave pools. MS Thesis, Office of Graduate Studies of Texas A&M University.

Manning, B., Hart, C., Iliffe, T., 1986. Mesozoic relicts in marine caves of Bermuda, Stygologia, 2, 156-166.

Martin, J.B., 2011. Tidal pumping of water between Bahamian blue holes, aquifers, and the ocean, accepted manuscript, University of Texas.

Morris, B., Barnes, J., Brown, F., Markham, J., 1977. The Bermuda Marine Environment, A report of the Bermuda inshore waters investigations, Bermuda Biological Station, Bermuda.

Mukai, A.Y., Westerink, J.J., Luettich, R.A., 2002. Guidelines for using eastcoast 2001 database of tidal constituents within western North Atlantic Ocean, Gulf of Mexico and Caribbean Sea. Coastal and Hydraulics Engineering Technical Note, IV. 40.

Mylroie, J.E., Carew, J.L., Vacher H.L., 1995. Karst development in the Bahamas and Bermuda, Geological Society of America Special Papers, 300, 251-267.

Mylroie, J.E., Mylroie, J.R., 2011. Void development on carbonate coasts: creation of anchialine habitats, Anchialine Ecosystems, 677(1), 15-32.

Neumann, A. C., 1963. Processes of recent carbonate sedimentation in Harrington Sound, Bermuda, Ph.D. Thesis, Lehigh University, PA, 131.

Neumann A.C. 1965. Processes of Recent Carbonate Sedimentation in Harrington Sound, Bermuda, Bulletin of Marine Science. 15(4): 987-1035.

NOAA. 2006. “Tide Predicting Machines” Tides & Currents. Web. 6 Nov. 2011 < http://co-ops.nos.noaa.gov/predmach.html>.

Oldfield, S., 1999. Biodiversity: The UK overseas territories. Joint Nature Conservation Committee, Chapter 4, 23-33.

Palmer, A.N., 1991. Origin and morphology of limestone caves, Geological Society of America Bulletin, 103, 1-21.

Pawlowiecz, R., Beardsley, B., Lentz, S., 2001. Classical tidal harmonic analysis including error estimates in MATLAB using T TIDE, Computers & Geoscience, 28, 929-937.

Pohlman, J.W., 2011. The biochemistry of anchialine caves: progress and possibilities, Hydrobiologia, 677(1), 33-51.

Poiseuille, J. L. M. 1840. Recherches experimentelles sur le movement des liquids dans les tubes de tres petits diameters, Comptes Rendu, 1041 1048(11), 961-967

Recktenwald, G., 2002, Fully-Developed Flow in a Pipe: A CFD Solution. Web. 7 September. 2011. <web.cecs.pdx.edu/~gerry/class/ME448/codes/fullyDevelopedPipeFlow.pdf>

Ritter, M. 2011. The Physical Environment. The Water Balance. Web. 6 June. 2011. <http://www.uwsp.edu/geo/faculty/ritter/geog101/textbook/hydrosphere/water_balance_1.html>.

Ritzi, R.W., Bukowski, J.M., Carney, C.K., Boardman, M.R., 2001. Explaining the thinness of the fresh water lens in the Pleistocene carbonate aquifer on Andros Island, Bahamas, Ground Water, 39(5), 713-720.

Rotzoll, K., El-Kadi, A.I., Gingerich, B., 2008. Analysis of an unconfined aquifer subject to asynchronous dual-tide propagation, Ground Water, 46, 239-250.

Shah, R. K., London, A.L., 1978. Laminar Flow Forced Convection in Ducts. Academic, New York.

Simmons, J.A.K., Jickells, T., Knap, A., 1985. Nutrient concentrations in ground waters from Bermuda: Anthropogenic effects. In: D.E. Caldwell et al. (Eds), Planetary ecology, Van Nostrand Reinhold Company, New York, 383-398.

Sket, B., Iliffe, T.M., 1980. Cave fauna of Bermuda, International Review of Hydrobiology, 65, 871-882.

Slooten, L.J., Carrera, J., Castro, E., Garcia, D. F., 2010. A sensitivity analysis of tide-induced head fluctuations in coastal aquifers. Journal of Hydrology. 393, 370-380.

Thomas, M.L., Eakins, E.E., Logan A., 1991. Physical characteristics of the anchaline ponds of Bermuda, Bulletin of Marine Science, 48, 125-136.

Thomas, M.L., 1996. Origin and Community Structure of the Harrington Sound Notch, Bermuda, Bulletin of Marine Science, 58(3), 753-763.

Townley, L.R., 1995. The response of aquifers to periodic forcing, Advances in Water Resources, 18, 125–146.

Trefry, M.G., 1999. Periodic forcing in composite aquifers, Advances in Water Resources, 22, 645–656.

Vacher, H.L., 1978. Hydrology of Bermuda – Significance of an across – the island variation in permeability, Journal of Hydrology, 39, 207-226.

Vacher, H.L., Wallis, T.N., 1992. Comparative hydrogeology of fresh-water lenses of Bermuda and Great Exuma Island, Bahamas, Ground Water, 30(1), 15-20.

Vacher, H.L., Quinn T.M., 2004. Geology and hydrogeology of carbonate islands, first ed. Elsevier Science, Amsterdam.

Verrill, A. E., 1907. The Bermuda Islands Pt 4, geology and paleontology, Trans. Conn. Acad. Arts Sci, 12, 316.

Vogt, P.R., Jung, W.Y., 2007. Origin of the Bermuda volcanoes and Bermuda Rise: History, Observations, Models, and Puzzles, Geological Society of America, 430, 553-591.

von Bodungen, B., Jickells, J.D., Smith, S.R., Ward, J.A., Hillier, G.B., 1982. The water column. In: The Bermuda marine environment: the final report of the Bermuda Inshore Waters Investigation 1975-1980, (Eds), Bermuda Biological Station. Special Publication No. 18:1-66

Wheatcraft, S.W., Buddemeier, R.W., 1981. Atoll island hydrology, Ground Water, 19, 311-320.

Whitaker, F.F., Smart, P.L., 1990. Active Circulation of saline ground waters in carbonate platforms: Evidence from the Great Bahama Bank, Geology, 18, 200-203

Whitaker, F.F., Smart, P.L., 1997. Hydrogeology of the Bahamian archipelago, Developments in Sedimentology, 54, 183-216

White, I., Falkland, T., 2009. Management of freshwater lenses on small Pacific islands, Hydrogeology, 18, 227-24.